

POLYTECHNIC UNIVERSITY OF TURIN

DEPARTMENT OF ENVIRONMENT, LAND AND INFRASTRUCTURE ENGINEERING

Master of Science in Georesources and Geoenergy Engineering

A.Y. 2024/2025

Underground CO₂ Storage: a general overview

Supervisor:	Candidate:
Prof. Vera Rocca	Mironshokh Ismoilov

Abstract

Global climate change entails big changes - such as rising ocean levels, due to which some countries may remain under water, and some, on the contrary, will feel a shortage of water, air pollution will lead to an increase in the number of diseases and deaths, the intensity of forest fires, strong hurricanes can negative effect to natural CO2 adsorbers, pollution of the oceans will lead to the death of marine animals, one of the ways to reduce these risks is to capture carbon dioxide, transport it storage facilities and safely store it underground.

Carbon dioxide capture and storage (CCS) represents a critical technology for climate change mitigation, with underground geological storage being the most technically mature and widely researched approach. This thesis provides a comprehensive analysis of underground CO₂ storage projects worldwide, examining the latest technical literature, technological practices, and regulatory considerations surrounding geological safe sequestration. The research focuses on literature revision, dataset definition, and analysis of existing 20 underground CO2 projects to provide a global overview of CO₂ storage implementation and to find the ones with the best properties and technological parameters, which suits for the safe, reliable and long-term CO2 underground storage.

The study investigates various storage mechanisms including structural, residual, solubility, and mineral trapping, analyzing their effectiveness across different geological formations. Through examination of operational projects such as Sleipner (Norway), Weyburn-Midale (Canada), and In Salah (Algeria), this work evaluates the thermodynamic properties of CO₂ under subsurface conditions, rock-fluid interactions, and the influence of reservoir heterogeneity on storage performance.

Key findings indicate that geological formations possess substantial storage capacity, with global estimates ranging from 1000 GtCO₂ to over 10,000 GtCO₂. However, operational challenges including site characterization, monitoring requirements, and public acceptance continue to limit widespread deployment. The analysis of 20 major storage projects reveals significant variations in storage efficiency, injection rates, and monitoring approaches, with success factors primarily dependent on geological characteristics, regulatory frameworks, and stakeholder engagement.

This master thesis contributes to the understanding of underground CO₂ storage by providing a systematic evaluation of project parameters and performance metrics, offering insights for future storage site selection and operation optimization.

Index

Abstract	2
Scope of the Work	6
1. Introduction	
2. Theoretical Background	9
2.1 Storage Locations	10
2.2 Storage Mechanisms	11
2.3 PVT Properties of CO ₂	13
2.4 Rock Properties and Fluid-Rock Interactions	17
3. Global Overview of CO ₂ Storage Projects	24
3.1 Technical Review of Existing CO ₂ Storage Projects	3
3.2 Reservoir Formation Petrophysical Properties	32
3.3 Reservoir Physical Conditions	37
3.4 Caprock Properties	45
3.5 Brine Characteristics	46
3.6 Fluid–Rock Interaction Properties	5(
3.7 Injectivity and Storativity	53
3.8 Trapping Mechanisms	56
3.9 Monitoring Technologies and Results	56
4. Risk Assessment and Management Strategies	57
4.1 Global and Local Risk Factors	57
4.2 Monitoring and Verification Requirements	58
5. 2025 Project Status Updates and Recent Developments	58
6. Comments and conclusions	60
References	62

List of Figures

Figure 1. Overview of carbon capture, transport, and storage [4]	9
Figure 2. Schematic of CO ₂ trapping mechanisms in the subsurface (Aminu et al. 2017) [3]	
Figure 3. Phase Diagram of CO ₂ [2]	13
Figure 4. CO ₂ density versus pressure at various temperatures	14
Figure 5. CO ₂ fingering in the reservoir [49]	
Figure 6. A review of recent developments in CO ₂ -mobility control in enhanced oil recovery [49]	15
Figure 7. Compressibility factor of CO ₂ versus pressure at various temperatures	16
Figure 8. Viscosity of CO ₂ versus pressure at various temperatures	16
Figure 9. Effect of temperature and pressure on the solubility of CO ₂ in water [1]	16
Figure 10. Schematic of capillary sealing mechanism in a pore throat of seal rock [33]	20
Figure 11. CO ₂ –Brine–Mineral Interactions in Ebeity Sandstone–Caprock [55]	22
Figure 12. A comparison between well orientation (a) vertical well (b) horizontal well [56]	23
Figure 13. Global CCS Map, Storage Projects Map for 2023 (credits to Scottish Carbon Capture &	
Storage http://sccs.org.uk/resources/global-ccs-map)	29
Figure 14. Global CCS Map, Injection Projects Map for 2023 (credits to Scottish Carbon Capture &	
Storage http://sccs.org.uk/resources/global-ccs-map)	30
Figure 15. Formation Type	31
Figure 16. Lithology	
Figure 17. Brine Salinity Classification for Underground CO ₂ Storage Sites	33
Figure 18. Reservoirs Average Porosities	34
Figure 19. Porosity Classification for Underground CO ₂ Storage Sites	35
Figure 20. Reservoirs Average Permeabilities	36
Figure 21. Permeability Classification for Underground CO ₂ Storage Sites	
Figure 22. Injection depths and formation's thicknesses	38
Figure 23. Injection Depth Classification for Underground CO ₂ Storage Sites	39
Figure 24. Formation Thickness Classification for Underground CO ₂ Storage Sites	40
Figure 25. Reservoir Pressure Classification for Underground CO ₂ Storage Sites	42
Figure 26. Reservoirs Pressure	43
Figure 27. Reservoirs Temperature	44
Figure 28. Reservoir Temperature Classification for Underground CO ₂ Storage Sites	
Figure 29. Formation Brine pH Distribution in Global CO ₂ Storage Projects	
Figure 30. Brine pH	
Figure 31. Brine Salinity Classification for Underground CO ₂ Storage Sites	
Figure 32. Brine Salinity	
Figure 33. Initial Water Saturation Distribution in Global CO ₂ Storage Projects	
Figure 34. CO ₂ -Water-Rock Contact Angle Distribution in Global CO ₂ Storage Projects	
Figure 35. CO ₂ Injection Rate Distribution in Global CO ₂ Storage Projects	54
Figure 36. Cumulative CO ₂ Storage Volume Distribution in Global CO ₂ Storage Projects	55

List of Tables

Table 1. Storage Mechanisms [57]	.11
Table 2. Summary of typical reservoir rock properties observed in major CO2 storage formations [14] .	.18
Table 3. Comprehensive Comparison of Major CO2 Storage Projects	.25
Table 4. Comprehensive Comparison of Major CO2 Storage Projects (Continued)	.26
Table 5. Comprehensive Comparison of Major CO2 Storage Projects (Continued)	.27
Table 6. Comprehensive Comparison of Major CO2 Storage Projects (Continued)	.28
Table 7. Monitoring Technologies Used in Major CO2 Storage Projects	.57
Table 8. Optimal Geological Parameters for Underground CO2 Storage Derived from Analyzed Projects	s60

Scope of the Work

This thesis includes a detailed description of underground carbon dioxide storage, an analysis of all the important parameters to maintain safe and long-term storage, a carbon dioxide storage map is provided to see carbon dioxide storage projects, carbon dioxide leakage paths and leak detection methods are described.

A detailed comparison of 20 underground carbon dioxide storage projects on important parameters is given to identify the best one in terms of the best parameters for safe and long-term carbon dioxide storage.

1. Introduction

Climate change is a global problem for the whole world, due to which some countries may remain under water, and some will experience water shortage, intensive melting of glaciers, frequent forest fires, death or complete disappearance of some species of animals or birds or marine animals, air pollution, change of seasons, all this is associated with emissions of carbon dioxide and other harmful gases into the atmosphere, which leads to the greenhouse effect and rising temperatures.

Rising atmospheric carbon dioxide concentrations, mainly due to anthropogenic activities, have made climate change one of the most important global challenges of the 21st century. The Intergovernmental Panel on Climate Change (IPCC) has stressed the urgent need for rapid and farreaching transformations in energy systems to limit global warming to 1.5°C above pre-industrial levels (IPCC, 2018). In April 2025, the global average temperature have reached about +1.49°C above the 1850–1900 pre-industrial level, bringing us dangerously close to the 1.5°C threshold, the point at which climate tipping points could lead to extreme and irreversible consequences. In this context, carbon capture and storage (CCS) has emerged as a key technology to achieve significant emission reductions, particularly from large stationary sources that remain difficult to decarbonise by alternative means. [14]

Carbon capture and storage (CCS) consist of a set of technologies that aim to prevent CO2 emissions from entering the atmosphere by capturing carbon dioxide from industrial and energy-related sources, transporting it to suitable storage sites, and storing it in safe way for long periods of time. While the full CCS chain includes capture, transport, and storage components, the ultimate climate benefit depends largely on the safety and durability of the storage phase. Underground geological storage has emerged as the most promising and technically advanced storage option, allowing CO2 to be retained over geological time periods.

The concept of geological CO2 storage involves injecting compressed CO2 into deep underground formations, typically at depths greater than 800 meters, where pressure and temperature conditions maintain the CO2 in a dense supercritical state. Suitable geological formations include depleted oil and gas reservoirs, deep saline aquifers, and unmined coal seams, each of which is characterized by sufficient porosity to accommodate the injected CO2 and overlying low-permeability seals to prevent its upward migration. Storage safety depends on multiple capture mechanisms acting over different time periods, from immediate structural capture to long-term mineral sequestration through geochemical reactions [12].

Several commercial-scale projects have demonstrated the technical feasibility of geological storage of CO2. Since 1996, the Sleipner project in the Norwegian North Sea has successfully stored over 25 million tonnes of CO2, while the Weyburn-Midale project in Canada has integrated CO2 storage with enhanced oil recovery operations. These pioneering projects have provided valuable insights into the behaviour of CO2 in the subsurface, storage mechanisms and monitoring requirements, laying the foundation for wider implementation [11].

Although alternative approaches to storage such as ocean storage and mineral carbonation have been explored, deep geological storage remains the most technically advanced and economically viable option for large-scale implementation. The cost-effectiveness of geological storage varies considerably depending on site characteristics and project scale, but it is generally the most promising technology for making a significant contribution to CO2 sequestration in climate change mitigation efforts [10].

Despite its proven technical feasibility, geological CO2 storage faces significant challenges that limit widespread adoption. These include uncertainty about the safety of long-term storage, high capital costs of infrastructure development, complex regulatory frameworks, and public acceptance issues. Risk management considerations span both global risks associated with potential CO2 releases undermining climate benefits and local risks including groundwater contamination and induced seismicity. Comprehensive monitoring, reporting, and verification systems are needed to ensure the integrity of the storage facility and maintain public confidence [7].

The global potential for geological storage of CO2 is significant, and theoretical estimates suggest that it could last for several centuries at current emission levels. However, the practical use of this potential depends on many factors, including site accessibility, infrastructure development, economic feasibility, and supportive policy frameworks. Current projections suggest that CO2 storage could reduce cumulative CO2 emissions by 220–2200 Gt by 2100, representing 10–20% of the required mitigation effort in scenarios consistent with limiting global warming to below 2°C [5].

The objective of this thesis is to conduct a comprehensive analysis of underground CO2 storage through a systematic literature review, dataset identification and analysis for a global overview of existing and projected projects. The study covers three main objectives: first, to examine the theoretical foundations of geological CO2 storage, including storage mechanisms, thermodynamic properties and rock-fluid interactions; second, to analyze the operating experience of large-scale storage projects to identify key performance factors and lessons learned; and third, to assess the global potential and limitations for scaling up geological CO2 storage as a climate change mitigation strategy.

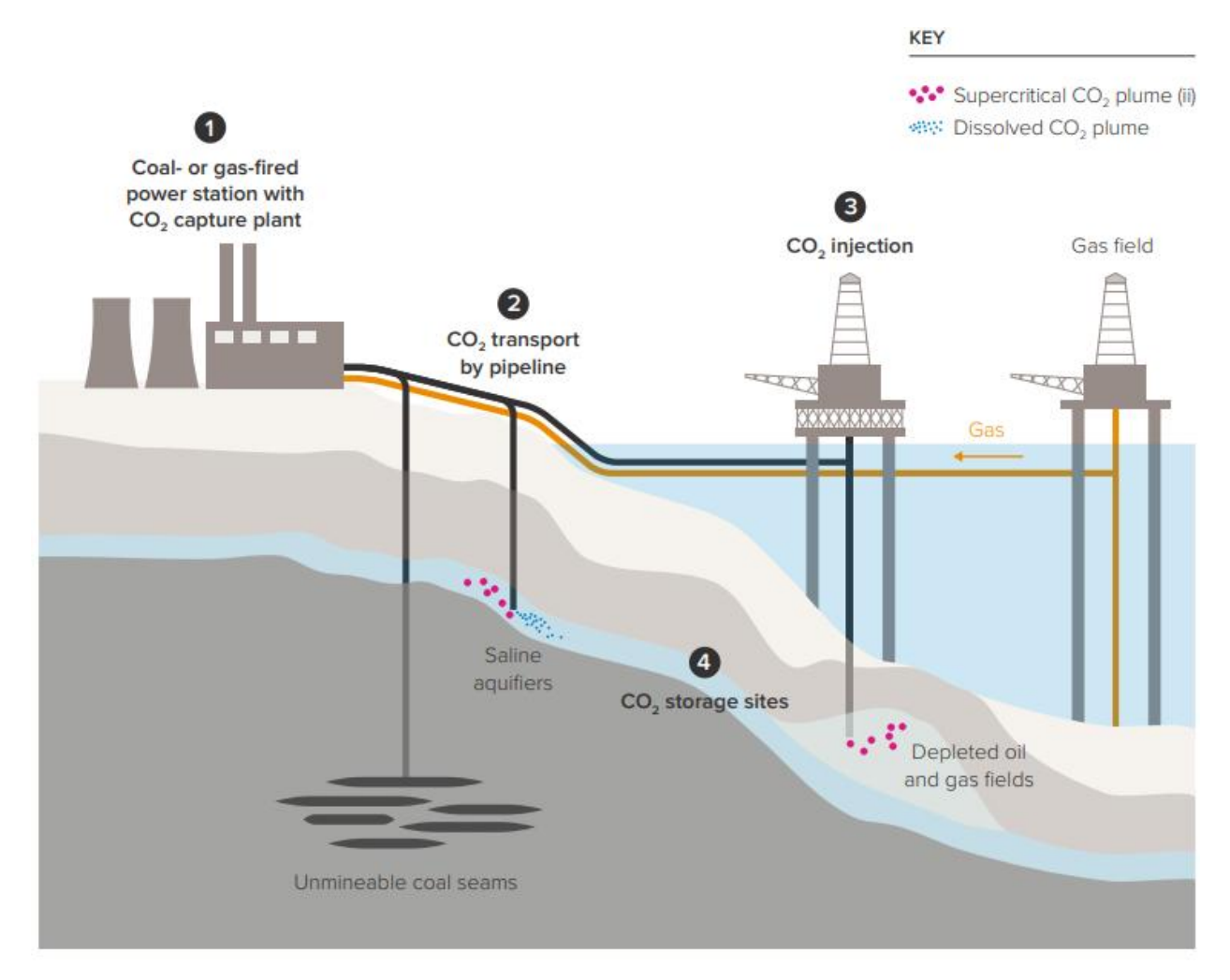
The analysis includes a detailed assessment of 20 major CO2 storage projects, examining their geological characteristics, operational parameters and performance indicators to inform future project development. This comprehensive data set allows for comparison of different storage approaches, identification of best practices and assessment of factors influencing project success or failure. Risk assessment considerations are incorporated throughout the analysis to provide a comprehensive basis for the assessment.

2. Theoretical Background

This section examines the fundamental principles underlying underground CO₂ storage through four key areas: storage locations (Fig.1), storage mechanisms, thermodynamic properties of CO₂, and rock properties with fluid-rock interactions. Understanding these theoretical foundations is essential for effective storage system design and risk assessment.

According to the IEA's 2023 assessment, if every announced carbon-capture-and-storage project proceeds, global CO₂ capture capacity could soar from about 45 Mtpa today to nearly 400 Mtpa by 2030. Yet the storage pipeline suggests we might be able to inject up to 615 Mtpa over the same period—outpacing capture capacity and underscoring the urgency of safe, reliable containment.

Effective reservoir management in CCS spans every stage—from choosing a geologically suitable basin and performing detailed subsurface characterization, to designing and simulating injection schemes, tracking the CO₂ plume in real time, and verifying long-term seal integrity. Only by integrating these technical and geological disciplines can we be confident that stored CO₂ will remain immobilized for centuries.



- i. Diagram is not to scale. The burial of CO₂ is typically at 1 5km, and 50 300km from the coastline.
- ii. Supercritical CO2 is the natural fluid state of CO2 at pressures deep underground.

Figure 1. Overview of carbon capture, transport, and storage [4]

2.1 Storage Locations

Underground CO₂ storage utilizes deep geological formations that possess the necessary characteristics for long-term CO₂ containment. The selection of appropriate storage locations depends on several critical factors including geological stability, storage capacity, injectivity, and the presence of effective sealing mechanisms. Two primary formation types represent the most promising targets for large-scale CO₂ storage implementation: depleted hydrocarbon reservoirs and deep saline aquifers.

Depleted hydrocarbon reservoirs represent one of the most attractive options for CO₂ storage due to their well-characterized geology and proven capacity to retain fluids over geological timescales [25, 26]. These formations have demonstrated their sealing integrity through natural hydrocarbon accumulation and retention, often for millions of years. The existing infrastructure including wells, pipelines, and surface facilities provides significant economic advantages by reducing initial capital requirements [27].

Depleted oil reservoirs typically exhibit porosity ranges of 10-35% and permeabilities varying from less than 1 mD to several hundred millidarcies, depending on the reservoir rock type and depositional environment [28]. The pressure depletion resulting from hydrocarbon extraction creates additional storage capacity while maintaining formation integrity below fracture pressures. The replacement of hydrocarbons with CO₂ can enhance oil recovery in certain cases, providing economic incentives for storage operations [29, 30].

Gas reservoirs generally offer higher storage capacities due to their typically higher porosity and permeability compared to oil reservoirs. The absence of residual oil saturation allows for more efficient CO₂ storage, with storage efficiencies potentially reaching 60-80% of the original gas in place [31]. However, the pressure history and potential for reservoir compartmentalization must be carefully evaluated to ensure uniform CO₂ distribution and containment [32].

Deep saline aquifers represent the largest potential storage resource globally, with estimated capacities orders of magnitude ranging from 400 to 10,000 gigatonnes [20, 33]. These formations consist of porous and permeable sedimentary rocks saturated with saline water that is not suitable for drinking or agricultural use due to high total dissolved solids concentrations, typically exceeding 10,000 mg/L [34].

Saline aquifers are typically found in sedimentary basins at depths ranging from 800 to 4000 meters, where pressure and temperature conditions favor CO₂ storage in its supercritical state [6]. The geological diversity of these formations encompasses various rock types including sandstones, carbonates, and volcanic rocks, each presenting unique storage characteristics and challenges [35].

The storage mechanism in saline aquifers relies primarily on structural and stratigraphic trapping, with CO₂ displacing formation water and accumulating beneath low-permeability seals. Over time, additional trapping mechanisms become active, including residual trapping through capillary forces, solubility trapping as CO₂ dissolves in formation water, and mineral trapping through reactions with rock minerals [36, 37].

The characterization of saline aquifers presents significant challenges compared to hydrocarbon reservoirs due to limited geological data and the absence of production history. Site characterization requires extensive geological and geophysical surveys, exploratory drilling, and reservoir modeling to assess storage capacity, injectivity, and containment security [38].

2.2 Storage Mechanisms

The security of underground CO₂ storage depends on multiple trapping mechanisms that operate over different timescales and provide complementary containment functions. Four primary trapping mechanisms ensure CO₂ containment security: structural trapping, residual trapping, solubility trapping, and mineral trapping (Table 1). Understanding these mechanisms is crucial for predicting long-term storage behavior and assessing storage security.

Table	1.	Storage	Mechanisms	1571
	4 .	Diologe.		1011

Mechanism	Description	Timescale	Capacity	Security Level	Controlling Factors
Structural	Buoyancy-driven accumulation beneath seals	Immediate	High	Good	Seal integrity, structure geometry
Residual	Capillary trapping in pore spaces	Years	Moderate	Very Good	Pore structure, wettability
Solubility	Dissolution in formation water	Decades	Moderate	Excellent	Pressure, temperature, salinity
Mineral	Chemical reaction forming carbonates	Centuries	Low- Moderate	Excellent	Mineralogy, reaction kinetics

The evolution of these trapping mechanisms over time is illustrated in Figure 2, showing how storage security increases as mobile CO₂ becomes increasingly immobilized through various processes.

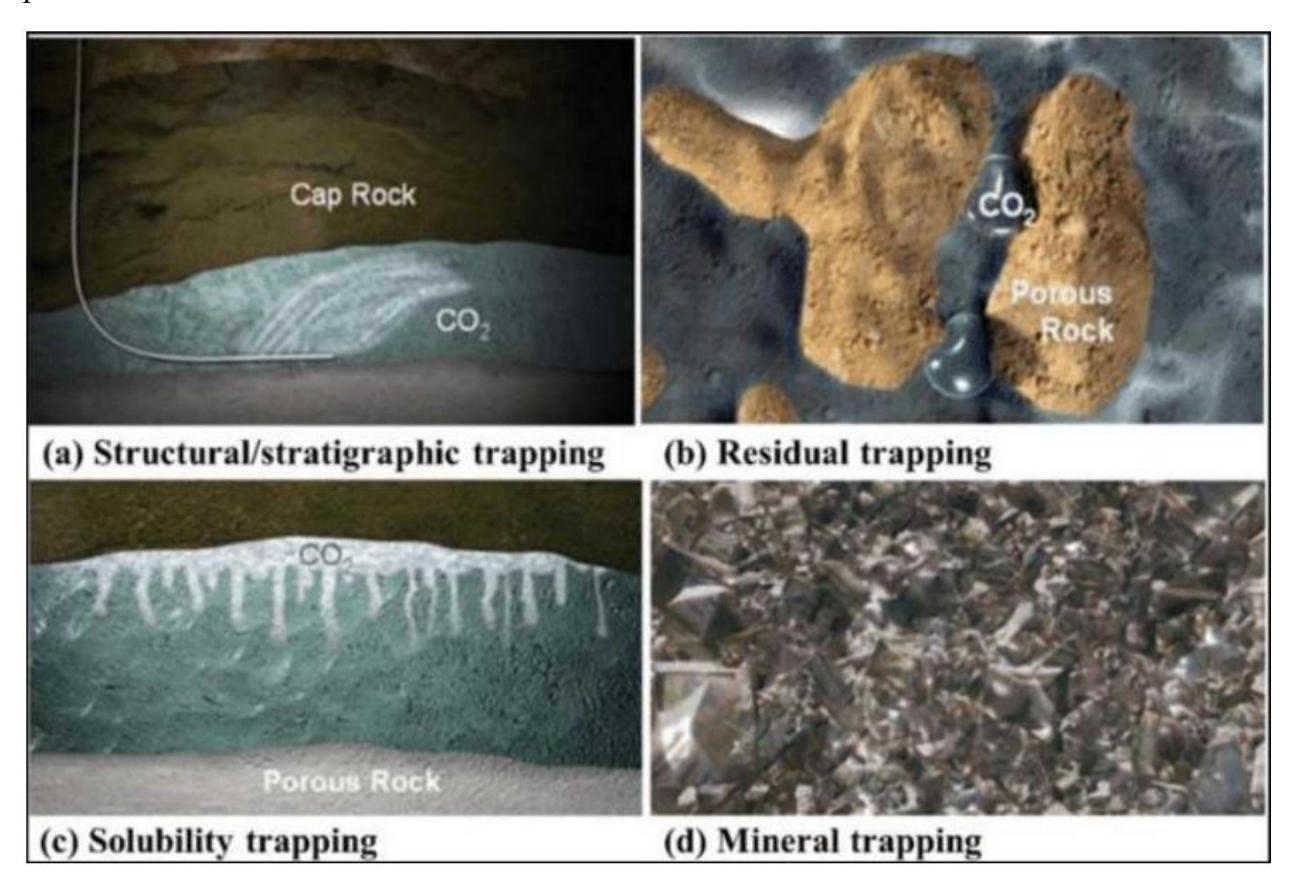


Figure 2. Schematic of CO₂ trapping mechanisms in the subsurface (Aminu et al. 2017) [3]

Structural and Stratigraphic Trapping

Structural trapping represents the primary containment mechanism during the initial phases of CO₂ injection, relying on buoyancy-driven accumulation of CO₂ beneath low-permeability sealing formations [39]. CO₂, being less dense than formation water, migrates upward until it encounters an impermeable barrier such as shale, evaporites, or tight carbonates that prevent further vertical migration [40].

The effectiveness of structural trapping depends on the geometry and lateral continuity of the seal, the permeability contrast between the reservoir and caprock, and the capillary entry pressure of the sealing formation [41]. Structural closures provide the most secure containment, but stratigraphic traps formed by permeability barriers or facies changes can also provide effective containment [6].

The integrity of structural traps must be evaluated considering potential leakage pathways including fractures, faults, and wellbores. Fault reactivation due to increased pore pressure from CO₂ injection represents a particular concern, requiring geomechanical analysis to ensure that injection pressures remain below critical thresholds [42, 43].

Residual Trapping

Residual trapping occurs when CO₂ becomes immobilized within pore spaces due to capillary forces and pore-scale heterogeneity [44, 45]. As CO₂ migrates through the reservoir, it displaces formation water, but a portion becomes trapped as disconnected ganglia in smaller pores and pore throats where capillary forces exceed buoyancy forces.

The magnitude of residual trapping depends on reservoir rock properties including pore size distribution, surface roughness, and wettability characteristics [46]. Laboratory studies suggest that residual CO₂ saturations typically range from 10-50% of the mobile CO₂, with higher values observed in rocks with more heterogeneous pore structures [47].

Residual trapping provides a significant contribution to storage security because trapped CO₂ cannot migrate regardless of pressure gradients or structural changes. This mechanism becomes increasingly important over time as CO₂ plume migration slows and more CO₂ becomes residually trapped behind the migration front [37].

Solubility Trapping

Solubility trapping involves the dissolution of CO₂ in formation water, forming a slightly acidic solution that is denser than the original formation water [48]. This density difference can drive convective mixing that accelerates CO₂ dissolution and enhances storage security by converting mobile CO₂ into an immobile aqueous phase [24].

The solubility of CO₂ in water increases with pressure and decreases with temperature and salinity, with typical values ranging from 10-60 kg CO₂/m³ of water under storage conditions [23]. While solubility trapping operates slowly compared to structural and residual trapping, it can ultimately dissolve substantial quantities of stored CO₂, particularly in large saline aquifers with active water circulation [22].

The kinetics of solubility trapping are controlled by mass transfer processes including molecular diffusion and convective mixing. Natural convection can develop when CO₂-saturated water becomes gravitationally unstable, leading to fingering instabilities that enhance dissolution rates [21]. This process is particularly important in thick, homogeneous formations with high permeability.

Mineral Trapping

Mineral trapping represents the most secure long-term storage mechanism, involving chemical reactions between dissolved CO₂ and rock minerals to form stable carbonate minerals [19]. These reactions are thermodynamically favorable but proceed slowly under typical reservoir conditions, requiring hundreds to thousands of years for significant conversion [18].

The rate and extent of mineral trapping depend on the availability of reactive minerals, particularly those containing calcium, magnesium, and iron such as plagioclase feldspars, pyroxenes, and olivine [17]. Sandstone reservoirs with volcanic components or carbonate formations typically show higher potential for mineral trapping compared to quartz-rich sandstones [16].

Experimental studies and numerical modeling suggest that mineral trapping can ultimately sequester most of the injected CO₂ in favorable geological settings [13]. However, the slow kinetics mean that other trapping mechanisms must provide containment security during the initial centuries following injection [15].

2.3 PVT Properties of CO₂

The thermodynamic properties of CO₂ under subsurface conditions fundamentally control its behavior during injection, migration, and long-term storage. Understanding these properties is essential for reservoir engineering design, storage capacity estimation, and risk assessment.

Phase Behavior and Density

Carbon dioxide exhibits complex phase behavior that varies significantly with pressure and temperature conditions encountered in subsurface storage (Fig. 3). At standard conditions, CO₂ exists as a gas with a density of approximately 1.98 kg/m³. However, under typical storage conditions at depths greater than 800 meters, CO₂ transitions to a supercritical state characterized by liquid-like density and gas-like viscosity.

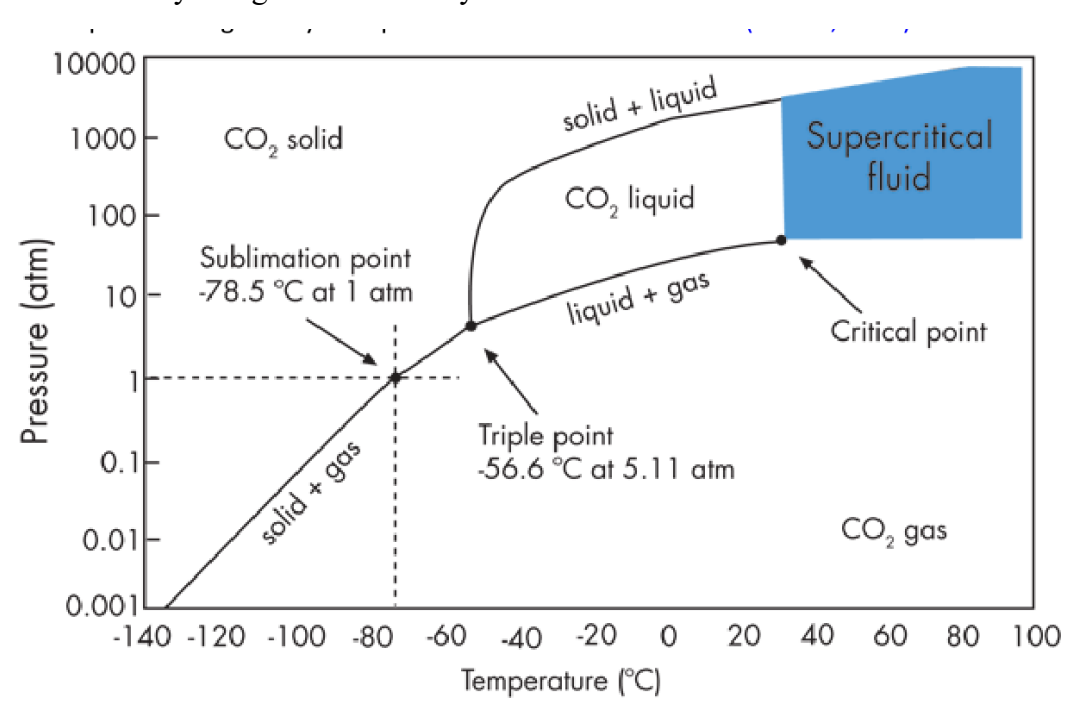


Figure 3. Phase Diagram of CO₂ [2]

The critical point of pure CO₂ occurs at 31.1°C and 7.38 MPa, above which distinct liquid and gas phases do not exist. In supercritical conditions, CO₂ density ranges from 600-900 kg/m³ depending on pressure and temperature. This high density is crucial for storage efficiency, allowing substantial quantities of CO₂ to be stored in available pore space.

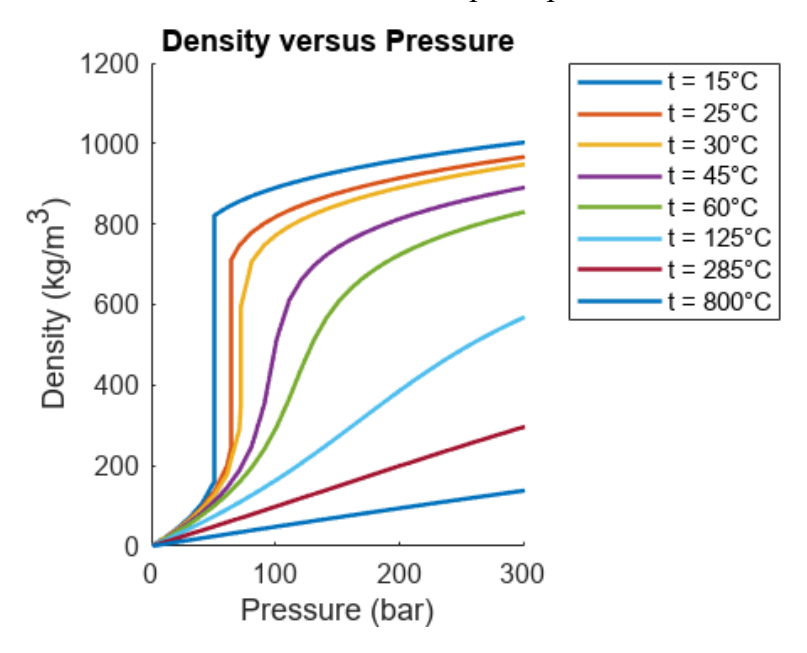


Figure 4. CO₂ density versus pressure at various temperatures

The density of supercritical CO₂ decreases with increasing temperature and increases with pressure, following relationships that can be predicted using equations of state such as the Peng-Robinson formulation. Figure 4 illustrates the relationship between CO₂ density and pressure at various temperatures typical of storage formations.

Compressibility and Viscosity

The compressibility of CO₂ varies significantly with pressure and temperature (Fig. 7), affecting both injectivity and storage capacity calculations. Near the critical point, CO₂ exhibits very high compressibility, which decreases at higher pressures and temperatures. Under typical storage conditions, CO₂ compressibility ranges from 10⁻⁴ to 10⁻³ MPa⁻¹, several orders of magnitude higher than water or rock compressibility.

Viscosity is another critical property affecting CO₂ flow behavior in porous media. Supercritical CO₂ viscosity is much lower than water viscosity, typically ranging from 0.02-0.08 mPa·s under storage conditions compared to 0.3-1.0 mPa·s for formation water. This low viscosity contributes to high CO₂ mobility but can also lead to viscous fingering instabilities when CO₂ displaces more viscous formation fluids (Fig. 5). In practice, such uneven sweep lowers the effective storage capacity—since only a portion of the pore network is occupied by CO₂—and, in enhanced oil recovery applications, results in suboptimal oil displacement [58] [59] [60].

To overcome these sweep inefficiencies, reservoir engineers have adapted enhanced-oil-recovery techniques. Water-alternating-gas (WAG) injection (Fig. 6) alternates water and CO₂ slugs to raise bulk viscosity and suppress viscous fingering [61]. Increasing the number of injection wells broadens areal coverage despite higher costs and combats heterogeneity [62]. Composition-swing injection (CSI) alternates CO₂ streams of differing density and viscosity to reduce buoyant override and enhance residual and solubility trapping [63]. Temperature-swing injection (TSI) exploits cooler CO₂ to induce controlled thermal stresses and improve injectivity [64], while

pressure-swing injection (PSI) varies injection pressures to optimize plume distribution and protect caprock integrity [65]. Dynamic reservoir modeling and real-time monitoring then guide these interventions to maximize sweep efficiency and secure long-term containment.

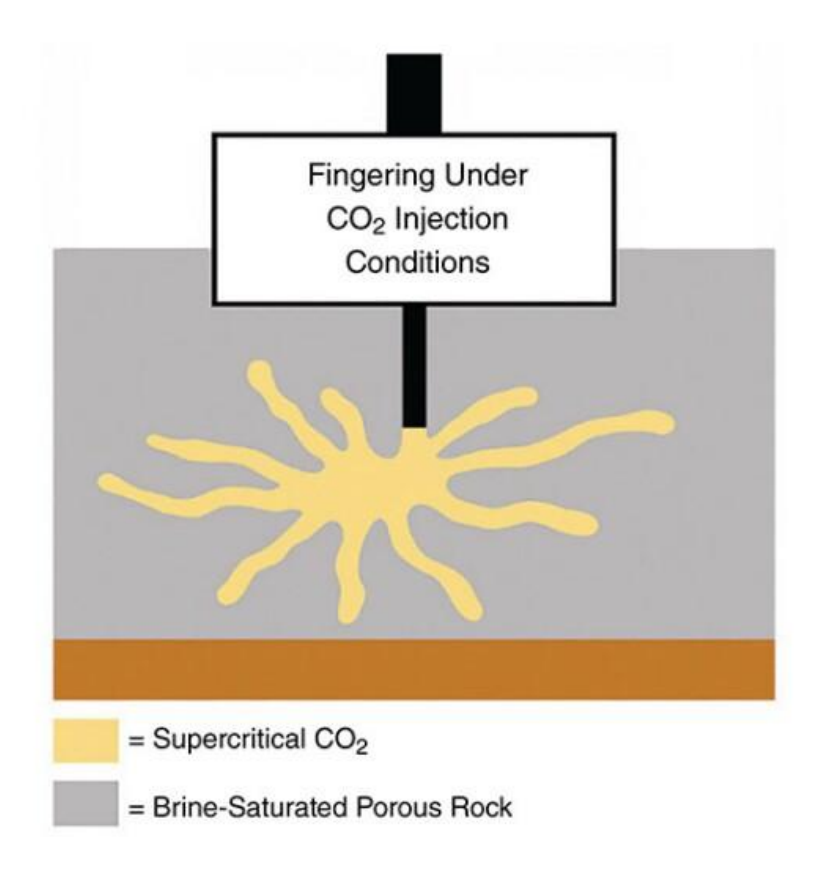


Figure 5. CO₂ fingering in the reservoir [49]

The temperature dependence of CO₂ viscosity is positive (Fig. 7), meaning viscosity increases with temperature, which is opposite to the behavior of most liquids but typical of gases. This relationship, combined with pressure effects, creates complex flow patterns during injection and migration that must be considered in reservoir simulation and risk assessment.

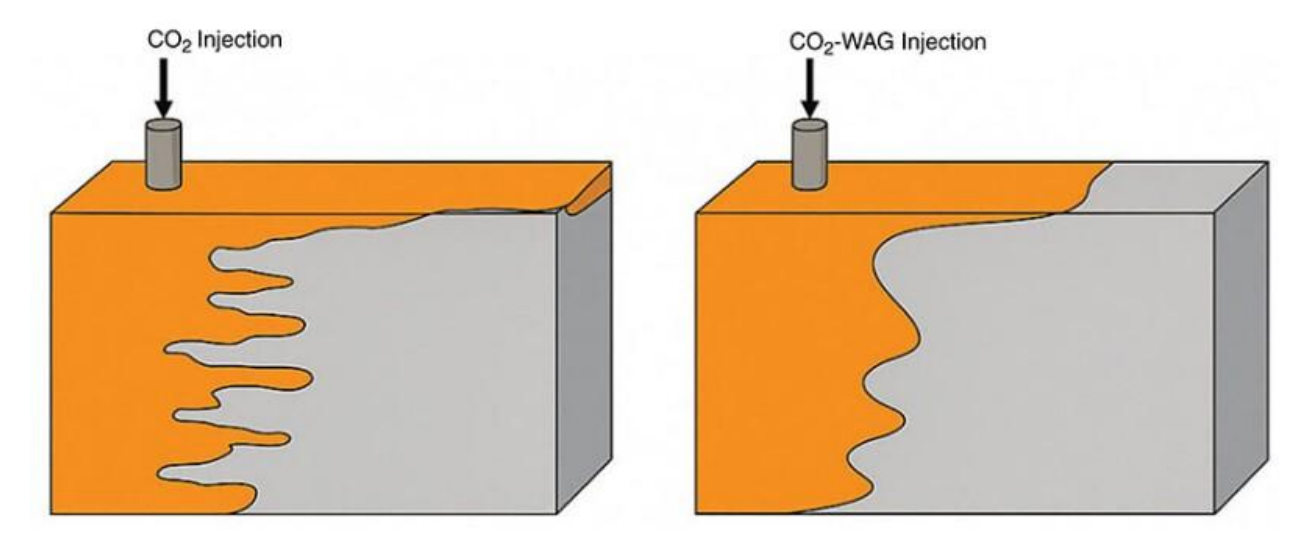


Figure 6. A review of recent developments in CO₂-mobility control in enhanced oil recovery [49]

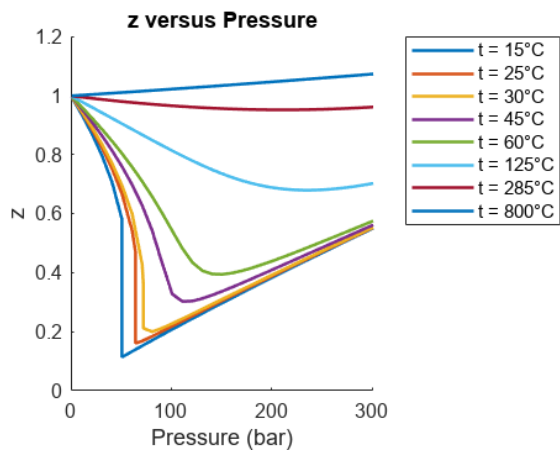


Figure 7. Compressibility factor of CO₂ versus pressure at various temperatures

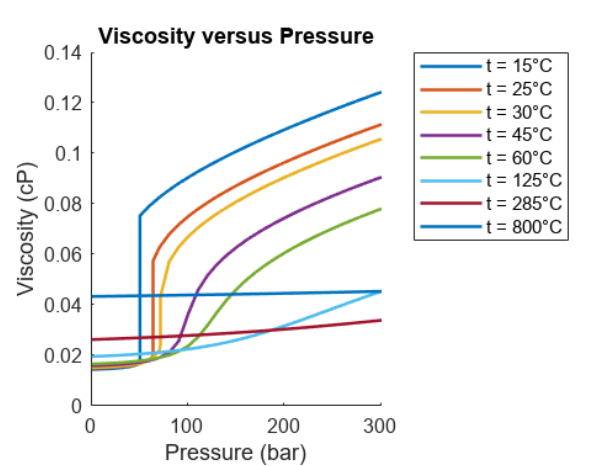


Figure 8. Viscosity of CO₂ versus pressure at various temperatures

Solubility in Formation Water

The solubility of CO₂ in formation water plays a crucial role in long-term storage security through solubility trapping mechanisms. CO₂ solubility is strongly dependent on pressure, temperature, and water salinity, with typical values under storage conditions ranging from 10-60 kg CO₂/m³ of water (Fig. 9).

Pressure has a positive effect on CO₂ solubility, with higher pressures allowing more CO₂ to dissolve. Temperature has a negative effect, with solubility decreasing at higher temperatures. Salinity also reduces CO₂ solubility, with the effect becoming more pronounced at higher salt concentrations typical of deep formation waters.

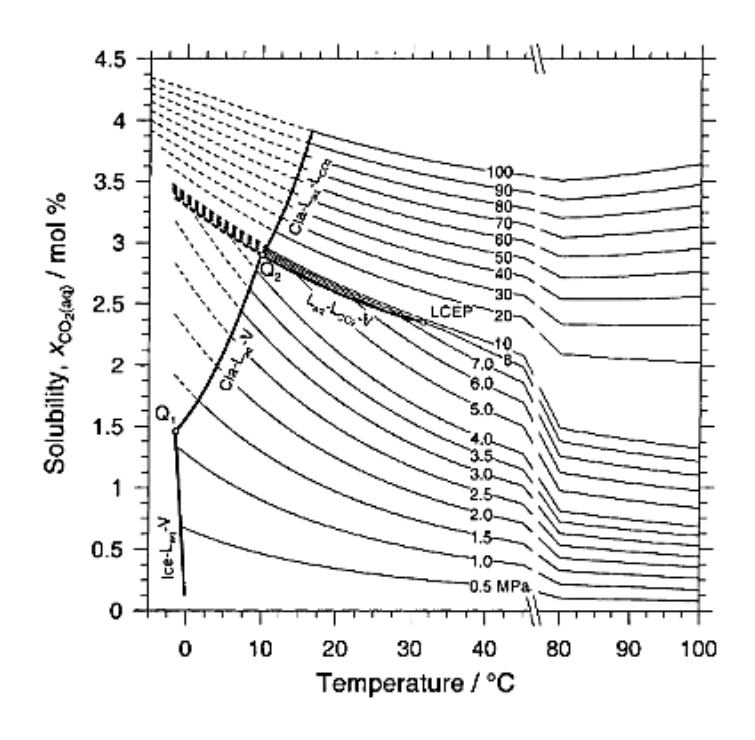


Figure 9. Effect of temperature and pressure on the solubility of CO_2 in water [1]

The dissolution of CO₂ in water forms carbonic acid (H₂CO₃), which dissociates to form bicarbonate (HCO₃⁻) and carbonate (CO₃²⁻) ions. This process acidifies the water, reducing pH from typical formation water values of 6-8 to approximately 3-4 in CO₂-saturated conditions. The acidification can enhance mineral dissolution and potentially impact formation integrity, requiring careful geochemical assessment.

Effects of impurities on storage capacity

Impurities present in the CO₂ gas stream can significantly impact various stages of carbon capture and storage (CCS), including capture, transport, and subsurface injection, in addition to influencing both the mechanisms of entrapment and overall storage efficiency within geological formations. Contaminants such as sulfur oxides (SO_x), nitrogen oxides (NO_x), and hydrogen sulfide (H₂S) are of particular concern due to their hazardous classification, which may necessitate stricter regulatory handling compared to pure CO₂ streams [50]. These impurities alter the thermophysical behavior of CO₂, especially its compressibility, thereby affecting the volumetric storage potential as they occupy pore space, reducing the amount of CO₂ that can be stored in its supercritical or free phase.

In enhanced oil recovery (EOR) applications, the chemical composition of the injected gas influences the solubility of CO₂ in crude oil and its effectiveness in mobilizing hydrocarbons. For instance, methane and nitrogen tend to suppress oil recovery, while components like hydrogen sulfide, propane, and heavier hydrocarbons generally enhance it [51]. The presence of SO_x may also improve recovery efficiency, whereas NO_x can hinder CO₂-oil miscibility, and oxygen may provoke exothermic reactions with reservoir hydrocarbons, potentially causing operational risks [52].

When CO₂ is injected into deep saline aquifers, impurity gases can interfere with dissolution and mineral precipitation dynamics, which govern both the rate and permanence of storage. Certain impurities, notably SO₂ and O₂, may catalyze the leaching of heavy metals from host rock minerals. While prior experiences with acid gas injection suggest minimal long-term impacts, research indicates that SO_x co-injection may drive distinct chemical and mineralogical transformations, necessitating further investigation into the permissible range of impurity compositions for storage operations [53].

Similarly, in coal seam storage scenarios, gas impurities may either enhance or reduce CO₂ storage capacity. For example, SO₂ and H₂S may be preferentially adsorbed due to their higher affinity for coal surfaces, consequently limiting CO₂ uptake. Oxygen, if present, may react irreversibly with coal, degrading the adsorption surface and reducing overall capacity. Nonetheless, certain impure gas mixtures—such as flue gases from coal combustion, predominantly composed of nitrogen and CO₂—can still be viable for enhanced coalbed methane (ECBM) recovery, owing to CO₂'s preferential sorption over methane and nitrogen [54].

2.4 Rock Properties and Fluid-Rock Interactions

The interaction between CO₂ and reservoir rocks controls storage capacity, injectivity, and long-term containment security. Understanding these interactions requires detailed characterization of rock properties and their evolution in response to CO₂ exposure. Key parameters include porosity and permeability characteristics, their anisotropic effects on storage operations, and the influence of wettability, interfacial tension, and capillary pressure on formation fluid displacement.

A key performance metric is **reservoir injectivity**, which measures how rapidly a formation accepts CO₂. It hinges on the rock's natural permeability and its connected pore network, typically quantified through well-test data and core-sample analyses (Alcalde et al., 2021). Furthermore, to keep CO₂ in its dense, supercritical state—and thus pack more molecules into each pore space—storage formations generally need to lie deeper than approximately 800 m, where pressure and temperature conditions transform CO₂ into liquid "fluid" that maximizes volumetric efficiency (IEAGHG, 2010).

Porosity and Permeability Effects

Porosity and permeability represent the fundamental rock properties controlling CO₂ storage capacity and injectivity. Porosity determines the volume of pore space available for CO₂ storage, while permeability controls the ability to inject CO₂ at economically viable rates and influences CO₂ migration patterns within the reservoir. The anisotropic nature of these properties significantly affects both storage capacity estimation and injection operation design.

Storage formations typically exhibit porosities ranging from 10-40% (Table 2), with higher values generally associated with better storage potential. However, the relationship between porosity and storage capacity is complex due to the influence of other factors including pore connectivity, heterogeneity, and trapping mechanisms. Effective porosity, representing the interconnected pore space accessible to fluid flow, is more relevant for storage capacity estimation than total porosity.

Formation Type	Lithology	Porosity (%)	Permeability (mD)	Depth Range (m)	Project	
Depleted Oil Fields	Carbonate	10-25	1-100	1000-3000	Weyburn- Midale	
Depleted Gas Fields	Sandstone	15-30	10-500	1500-4000	Sleipner	
Saline Aquifers	Sandstone	20-40	100-5000	800-3000	Utsira Fromation	
Tight Formations	Shale/Tight Shale	5-15	0.001-1	2000-4000	In Salah	
Volcanic Rocks	Basalt	10-30	1-1000	1000-2500	CarbFix	

Table 2. Summary of typical reservoir rock properties observed in major CO2 storage formations [14]

Permeability shows much greater variability than porosity, spanning several orders of magnitude even within individual formations. Horizontal permeabilities in storage formations typically range from less than 1 mD in tight formations to several thousand millidarcies in highly permeable rocks. Vertical permeability is generally lower than horizontal permeability due to depositional layering and compaction effects, with anisotropy ratios (kh/kv) commonly ranging from 2-100, as shown in the project analysis detailed in Section 3.

The anisotropic nature of permeability significantly affects CO₂ migration patterns and plume geometry. High horizontal permeability facilitates lateral CO₂ spreading, which can be beneficial for storage by increasing the contact area with caprocks and formation water. However, preferential flow along high-permeability layers can also lead to early breakthrough at monitoring wells or increased migration distances.

Wettability, Interfacial Tension and Capillary Pressure

Wettability describes the preference of rock surfaces for one fluid over another and fundamentally controls the distribution of CO₂ and water within pore spaces. This property directly affects the displacement efficiency of formation fluids, whether hydrocarbons or brine. Most reservoir rocks are water-wet under initial conditions, meaning that water preferentially occupies smaller pores and coats rock surfaces while CO₂ occupies larger pore spaces as a non-wetting phase [25][36].

The wetting behavior affects capillary pressure relationships, which control the saturation distribution and residual trapping of CO₂. In water-wet systems, CO₂ as the non-wetting phase requires higher pressures to invade smaller pores, leading to preferential occupation of larger pores and higher residual water saturations. This behavior affects both storage capacity and security by influencing the fraction of CO₂ that becomes residually trapped [36][47].

Interfacial tension (IFT) is a key physical property influencing capillary pressure and fluid distribution within the pore network. IFT refers to the force per unit length existing at the interface between two immiscible fluids—in this case, CO₂ and brine. It is a critical factor in determining the capillary entry pressure and governs how easily CO₂ can displace brine within pore spaces. CO₂-brine IFT values typically range from 20 to 75 mN/m under reservoir conditions, depending on temperature, pressure, and salinity. At higher pressures and temperatures especially near the CO₂ critical point, the IFT decreases, which can facilitate CO₂ invasion into finer pore spaces. This has a direct impact on the efficiency of pore-scale displacement and affects both residual trapping and migration behavior. Reduction in IFT, while beneficial for enhancing injectivity and increasing contact between CO₂ and the rock matrix, can also reduce capillary entry pressures, potentially increasing the risk of leakage if not properly managed. Conversely, higher IFT values lead to greater capillary barriers, reinforcing CO₂ containment within target formations. Therefore, understanding and accurately measuring interfacial tension under in-situ conditions is crucial for modeling multiphase flow behavior, predicting storage capacity, and assessing the long-term security of geological CO₂ storage [41][47].

Capillary pressure measurements show that CO₂-water systems typically exhibit entry pressures of 0.1-10 kPa in reservoir rocks, depending on pore throat size distribution and wettability. These values are much lower than typical CO₂-oil entry pressures, facilitating CO₂ injection into water-saturated formations. However, the low entry pressures also mean that relatively small pressure gradients can mobilize CO₂, affecting migration and containment assessments [45][65].

The anisotropic nature of reservoir rocks creates directional variations in capillary pressure behavior, with different values measured parallel and perpendicular to bedding planes. These variations can significantly affect CO₂ distribution and trapping, with implications for storage capacity estimation and risk assessment [39][42].

Sealing efficiency of caprock

A critical aspect of safe and effective gas storage, whether for natural gas, hydrogen, or carbon dioxide, is the sealing performance of the caprock. The caprock, typically composed of fine-grained, low-permeability rocks such as shale or anhydrite, acts as a natural hydraulic barrier, preventing the upward migration of fluids from the reservoir. Its integrity is essential to ensure containment over operational and geological timescales. In porous geological formations where two or more immiscible fluid phases coexist, a multiphase flow regime is established, inherently governed by capillary phenomena. The interaction at the interface between the wetting phase—typically brine, which predominantly saturates the sealing (caprock) layers and the non-wetting phase such as gas (CO2) or oil stored within the reservoir results in capillary forces that critically influence fluid displacement dynamics. These capillary forces play a decisive role in determining

the sealing capacity of the rock, specifically its effectiveness in impeding the upward migration of the non-wetting phase [33]

The capillary pressure (Pc) across a single pore throat can be described by the Young-Laplace equation:

$$P_c = P_n - P_w = \frac{2\sigma}{r} cos\theta$$

where:

- σ is the interfacial tension (IFT) between the non wetting phase (hydrocarbon or hydrogen) and wetting phase (typically brine),
- r is the equivalent radius of the pore throat,
- θ is the contact angle, which reflects the wettability of the solid surface.

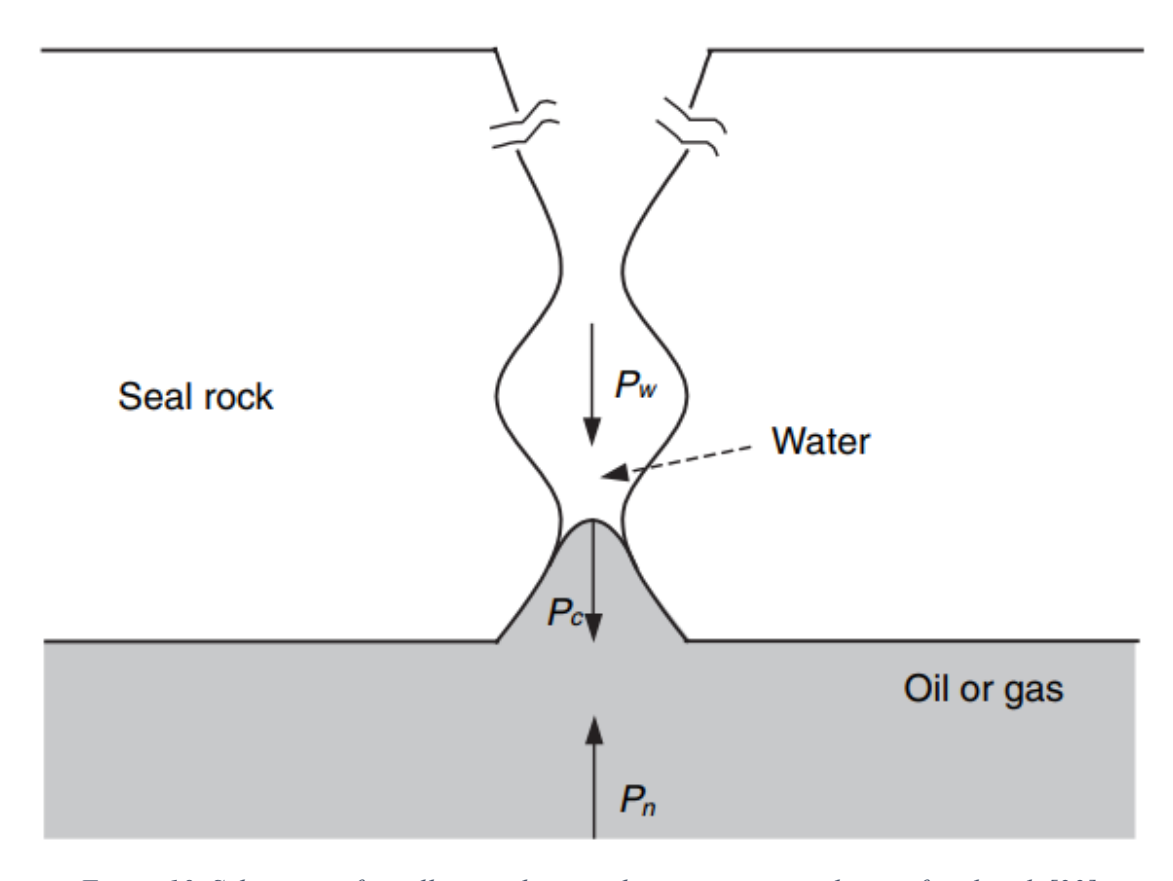


Figure 10. Schematic of capillary sealing mechanism in a pore throat of seal rock [33]

Figure 10. schematically illustrates a pore throat within a seal rock (caprock), displaying a curved interface between the wetting and non-wetting fluid phases. The capillary pressure (Pc) at the meniscus formed within the pore throat represents the pressure differential required to displace the wetting phase with the non-wetting phase.

In this context, Pn refers to the pressure of the non-wetting phase (gas), and Pw represents the pressure of the wetting phase (brine). The capillary pressure (Pc = Pn - Pw) acts as a barrier that inhibits the migration of the non-wetting phase into the seal rock under normal conditions. When the pressure differential (Pn - Pw) exceeds the capillary entry pressure of a given pore throat, the non-wetting phase is able to invade the pore space.

The breakthrough pressure is a fundamental parameter used to quantify the sealing efficiency of caprocks in both natural and engineered subsurface systems. It has widespread applications, including:

- Evaluating seal integrity during hydrocarbon reservoir assessment;
- Conducting basin modeling and hydrocarbon migration studies;
- Assessing the potential for secondary migration in petroleum systems;
- Screening and selecting candidate geological formations for the underground storage of natural gas, hydrogen, CO₂.

Accurate determination of breakthrough pressure is therefore critical for the design and risk assessment of underground storage systems, especially in the context of energy transition technologies such as Carbon Capture, Utilization, and Storage (CCUS).

Geotechnical Reactions and Rock Alteration

The injection of CO₂ into geological formations initiates a complex series of geochemical reactions (Fig. 11) that can alter rock properties and affect long-term storage security. The dissolution of CO₂ in formation water creates an acidic environment that can dissolve carbonate minerals and feldspars while potentially precipitating other minerals such as clays and carbonates.

Mineral dissolution reactions can increase porosity and permeability by removing cementing materials, but they can also weaken rock mechanical properties and potentially compromise seal integrity. The rate and extent of dissolution depend on the mineralogical composition, surface area, temperature, and residence time of acidified water.

Precipitation reactions can reduce porosity and permeability by forming new minerals in pore spaces. Clay mineral precipitation is particularly significant because of the large volume changes associated with hydration and the potential for pore plugging. However, carbonate precipitation through mineral trapping reactions provides beneficial long-term storage security by permanently fixing CO₂ in solid form.

The geochemical evolution of CO₂ storage systems must be evaluated using reactive transport modeling that couples fluid flow, chemical reactions, and rock property changes. These models require extensive input data including mineral compositions, reaction kinetics, and thermodynamic properties, but they provide essential insights into long-term storage behavior and security.

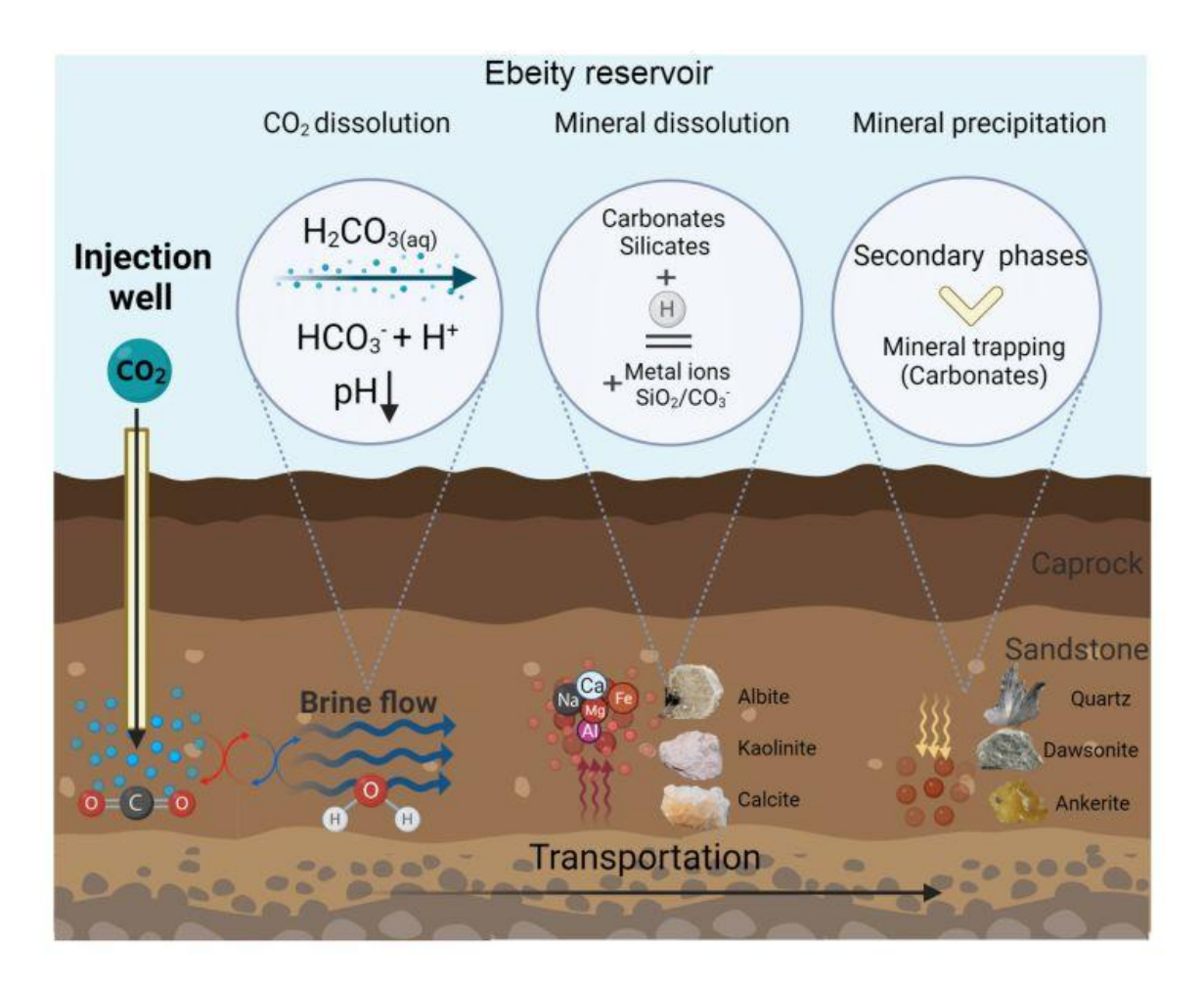


Figure 11. CO₂—Brine—Mineral Interactions in Ebeity Sandstone—Caprock [55]

Impact of Well Construction and Design

The design of the injection well is as critical as plume-control techniques for effective CO₂ storage. Well architecture can either constrain or greatly enhance reservoir performance.

In heterogeneous formations, a single vertical well typically floods high-permeability layers, leaving tighter strata unswept and causing the buoyant CO₂ to override toward the top under gravity. This results in early breakthrough against the caprock, reduced storage efficiency, and elevated fracture risk (Birkholzer et al., 2009; Hovorka et al., 2016).

A salient example is Norway's Snøhvit CCS project, where injection into the Tubåen Formation was suspended after roughly three years and 1.1 Mt of CO₂, as reservoir pressures neared caprock fracture thresholds (Zhang et al., 2012). A subsequent workover recompleted the well in a higher-permeability zone, relieving bottomhole pressures and restoring injectivity.

By contrast, the Sleipner field has sustained stable pressure and uniform plume advance for over two decades via a long-reach, near-horizontal injector. Horizontal or multilateral wells—common in hydrocarbon production (Fig. 12) —expand the well-reservoir contact area, boosting injectivity and enabling target injection rates at lower pressure drawdown (Buscheck & Nitao, 2008; Fang et al., 2014). Simulation studies demonstrate that horizontal injection yields a wider swept volume and more homogeneous saturation than vertical wells, substantially increasing residual trapping and CO₂ dissolution (Buscheck et al., 2011; Jessen et al., 2013).

Furthermore, downhole outflow control devices (OCDs) can be deployed in deviated wells to tailor the injection profile. By throttling flow into high-permeability sections, OCDs divert CO₂ into lower-permeability zones, evening out along-borehole distribution, minimizing local overpressure, and reducing the risk of caprock breach (He et al., 2015; Kulkarni et al., 2006).

Field experience at Sleipner and Snøhvit, coupled with numerous modeling studies, clearly indicates that moving from simple vertical completions to engineered horizontal or multilateral configurations—with integrated flow-control technologies—markedly improves CO₂ injectivity, optimizes plume geometry, and mitigates the early-pressure limitations inherent to geological storage (Birkholzer et al., 2013; Hovorka et al., 2016).

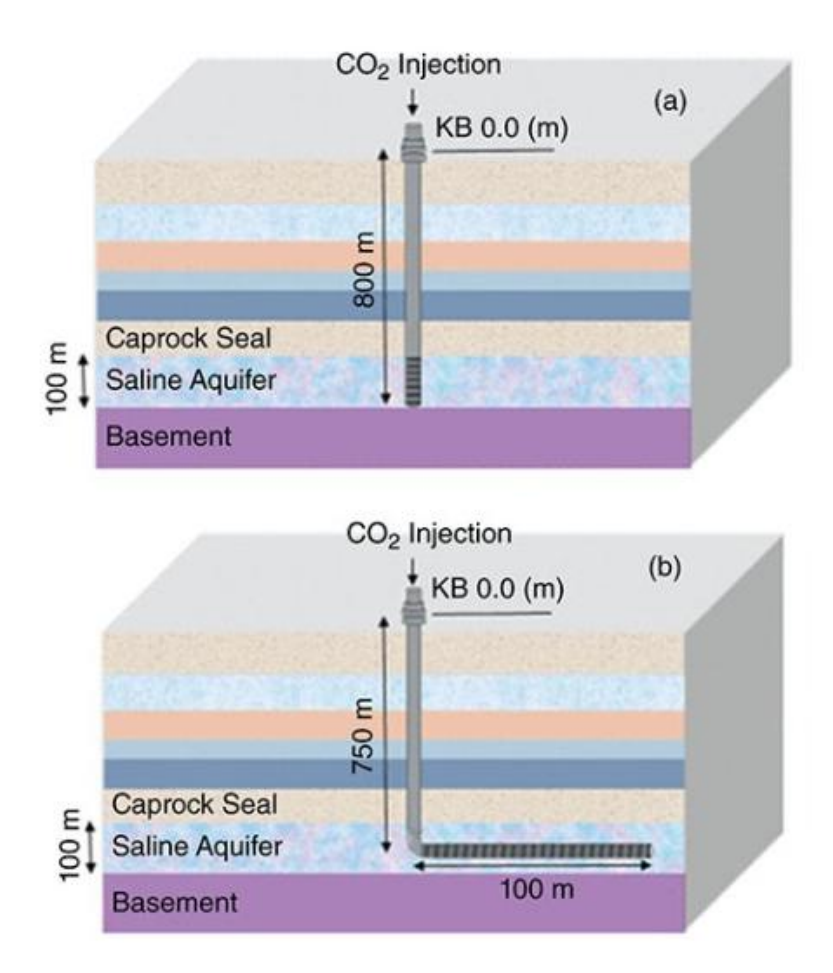


Figure 12. A comparison between well orientation (a) vertical well (b) horizontal well [56]

In summary, as geological CO₂ storage moves toward gigaton-scale deployment, advanced reservoir management becomes indispensable. Composition-, temperature- and pressure-swing injection techniques provide operators with dynamic levers to direct plume migration, enhance areal sweep and curb gravitational segregation (Nazarian et al., 2014; Kulkarni et al., 2006). Concurrently, engineered well architectures—long-reach horizontal and multilateral completions equipped with downhole flow-control devices—substantially increase injectivity, optimize plume uniformity and mitigate overpressure risks (Buscheck & Nitao, 2008; He et al., 2015). These strategies exemplify how petroleum-industry know-how can be repurposed for secure CO₂ storage. Yet, to transition from conceptual frameworks to large-scale impact, a concerted expansion of pilot and field-scale trials is required. Achieving the ambition of sequestering billions of tonnes of CO₂ will demand reservoir management approaches that are as intelligent, adaptive and data-driven as the capture technologies themselves (IEAGHG, 2010).

3. Global Overview of CO₂ Storage Projects

The global landscape of underground CO₂ storage encompasses a diverse range of projects at various stages of development, from pilot-scale demonstrations to commercial operations. In this chapter we will thoroughly study 20 significant CO₂ storage projects worldwide, evaluating their geological characteristics, operational parameters, and performance metrics to identify the "key success factors" contributing to their success and the insights gained from them.

Depending on the operational status and scale, CO₂ storage projects can be classified into several categories:

- operational commercial projects,
- completed demonstration projects,
- projects under development, and
- cancelled or suspended projects.

Each category provides valuable insights into different aspects of storage implementation, including technical feasibility, economic viability and regulatory frameworks.

Table 3 presents a detailed comparison of 20 major CO₂ storage projects worldwide analyzed in this study, highlighting their key technical parameters and operational characteristics. This data serves as the foundation for identifying key success factors and best practices for geological storage of CO₂.

Figure 13 illustrates the global distribution of these major and all global storage projects, highlighting regional differences in geological suitability and deployment strategies.

Figure 14 shows Annual Injection Capacity of Global CO2 Storage Projects.

Operational projects represent the most mature segment, with facilities like Sleipner, Weyburn-Midale, and Gorgon demonstrating long-term storage at commercial scale. These projects have decades of operational experience, providing valuable insights into subsurface CO₂ behavior, storage mechanisms, and monitoring techniques. Their successful operations have played an important role in proving that geological storage of CO₂ is a viable option for climate change mitigation.

Small-scale demonstration projects that have been completed helped us to learn more and get insights about CO2 storage. Projects like In Salah, Ketzin, and Tomakomai have provided valuable data on different geological settings and operational techniques, advancing the technical knowledge and helping to design future projects.

Table 3. Comprehensive Comparison of Major CO2 Storage Projects

Project Name	Country	Formation Type	Primary Storage Formation	Lithology	Age	Primary Minerals	Clay Content (%)	Carbonate Content (%)	Top of Formation (m)	Formation Thickness (m)	Injection Depth (m)	Pore Volume (km³)
Sleipner	Norway	Saline Aquifer	Utsira Sand	Sandstone	Pliocene	Quartz, Feldspar	8	2	800	50-300	800-900	450
Snøhvit	Norway	Saline Aquifer	Tubåen Formation	Sandstone	Jurassic	Quartz, Feldspar	12	5	2400	15-100	2600	15
Weyburn- Midale	Canada	Enhanced Oil Recovery	Midale Formation	Carbonate	Mississippian	Calcite, Dolomite	5	85	1400	25	1450-1500	2.5
Quest	Canada	Saline Aquifer	Basal Cambrian Sands	Sandstone	Cambrian	Quartz, Feldspar	15	8	1950	125	2000-2200	25
Boundary Dam	Canada	Saline Aquifer	Deadwood Formation	Sandstone	Cambrian	Quartz, Feldspar	18	3	3200	30	3300	55
In Salah	Algeria	Depleted Gas Field	Krechba Formation	Sandstone	Carboniferous	Quartz, Feldspar	10	12	1750	20	1800-1900	8.5
Gorgon	Australia	Saline Aquifer	Dupuy Formation	Sandstone	Jurassic	Quartz, Feldspar	14	6	2200	50-200	2300-2500	95
Otway	Australia	Saline Aquifer	Waarre Formation	Sandstone	Cretaceous	Quartz, Feldspar	16	4	1950	40	2000-2100	12
Cranfield	USA	Enhanced Oil Recovery	Tuscaloosa Formation	Sandstone	Cretaceous	Quartz, Feldspar	12	8	3100	15	3200	48
Illinois Basin- Decatur	USA	Saline Aquifer	Mt. Simon Sandstone	Sandstone	Cambrian	Quartz, Feldspar	20	2	1950	60	2000	125
Frio Brine Pilot	USA	Saline Aquifer	Frio Formation	Sandstone	Oligocene	Quartz, Feldspar	15	5	1476	24	1500	5.8
Petra Nova	USA	Enhanced Oil Recovery	Miocene Formation	Sandstone	Miocene	Quartz, Feldspar	18	7	2200	45	2300	32
CNPC Jilin	China	Enhanced Oil Recovery	Fuyu Formation	Sandstone	Cretaceous	Quartz, Feldspar	22	3	1150	35	1200-1400	4.2
Sinopec Qilu	China	Enhanced Oil Recovery	Shengli Formation	Sandstone	Paleogene	Quartz, Feldspar	19	4	1750	28	1800	5.0
Yanchang CCS	China	Enhanced Oil Recovery	Yanchang Formation	Sandstone	Triassic	Quartz, Feldspar	17	6	1550	42	1600	7.1
Nagaoka	Japan	Saline Aquifer	Haizume Formation	Sandstone	Pleistocene	Quartz, Feldspar	25	1	1088	12	1100	0.25
Tomakomai	Japan	Saline Aquifer	Moebetsu Formation	Sandstone	Paleogene	Quartz, Feldspar	23	2	950	18	1000-1200	0.38
Al Reyadah	UAE	Industrial Capture	Arab Formation	Carbonate	Jurassic	Calcite, Anhydrite	3	90	2050	55	2100	6.6
Northern Lights	Norway	Saline Aquifer	Johansen Formation	Sandstone	Jurassic	Quartz, Feldspar	13	5	2400	150	2500-3100	125
Porthos	Netherlands	Saline Aquifer	Bunter Sandstone	Sandstone	Triassic	Quartz, Feldspar	16	4	2900	200	3000-4000	320

Table 4. Comprehensive Comparison of Major CO2 Storage Projects (Continued)

Project Name	Country	Average Porosity (%)	Porosity Range (%)	Average Permeability (mD)	Horizontal Permeability (mD)	Vertical Permeability (mD)	Permeability Anisotropy (kh/kv)	Caprock Lithology	Caprock Thickness (m)	Caprock Permeability (mD)	Entry Pressure (MPa)
Sleipner	Norway	37	35-40	4000	1000-8000	800-6000	1.2	Shale	100-150	0.001	2.5
Snøhvit	Norway	17	15-19	750	100-1000	50-500	2.0	Shale	50-80	0.0005	3.2
Weyburn- Midale	Canada	18	7-25	150	1-300	0.5-25	3.0	Anhydrite/Shale	15-25	0.0001	4.5
Quest	Canada	15	11-19	500	20-500	20-200	5.0	Salt/Shale	150-200	0.00001	8.0
Boundary Dam	Canada	20	10-30	25	1-25	2-30	5.0	Shale	30-50	0.001	2.8
In Salah	Algeria	15	15	10	10	0.2-2	5.0	Shale	20-40	0.0005	3.5
Gorgon	Australia	15	10-20	50	50	2-10	5.0	Shale	40-80	0.001	2.2
Otway	Australia	22	20-25	2000	2000	20-500	5.0	Mudstone	25-45	0.002	1.8
Cranfield	USA	26	25-27	2700	2400-2900	10-500	5.0	Shale	10-20	0.001	2.0
Illinois Basin- Decatur	USA	21	20-22	200	20-200	4-40	5.0	Shale	80-120	0.0005	3.8
Frio Brine Pilot	USA	31	28-34	1250	1000-2500	100-500	5.0	Shale	15-25	0.002	1.5
Petra Nova	USA	20	15-25	150	50-500	10-100	5.0	Shale	20-35	0.001	2.3
CNPC Jilin	China	12	11-13	20	5-50	1-10	5.0	Mudstone	12-20	0.003	1.2
Sinopec Qilu	China	13	12-15	35	10-80	2-16	5.0	Shale	18-30	0.002	1.6
Yanchang CCS	China	10	8-13	25	8-60	1.6-12	5.0	Mudstone	15-25	0.002	1.4
Nagaoka	Japan	23	23	10	2-20	0.4-4	5.0	Mudstone	8-15	0.005	0.8
Tomakomai	Japan	19	16-22	15	5-30	1-6	5.0	Mudstone	10-18	0.004	1.0
Al Reyadah	UAE	10	15-25	60	10-100	0.4-20	5.0	Anhydrite	25-40	0.0001	5.2
Northern Lights	Norway	23	20-25	800	100-1000	40-200	5.0	Shale	80-120	0.0008	3.0
Porthos	Netherlands	13	13	254	254	6-60	5.0	Shale	100-150	0.0005	3.5

Table 5. Comprehensive Comparison of Major CO2 Storage Projects (Continued)

Project Name	Country	Salinity (mg/L TDS)	pН	Water Saturation (%)	Contact Angle (°)	Wettability Index	Reservoir Temperature (°C)	Geothermal Gradient (°C/km)	Initial Reservoir Pressure (MPa)	Pressure Gradient (MPa/km)	Fracture Pressure (MPa)	Rock Compressibility (1/MPa)	Maximum Pressure Increase (MPa)	Surface Uplift (mm)
Sleipner	Norway	35000	7.8	75	25	0.8	37	35	8.0	10.0	12.5	4.5E-04	4.5	0
Snøhvit	Norway	45000	7.5	80	30	0.7	98	32	26.5	10.2	35.8	3.8E-04	9.3	0
Weyburn- Midale	Canada	180000	7.2	45	55	0.3	55	25	14.5	10.0	20.2	5.2E-04	6.0	0
Quest	Canada	15000	8.1	78	28	0.8	75	30	20.0	10.0	28.5	4.2E-04	8.5	0
Boundary Dam	Canada	250000	7.0	55	50	0.4	105	28	33.0	10.0	45.0	4.0E-04	12.0	0
In Salah	Algeria	85000	7.3	40	45	0.5	90	35	18.0	10.0	26.5	3.5E-04	8.5	15
Gorgon	Australia	120000	7.4	65	35	0.6	85	32	23.0	10.0	32.8	3.8E-04	9.8	0
Otway	Australia	95000	7.6	72	32	0.7	68	30	20.0	10.0	28.0	4.5E-04	8.0	0
Cranfield	USA	200000	6.8	55	48	0.4	120	35	32.0	10.0	44.5	3.2E-04	12.5	0
Illinois Basin- Decatur	USA	125000	7.5	70	35	0.6	60	25	20.0	10.0	28.0	4.8E-04	8.0	0
Frio Brine Pilot	USA	85000	7.8	80	25	0.8	58	35	15.0	10.0	21.8	5.2E-04	6.8	0
Petra Nova	USA	150000	7.2	62	42	0.5	78	30	23.0	10.0	32.0	3.8E-04	9.0	0
CNPC Jilin	China	35000	7.9	68	30	0.7	48	28	13.0	10.0	19.5	6.2E-04	6.5	0
Sinopec Qilu	China	55000	7.6	65	35	0.6	65	32	18.0	10.0	26.0	5.8E-04	8.0	0
Yanchang CCS	China	45000	7.7	70	32	0.7	55	30	16.0	10.0	23.5	5.5E-04	7.5	0
Nagaoka	Japan	15000	8.2	85	22	0.9	45	35	11.0	10.0	16.8	8.5E-04	5.8	0
Tomakomai	Japan	18000	8.0	82	24	0.8	42	35	10.5	10.0	16.2	7.8E-04	6.2	0
Al Reyadah	UAE	220000	6.9	48	52	0.3	82	35	21.0	10.0	30.5	4.8E-04	9.5	0
Northern Lights	Norway	55000	7.6	72	33	0.7	88	30	26.0	10.0	38.5	3.5E-04	12.5	0
Porthos	Netherlands	180000	7.1	58	46	0.4	110	30	35.0	10.0	50.0	3.2E-04	15.0	0

Table 6. Comprehensive Comparison of Major CO2 Storage Projects (Continued)

Project Name	Country	Injectio n Rate (Mt/yea r)	Injection Strategy	Injection Well Type	Numbe r of Injectio n Wells	Total Injecte d (Mt)	Estimat ed Storage Capacit y (Mt)	Storage Efficien cy (%)	Structur al Trappin g (%)	Residu al Trappi ng (%)	Solubili ty Trappin g (%)	Minera l Trappi ng (%)	Seismic Monitoring	Well Monitoring	Geochemic al Monitorin g
Sleipner	Norway	1.0	Continuous	Vertical	1	23	600000	4-8	60	25	10	5	4D Seismic	Pressure/Temperat ure	Water Sampling
Snøhvit	Norway	0.7	Continuous	Vertical	2	10.7	23000	5-10	70	20	8	2	4D Seismic	Pressure/Temperat ure	Water Sampling
Weyburn- Midale	Canada	2.8	Cyclic	Horizontal/Verti cal	127	40	30000	15-25	80	15	3	2	4D Seismic	Comprehensive	Extensive
Quest	Canada	1.0	Continuous	Vertical	3	9.5	27000	6-12	65	22	10	3	4D Seismic	Pressure/Temperat ure	Water Sampling
Boundary Dam	Canada	1.0	Continuous	Vertical	1	6.6	40000	5-8	55	28	12	5	Baseline	Pressure/Temperat ure	Limited
In Salah	Algeria	1.2	Continuous	Horizontal	3	3.8	17000	8-12	75	18	5	2	InSAR/Microseis mic	Pressure/Temperat ure	Water Sampling
Gorgon	Australia	3.4	Continuous	Vertical	9	11	120000	8-15	68	20	8	4	4D Seismic	Pressure/Temperat ure	Water Sampling
Otway	Australia	0.065	Pilot	Vertical	1	0.095	15000	3-6	62	25	12	3	4D Seismic	Comprehensive	Extensive
Cranfield	USA	1.4	Continuous	Vertical	23	5	125000	10-20	72	20	6	2	4D Seismic	Pressure/Temperat ure	Water Sampling
Illinois Basin- Decatur	USA	1.0	Continuous	Vertical	1	3.4	75000	4-8	58	28	12	2	4D Seismic	Pressure/Temperat ure	Water Sampling
Frio Brine Pilot	USA	0.003	Pilot	Vertical	1	0.0016	6000	3-5	60	30	15	1	None	Comprehensive	Extensive
Petra Nova	USA	1.4	Continuous	Vertical	90	3.9	35000	8-12	65	22	8	5	Limited	Pressure/Temperat ure	Water Sampling
CNPC Jilin	China	0.6	Continuous	Horizontal	5	3.2	8000	12-18	55	30	12	3	Limited	Pressure/Temperat ure	Limited
Sinopec Qilu	China	0.4	Continuous	Vertical	73	3	12000	10-15	58	28	10	4	Limited	Pressure/Temperat ure	Limited
Yanchang CCS	China	0.41	Continuous	Vertical	20	1.5	15000	8-14	62	26	9	3	Limited	Pressure/Temperat ure	Limited
Nagaoka	Japan	0.02	Pilot	Vertical	1	0.0104	300	2-4	45	35	18	2	None	Comprehensive	Extensive
Tomakom ai	Japan	0.1	Demonstrati on	Vertical	2	0.3	600	3-5	48	32	16	2	4D Seismic	Comprehensive	Extensive
Al Reyadah	UAE	0.8	Continuous	Vertical	5	7.2	22000	6-10	85	12	2	1	Limited	Pressure/Temperat ure	Limited
Northern Lights	Norway	1.5	Under Constructio n	Vertical	1	0.001	80000	8-12	68	24	6	2	Planned 4D	Planned	Planned
Porthos	Netherlan ds	2.5	Planned	Vertical	8	0	150000	6-10	62	26	8	4	Planned 4D	Planned	Planned

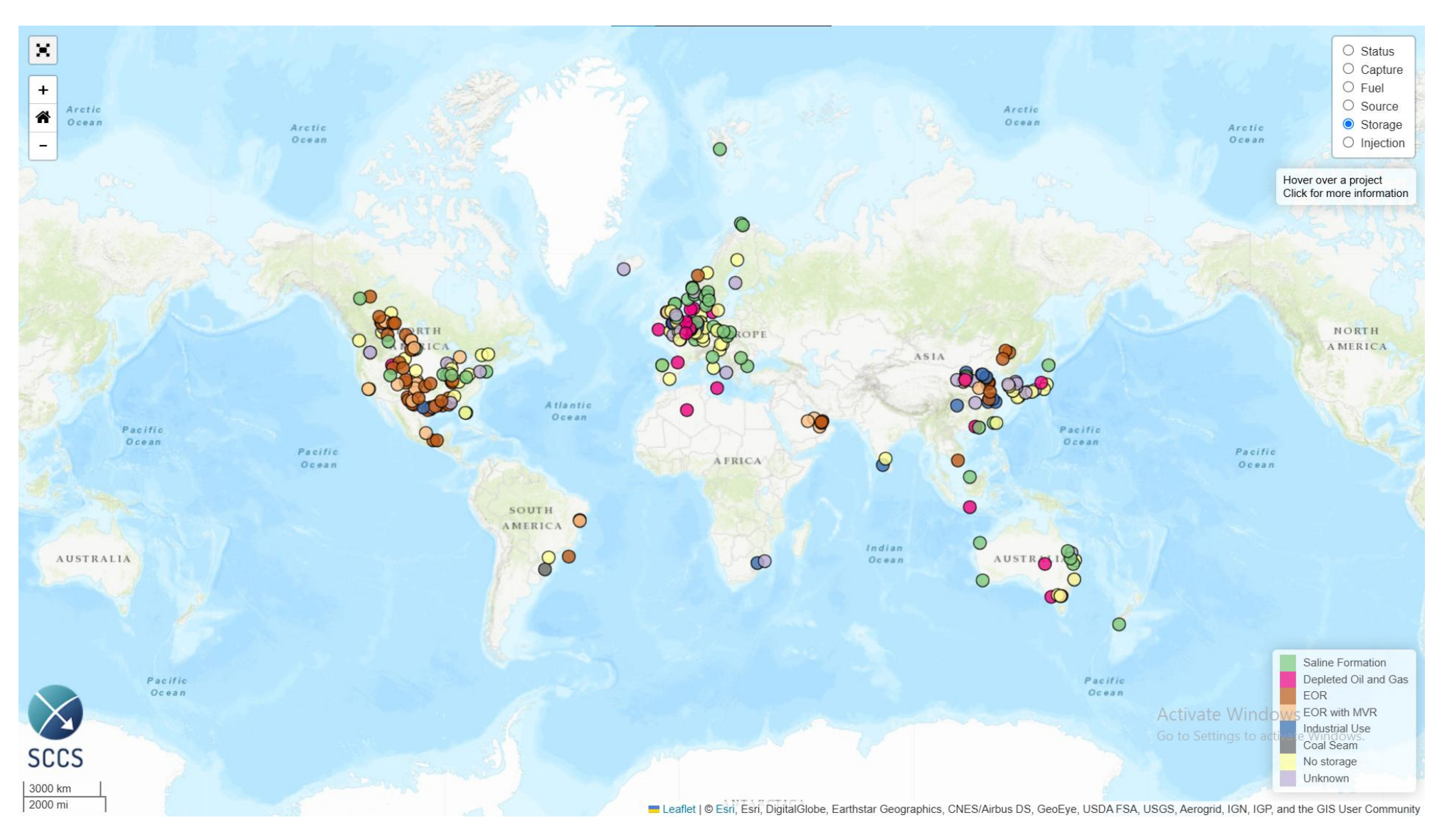


Figure 13. Global CCS Map, Storage Projects Map for 2023 (credits to Scottish Carbon Capture & Storage http://sccs.org.uk/resources/global-ccs-map)

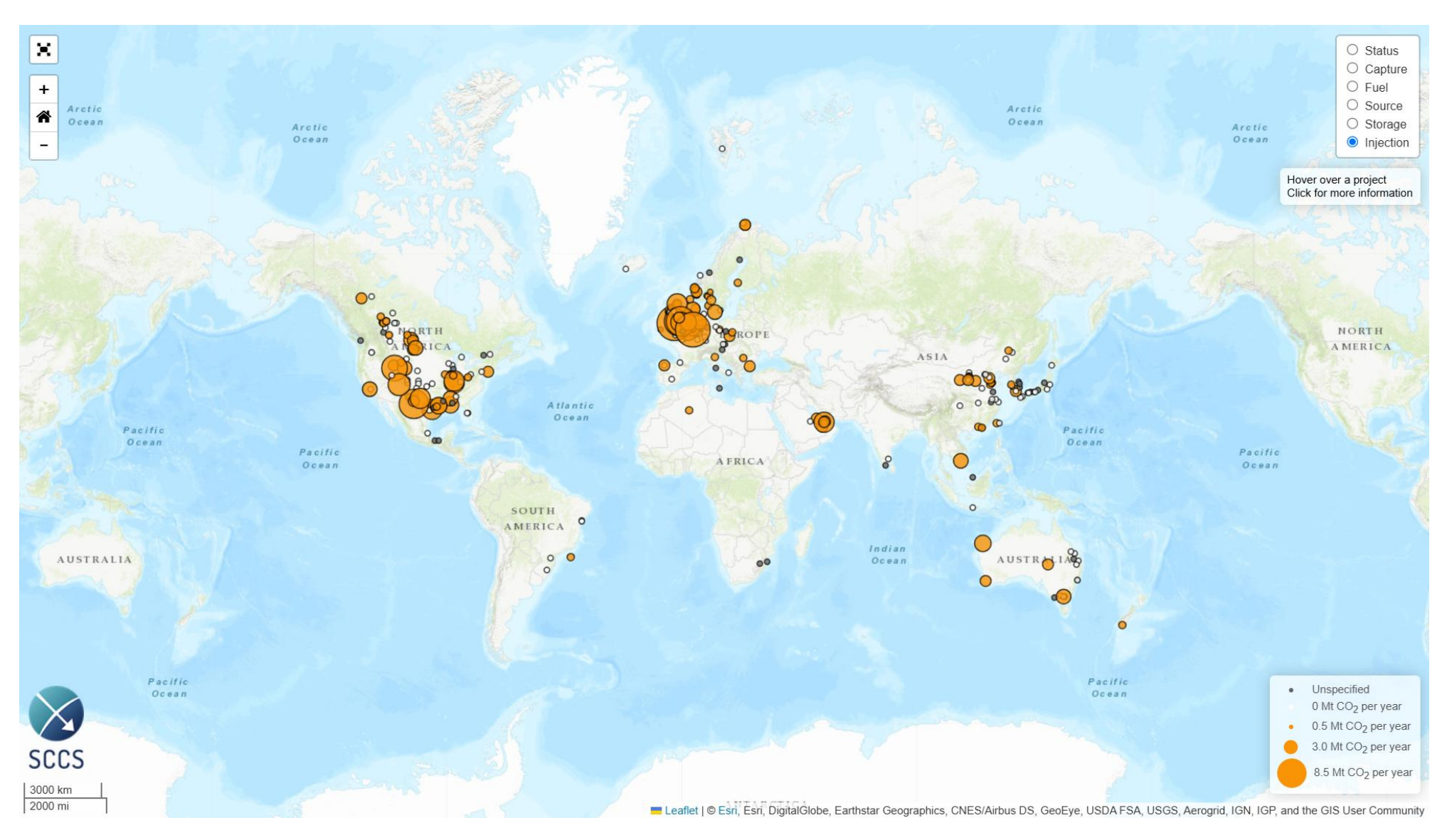


Figure 14. Global CCS Map, Injection Projects Map for 2023 (credits to Scottish Carbon Capture & Storage http://sccs.org.uk/resources/global-ccs-map)

3.1 Technical Review of Existing CO₂ Storage Projects

Based on the analysis of 20 advanced CO2 projects worldwide, it's clear that saline aquifers are the preferred choice, making up 60% of the projects studied (Fig. 15). This trend highlights fundamental technical advantages that reservoir engineers consider as critical for large-scale carbon storage implementation. Major saline aquifer projects such as Sleipner, Quest, Gorgon, and Northern Lights demonstrate large potential storage capacity (or storage volume), with theoretical maximum capacities ranging from 15,000 Mt at Otway to over 600,000 Mt at Sleipner. The widespread geographical distribution of deep saline formations provides strategic advantages by allowing CO2 to be stored closer to its industrial emission sources. This reduces cost of logistics and transportation of CO2 and increases storage safety through reliable geological trapping mechanisms.

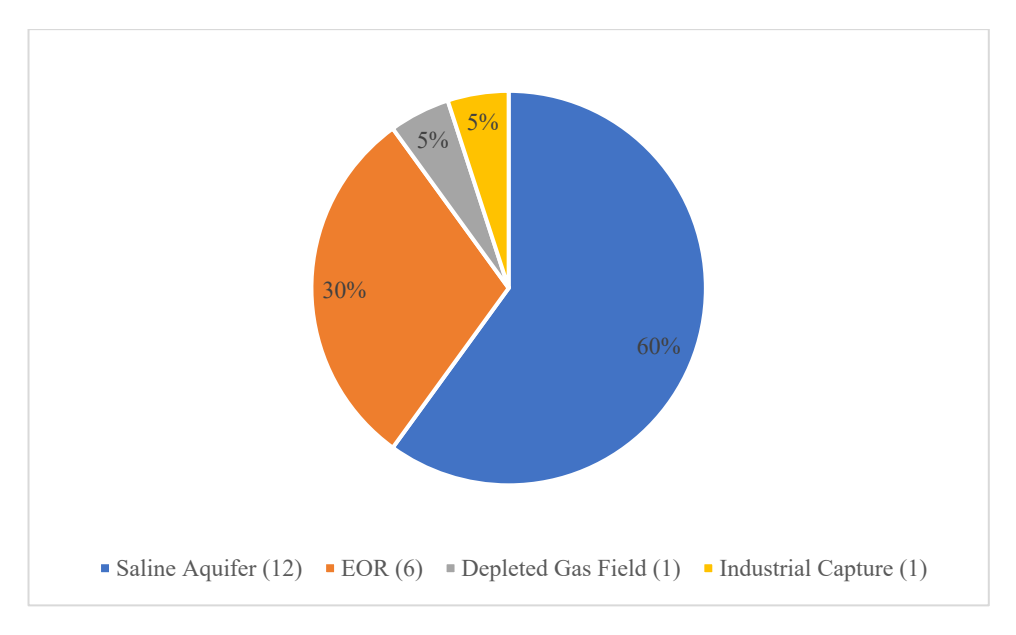


Figure 15. Formation Type

Enhanced oil recovery (EOR) applications accounts for about 35% of current storage operations, as it allows to use existing infrastructure and reservoir characterization data to reduce development risks and accelerate project deployment. For example, the Weyburn-Midale project, which has been in operation in mature carbonate reservoirs since 2000, with more than 200 injection wells and over 38 Mt of cumulative CO2 storage capacity. EOR projects are attractive and economically feasible, because they produce additional oil production, which helps to cover storage costs while also proving that CO2 can remain safely trapped in formations that have already retained hydrocarbons for millions of years. In China many projects including CNPC Jilin, Sinopec Qilu, and Yanchang CCS represent significant EOR developments with combined storage capacity exceeding 35,000 Mt and injection rates around 1.41 Mt/year.

Depleted hydrocarbon reservoir storage, represented primarily by the In Salah project, constitutes 5% of current operations but provides important technical advantages including comprehensive geological characterization, existing infrastructure, and proven containment integrity. The experience in In Salah has demonstrated both opportunities and challenges associated with depleted hydrocarbon reservoir storage, as injection of CO2 causes pressure build-up that results in detectable surface uplift requiring adjustment of operational pressure management. Recent trends in 2025 show growing interest in using depleted hydrocarbon reservoir for CO2 storage,

particularly offshore applications where existing platform infrastructure provides cost-effective development opportunities for large-scale storage implementation.

3.2 Reservoir Formation Petrophysical Properties

Lithology

Sandstone formations make up the majority of global CO₂ storage projects, accounting for 85% of operational projects due to their favorable combination of porosity, permeability, and geochemical stability characteristics. Typical sandstone reservoirs demonstrate porosity values ranging from 16% at CNPC Jilin to 37% at Sleipner, with the majority of formations exhibiting values between 18% and 28%. Studies of depositional formations highlight that fluvial and shallow marine sandstones are well-suited for storage, because they have well-sorted grain sizes between 0.1 and 0.5 millimeters which provides good pore connectivity and permeability. In the case of The Utsira Sand at Sleipner, where Pliocene marine deposits created highly uniform reservoir across an estimated formation volume of 450 km³, making it ideal for CO2 storage.

Quartz-dominated sandstone compositions provide superior long-term stability under CO₂ storage conditions, with quartz content typically ranging from 60% to 85% in optimal storage formations. The Quest project's Basal Cambrian Sands demonstrate excellent quartz content with minimal reactive feldspar, contributing to formation stability during CO₂ injection operations. Arkosic sandstones containing significant feldspar content, such as those at Illinois Basin-Decatur, present increased geochemical reactivity potential requiring careful monitoring of dissolution and secondary mineral precipitation processes that may affect long-term reservoir properties.

Carbonate reservoir, seen in Weyburn-Midale and Al Reyadah projects, account for about 15% of current CO2 storage operations. Carbonate formations pose specific technical challenges due to their complex pore network structure and higher geochemical reactivity compared to sandstones. Carbonates usually exhibit dual-porosity behavior with matrix porosity between 8% to 16% and fracture porosity providing main pathways for fluid movement. The Weyburn field developed in Mississippian carbonate reservoir has demonstrated that CO2 storage in such complex carbonate systems is possible. However, this requires enhanced monitoring requirements and geochemical management protocols to maintain reservoir performance and ensure long-term storage security.

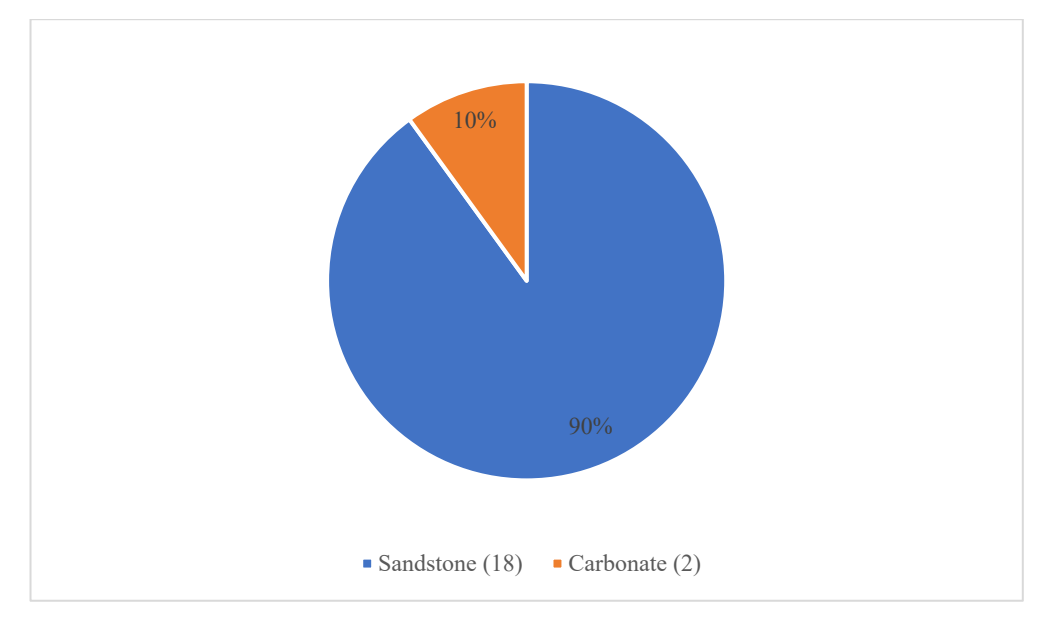
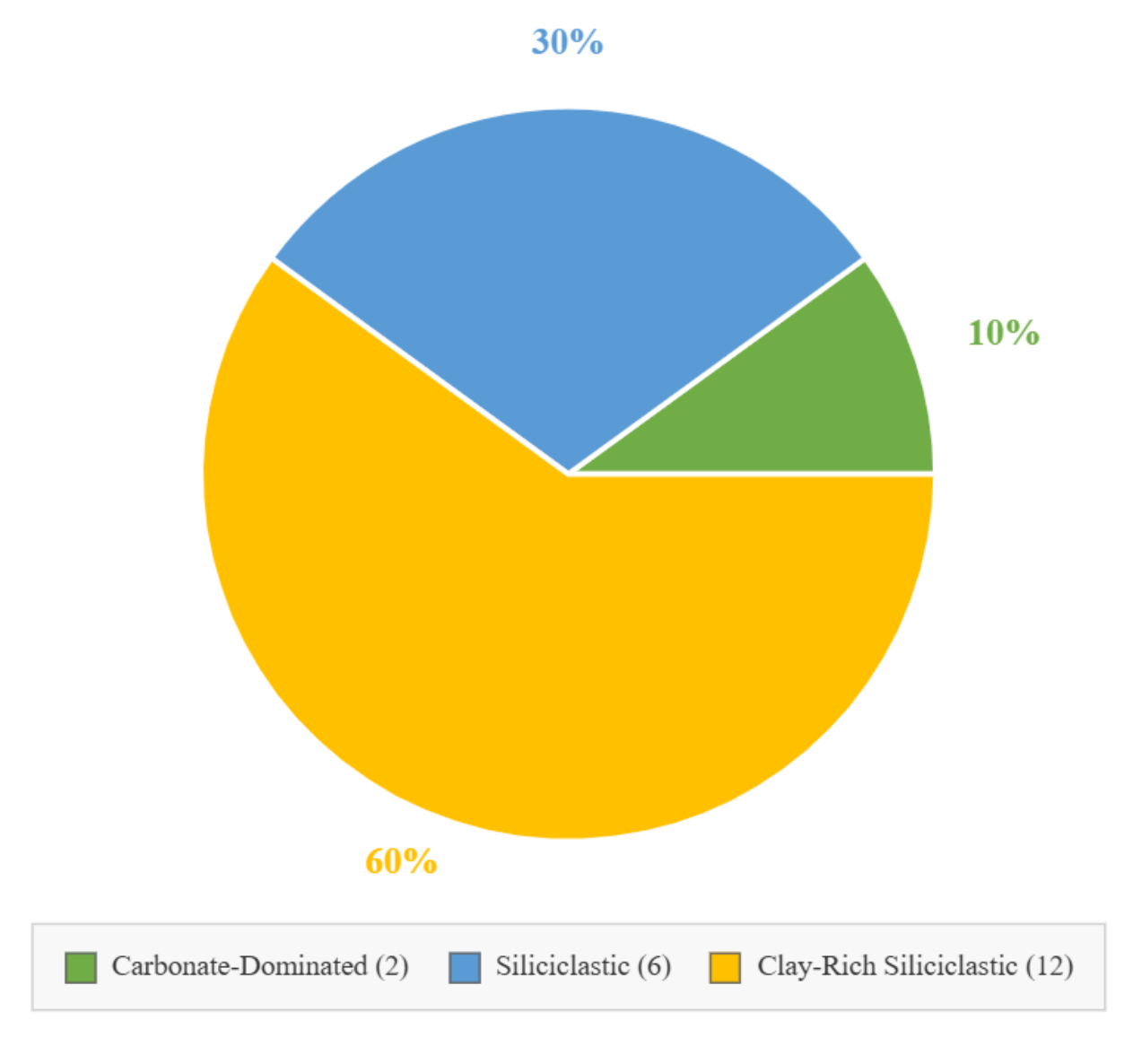


Figure 16. Lithology

Mineralogy

Analysis of the mineral composition in CO2 projects highlights the key relationships between the types of minerals and how CO2 behaves in storage over long periods of time. Reservoir rich in quartz offer excellent chemical stability, with dissolution rates sufficiently slow to maintain reservoir integrity over storage timeframes exceeding 1000 years. The Sleipner project's extensive geochemical monitoring demonstrates minimal quartz dissolution and stable reservoir properties throughout 25+ years of continuous injection operations [9]. Typically these reservoirs contain quartz (60-85%), feldspars (5-25%), and clay minerals (8-25%), with variations reflecting depositional environment and diagenetic history influences on reservoir quality.



Carbonate-Dominated: >50% carbonate content (2 projects, 10%)

Siliciclastic: <15% clay, ≤50% carbonate (6 projects, 30%)

Clay-Rich Siliciclastic: ≥15% clay, ≤50% carbonate (12 projects, 60%)

Classification based on reservoir rock mineralogy for CO₂ storage formations

Figure 17. Brine Salinity Classification for Underground CO₂ Storage Sites

Characterization of clay minerals and their analysis are crucial for predicting possible formation damage and optimizing the chemistry of injection fluid to maintain reservoir performance. In most storage sites, illite and kaolinite are the main clay minerals, exhibiting minimal swelling behavior under CO₂ injection conditions. The Quest project's detailed analysis of clays reveals illite-dominated assemblages with minor kaolinite content, contributing to stable permeability characteristics during CO₂ injection operations. However, when smectite clays are present, they require careful assessment due to potential swelling and permeability impairment effects that may compromise injection performance and storage efficiency.

Carbonate mineral distributions significantly influence geochemical reactivity and storage mechanism evolution, particularly in formations containing calcite, dolomite, and ferroan carbonates. The Weyburn field's complex carbonate mineralogy includes calcite cement, dolomite matrix, and ankerite replacement phases exhibiting different dissolution kinetics under CO₂-saturated conditions. Reactive transport modeling indicates calcite dissolution rates ranging from 10^{-13} to 10^{-11} mol/m²/s depending on temperature and pH conditions, with secondary carbonate precipitation providing potential mineral trapping enhancement over extended storage timeframes.

Porosity

Total porosity measurements from various CO2 storage projects demonstrate remarkable heterogeneity, ranging from 12% in tight carbonate formations at Al Reyadah to 37% in high-quality sandstone aquifers at Sleipner. Statistical analysis indicates average porosity of 21.3% for sandstone formations and 15.5% for carbonate reservoirs, highlighting key differences in pore system development and preservation during diagenesis. In well-sorted sandstone formations effective porosity typically comprises 85% to 95% of total, while carbonate reservoirs may exhibit lower effective porosity ratios due to isolated moldic and vuggy porosity components.

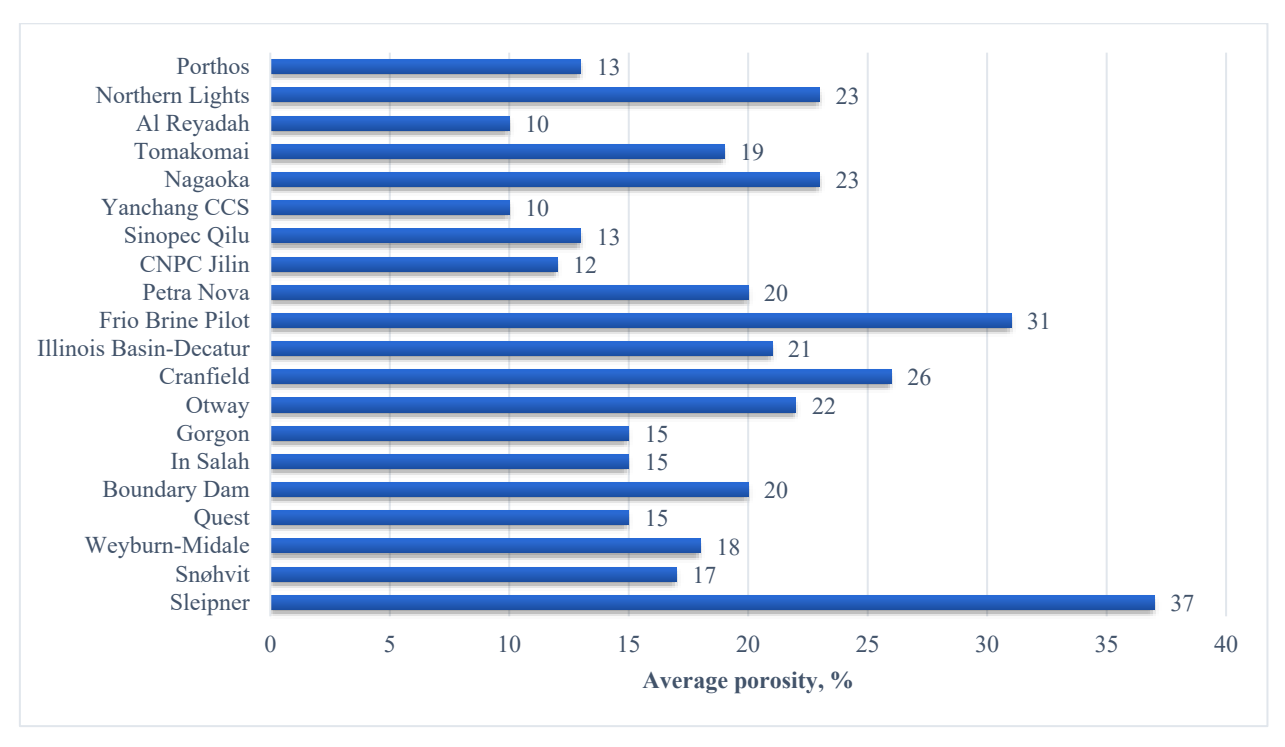


Figure 18. Reservoirs Average Porosities

Variations in porosity distribution (heterogeneity) significantly impact CO₂ plume development (and movement) and storage efficiency by influencing flow patterns and sweep behavior. Vertical porosity variations, commonly observed in deltaic and fluvial systems, create preferential flow

pathways that influence injection pressure requirements and storage capacity utilization. The Quest project demonstrates significant porosity layering with high-porosity flow units separated by lower-porosity barriers affecting vertical flow communication and requiring optimized completion strategies to maximize storage efficiency.

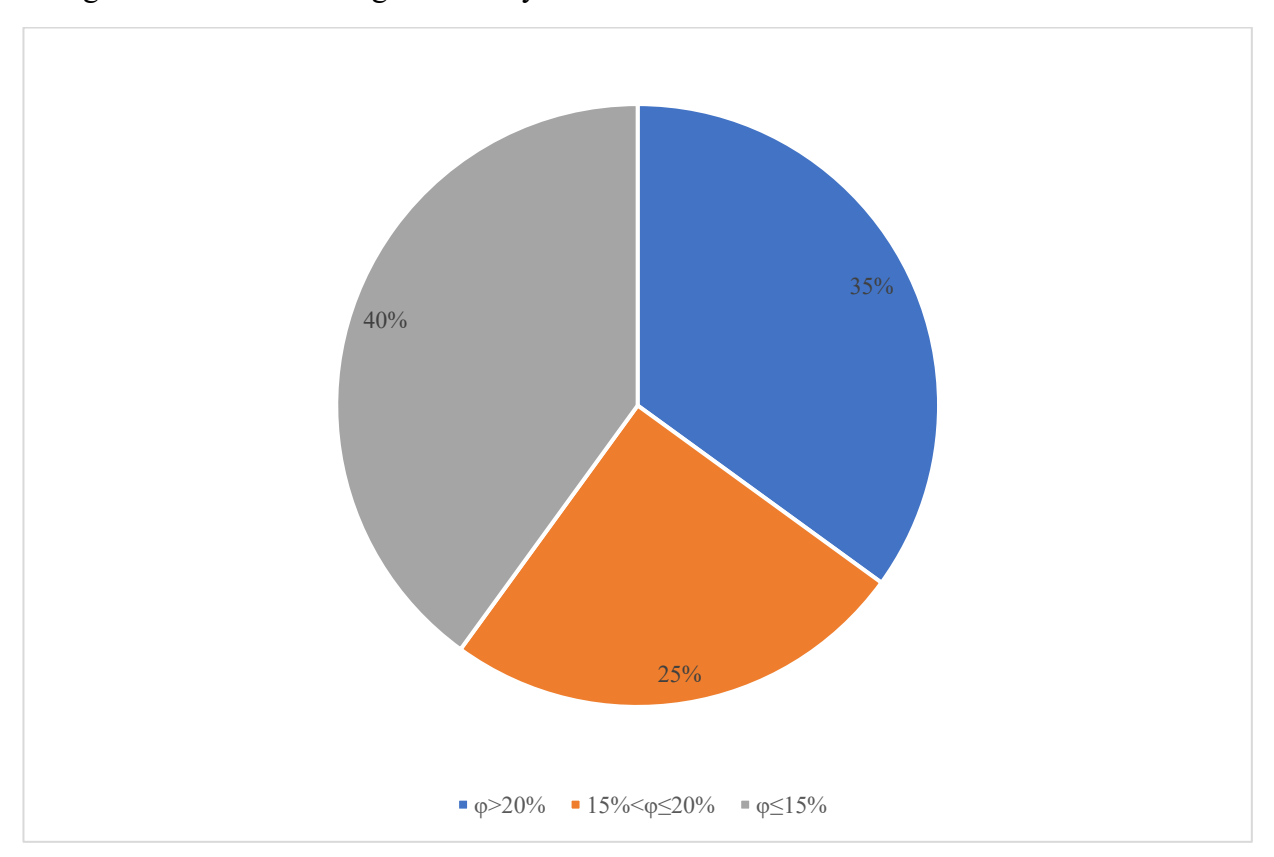


Figure 19. Porosity Classification for Underground CO₂ Storage Sites

Sleipner (Utsira Sand) and Illinois Basin-Decatur formations consist of sandstone with relatively high porosity, which supports good injectivity and storage capacity, while Weyburn-Midale and In Salah formations consist of carbonate with heterogeneous porosity, where secondary vugs and fractures locally enhance storage, but creates more complex flow behavior that must be carefully modelled.

Understanding of stress-dependent porosity behavior is crucial for deep storage formations, where effective stress conditions exceed 30 MPa. Laboratory measurements show that porosity can decrease by 1% to 3% for every 10 MPa increase in confining pressure, depending on rock fabric and cementation characteristics. The Porthos project's ultra-deep storage formations at 3000-4000 meters require careful consideration of stress-dependent porosity changes, affecting both storage capacity assessments and injection performance predictions throughout the project lifecycle.

Permeability

Horizontal permeability in CO2 storage projects varies widely spanning four orders of magnitude from 5 mD at CNPC Jilin to 4000 mD at Sleipner (Fig. 18). This dramatic range reflects fundamental differences in depositional environment, diagenetic modification, and structural alteration that directly control injection performance and economic viability. High-permeability formations enable sustainable injection rates above 1 Mt/year with minimal pressure buildup, while low-permeability formations require enhanced completion technologies and optimized injection strategies to achieve target storage rates.

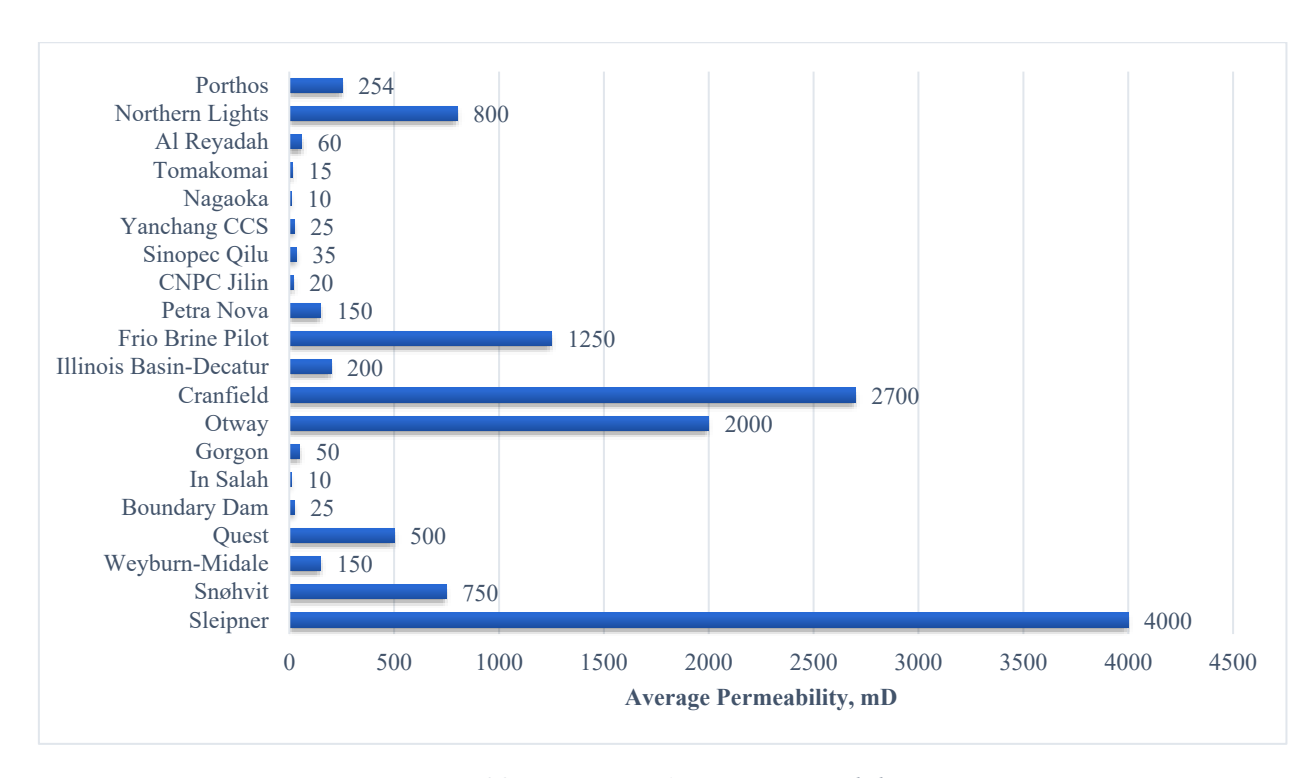


Figure 20. Reservoirs Average Permeabilities

Analysis of permeability anisotropy shows vertical-to-horizontal permeability ratios typically ranging from 0.2 to 0.8, with lower ratios indicating greater flow anisotropy that creates laterally extensive but vertically restricted CO₂ plumes. The Sleipner project's detailed permeability characterization demonstrates complex anisotropy patterns controlled by thin shale interbeds creating multiple storage compartments within the overall formation. Horizontal wells become particularly attractive for highly anisotropic formations, providing enhanced injection performance through increased contact area with high-permeability flow zones.

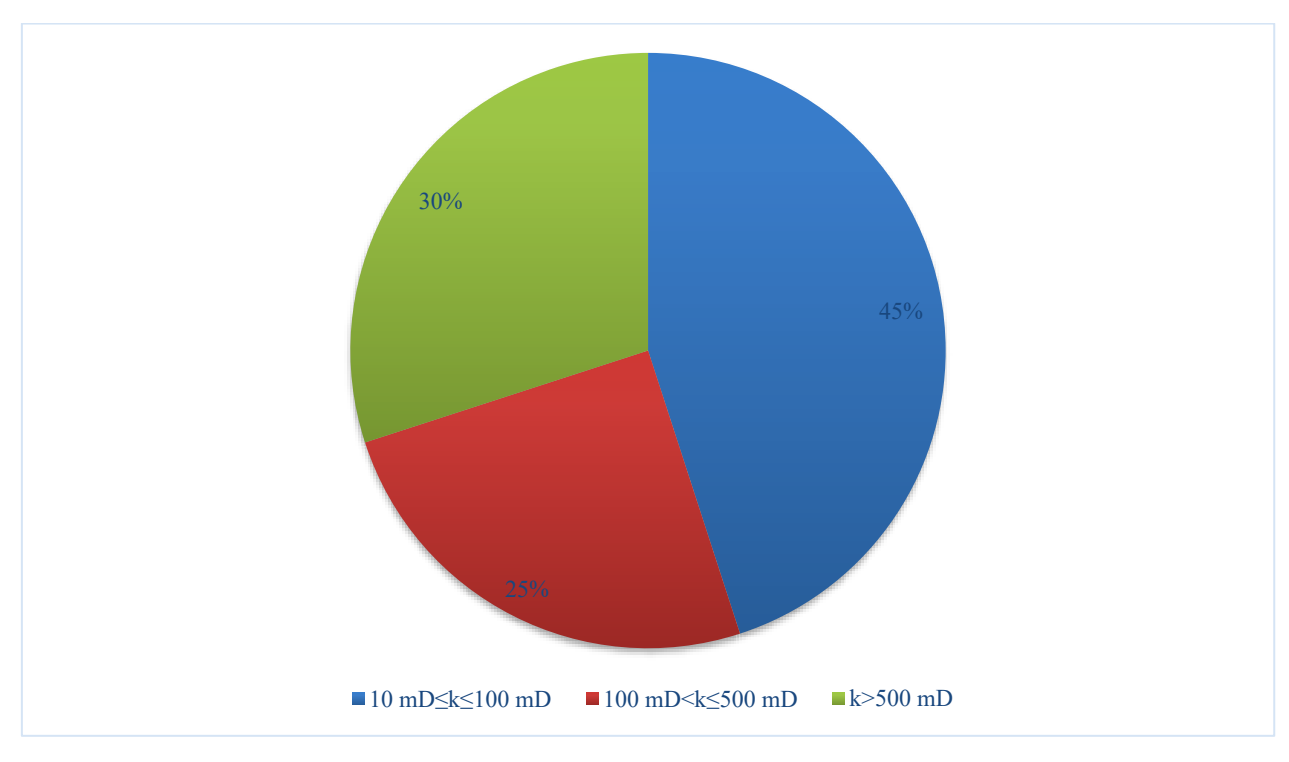


Figure 21. Permeability Classification for Underground CO2 Storage Sites

Stress-dependent permeability effects are crucial for deep storage operations, where pressure changes from injection can significantly affect flow properties. Laboratory core analysis shows permeability reductions of 10% to 40% for every 10 MPa increase confining pressure, with tighter formations exhibiting greater stress sensitivity. The Boundary Dam project's deep injection operations require careful pressure control and management to ensure consistent injection performance and prevent significant permeability impairment that could compromise long-term storage capacity utilization.

Geomechanical Properties

Comprehensive geomechanical characterization of CO2 storage projects reveals critical parameters controlling injection safety and operational pressure limits. Young's modulus values range from 8 GPa in poorly consolidated sandstones to 45 GPa in well-cemented carbonate formations, directly influencing formation deformation response and fracture pressure calculations. The Weyburn field's carbonate reservoirs demonstrate high mechanical strength with Young's modulus values of 25-35 GPa, enabling higher injection pressures while maintaining formation integrity throughout enhanced oil recovery (EOR) operations.

Fracture pressure gradients represent ultimate operational constraints, typically ranging from 0.65 psi/ft in normal pressure regimes to 0.90 psi/ft in overpressured formations depending on regional stress conditions and formation mechanical properties. Conservative operational practices maintain injection pressures at 80-90% of calculated fracture pressure to ensure adequate safety margins while maximizing injection rates. The In Salah project's operational experience demonstrates the importance of real-time geomechanical monitoring, where surface uplift measurements exceeding 15 mm indicated approaching mechanical integrity limits requiring injection pressure reductions.

Measurements of rock compressibility provide essential input for reservoir simulation and pressure prediction, with values ranging from 3.2×10^{-4} to 8.5×10^{-4} MPa⁻¹ depending on lithology and porosity of the formation. Higher compressibility formations accommodate pressure increases more readily but may experience greater porosity and permeability reduction during injection operations. Surface uplift monitoring in various projects shows acceptable deformation levels below 5 mm for most storage operations, while formations with compressibility exceeding 6×10^{-4} MPa⁻¹ require enhanced monitoring protocols to ensure operational safety and public acceptance.

3.3 Reservoir Physical Conditions

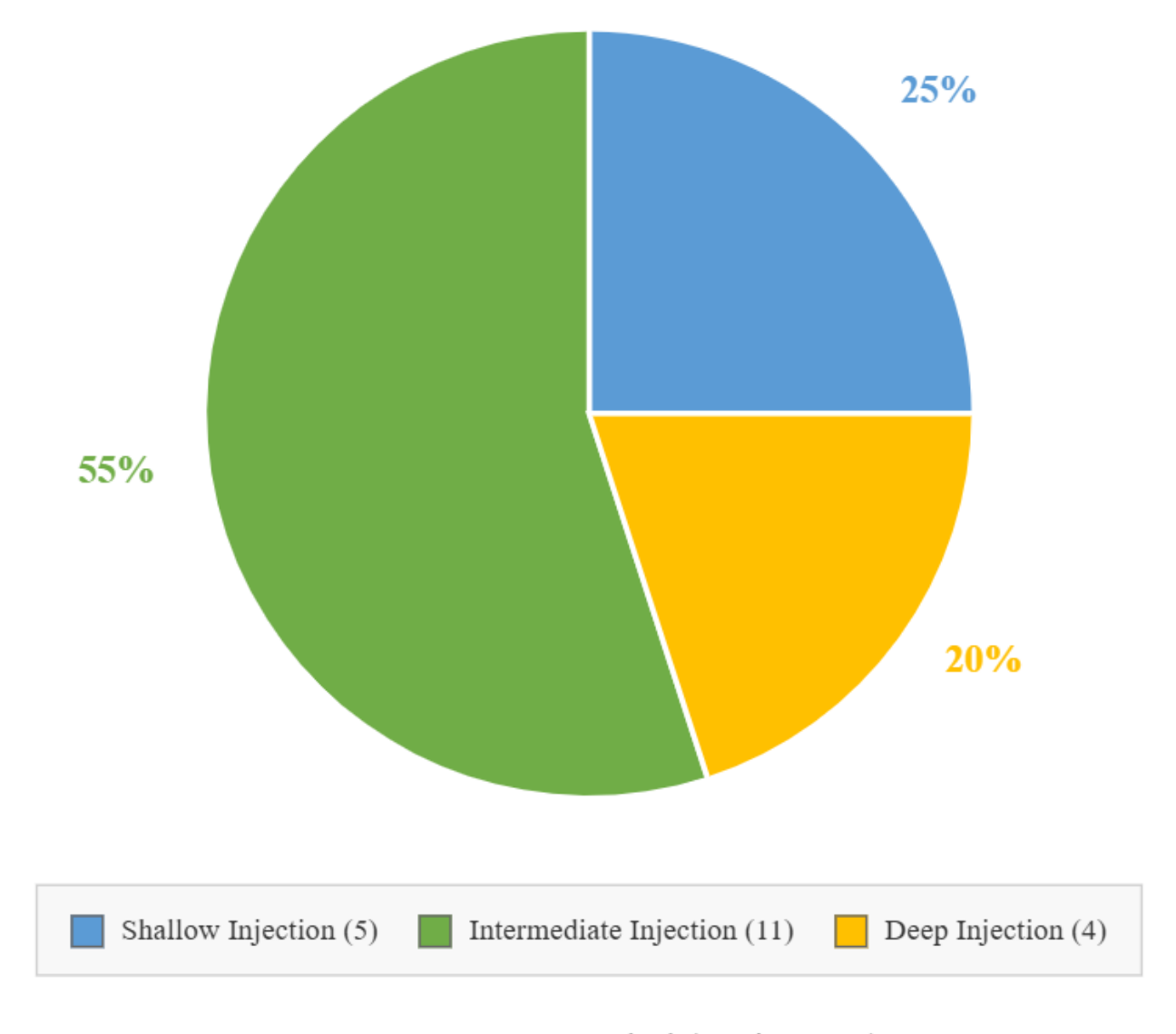
Depth

Storage formation depths in various projects range from 800 meters at Sleipner to 3100 meters at Porthos (Fig. 19), reflecting diverse geological settings and regional basin characteristics that influence both technical feasibility and project economics. Storage depth or injection depth affects fundamental CO₂ properties including density, viscosity, and phase behavior that control injection performance and storage efficiency. Optimal storage depths typically fall between 1000 and 3000 meters, where supercritical CO₂ conditions ensure maximum storage density while avoiding excessive pressure and temperature challenges that increase infrastructure costs and operational complexity.



Figure 22. Injection depths and formation's thicknesses

Recent developments in 2025 indicate growing interest in ultra-deep storage formations exceeding 3500 meters, where enhanced storage security and increased CO₂ density offset higher development costs. The Porthos project represents frontier technology deployment at 3000-4000 meters depth, targeting massive Bunter Sandstone formations with theoretical storage capacity exceeding 150,000 Mt. Deep storage operations require specialized injection equipment rated for extreme pressure conditions, with wellhead pressures potentially exceeding 40 MPa and corresponding safety system enhancements to manage operational risks.



Shallow Injection: <1500m depth (5 projects, 25%)

Intermediate Injection: 1500-2500m depth (11 projects, 55%)

Deep Injection: >2500m depth (4 projects, 20%)

Classification coherent with thermal gradient depth intervals for CO2 storage

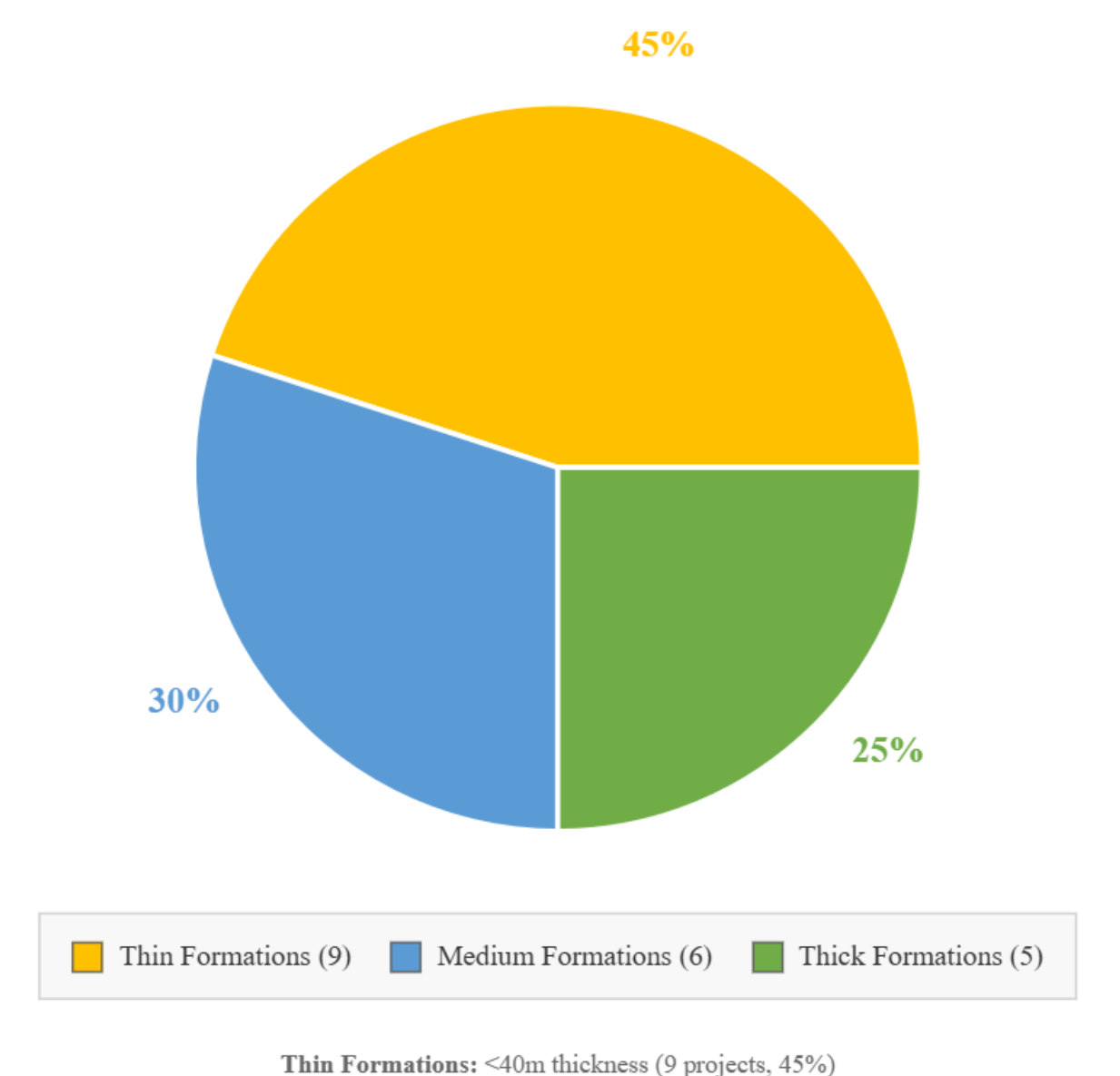
Figure 23. Injection Depth Classification for Underground CO₂ Storage Sites

Shallow CO2 storage at depths below 1200 meters present unique technical challenges related to CO2 phase behavior and storage efficiency optimization. The CNPC Jilin project operates near this lower depth limit at 1200-1400 meters, requiring careful pressure management to maintain stable supercritical conditions during injection. Temperature and pressure monitoring data indicate successful shallow storage implementation, however the lower CO2 density reduces storage efficiency and may require larger pore volumes to achieve target storage capacities compared with deeper formations.

Formation Thickness

Storage formation thickness demonstrates significant variation from 12 meters at Nagaoka to 300 meters at Sleipner, directly influencing storage capacity and injection well productivity over the project lifecycles. Thick formations provide several operational advantages including greater

storage volume per unit area, improved pressure distribution during injection, and enhanced flexibility for multi-zone completion strategies that optimize performance while maintaining formation integrity. The Northern Lights project illustrates the advantages of thick formation with 150 meters of high-quality Johansen Formation sandstone providing exceptional storage capacity exceeding 80,000 Mt.



Medium Formations: 40-100m thickness (6 projects, 30%)

Thick Formations: >100m thickness (5 projects, 25%)

Classification based on reservoir storage capacity and pressure management efficiency

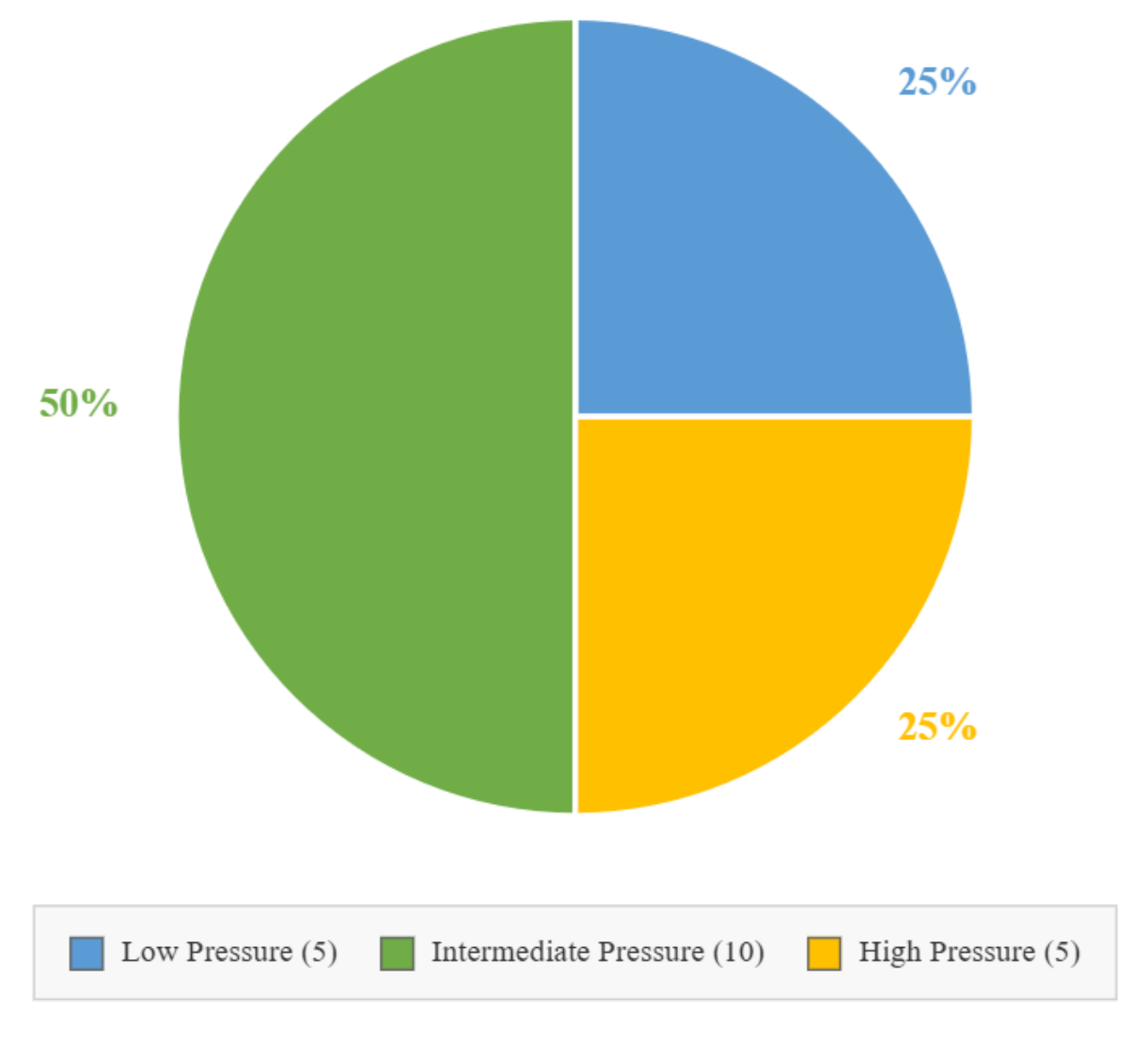
Figure 24. Formation Thickness Classification for Underground CO2 Storage Sites

Storing CO2 in thin formations require specialized well completion technologies and injection strategies to achieve adequate injectivity while maintaining formation pressure below fracture limits. The Nagaoka demonstration project successfully operated in a 12-meter-thick formation through precise pressure management and distributed injection strategies that prevented excessive pressure buildup. Horizontal well completions become particularly attractive for thin formations, providing 3-5 times greater contact area compared to vertical completions while enabling access to multiple reservoir compartments through extended lateral sections.

Recent 2025 project developments highlight the importance of optimizing formation thickness using detailed 3D seismic interpretation and geostatistical modeling to guide injection well placement and completion design. Advanced reservoir characterization techniques including seismic inversion and multi-attribute analysis enable identification of optimal thickness zones within heterogeneous formations, supporting enhanced storage efficiency and reduced development risks through improved geological understanding and operational planning.

Reservoir Pressure

Initial reservoir pressure conditions range from 8.0 MPa at Sleipner to 35.0 MPa at Porthos (Fig. 20), reflecting hydrostatic gradient variations and formation depletion history that significantly influence injection performance and storage capacity utilization. Normal pressure gradients between 10.0-10.2 MPa/km characterize most saline aquifer storage systems, while depleted hydrocarbon reservoirs often exhibit underpressured conditions providing additional capacity for CO₂ injection without exceeding fracture pressure limits. The Weyburn field is a clear example with current reservoir pressure approximately 60% of original hydrostatic values, enabling enhanced injection rates while maintaining geomechanical stability.



Low Pressure: 80-150 bar (8-15 MPa) (5 projects, 25%)

Intermediate Pressure: 150-250 bar (15-25 MPa) (10 projects, 50%)

High Pressure: >250 bar (>25 MPa) (5 projects, 25%)

Classification coherent with depth intervals for CO2 storage formations

Figure 25. Reservoir Pressure Classification for Underground CO₂ Storage Sites

Injection-induced pressure responses provide critical operational feedback for performance optimization and storage security assessment through continuous monitoring systems deployed across observation well networks. Pressure buildup analysis enables real-time evaluation of reservoir connectivity, boundary effects, and potential compartmentalization that affects long-term storage behavior and capacity utilization. The Quest project's comprehensive pressure monitoring program demonstrates successful pressure management with maximum increases below 8.5 MPa throughout three years of continuous injection operations.

Maximum allowable injection pressures are constrained to 80-90% of calculated fracture pressure across all operational projects. This provides adequate safety margins while maximizing injection efficiency and storage utilization. Advanced pressure management systems incorporate real-time monitoring, automated control systems, and emergency shutdown procedures to ensure operational safety and environmental protection throughout injection operations. Recent technological

developments include fiber-optic pressure sensing and distributed acoustic monitoring. They enhance pressure measurement accuracy and provide early warning of potential operational issues.

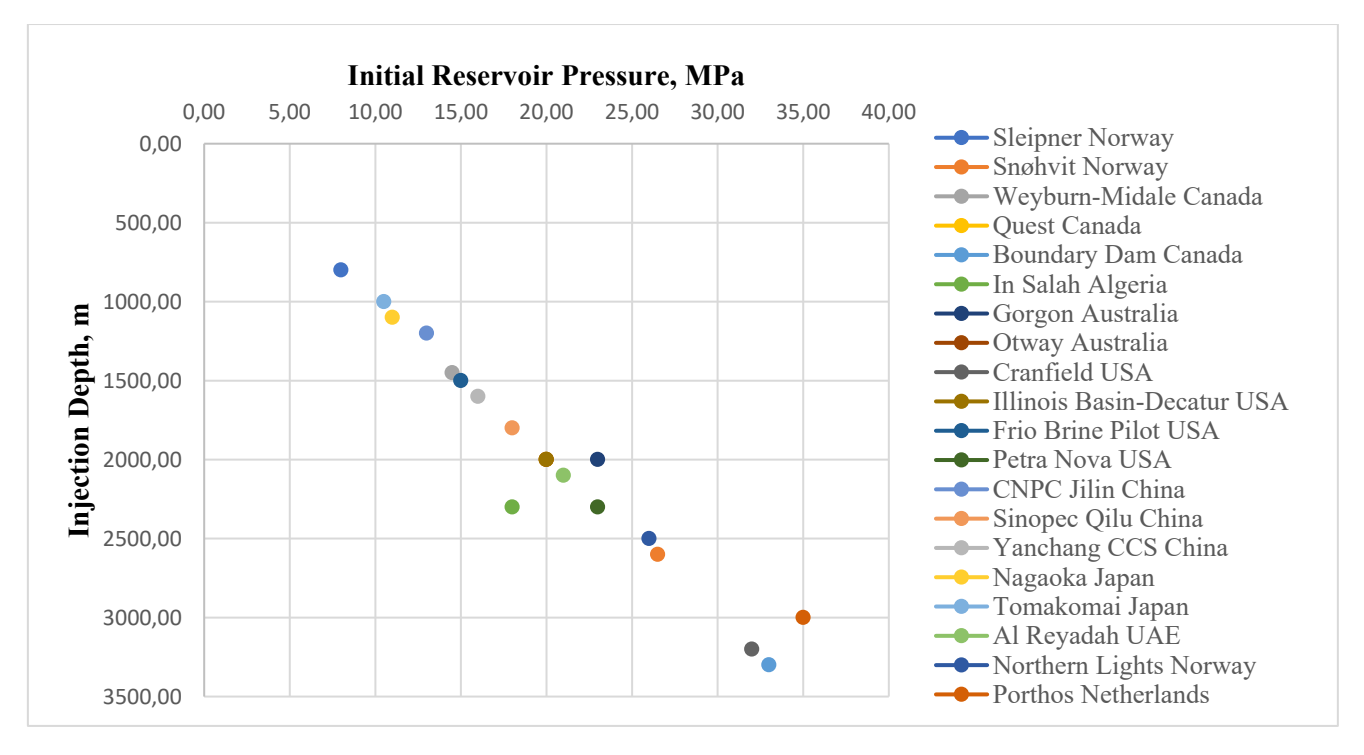


Figure 26. Reservoirs Pressure

Reservoir Temperature

Storage formation temperatures range from 37°C at Sleipner to 120°C at Cranfield (Fig. 21), directly influencing CO₂ physical properties and storage mechanisms controlling injection performance and long-term storage behavior. Higher temperatures tend to decrease CO₂ density while increasing its dissolution rates in formation brines, creating complex trade-offs between storage efficiency and trapping mechanism effectiveness. For example, under typical storage pressures conditions, CO₂ solubility in water decreases from approximately 1.8 mol/kg H₂O at 40°C to 1.2 mol/kg H₂O at 100°C.

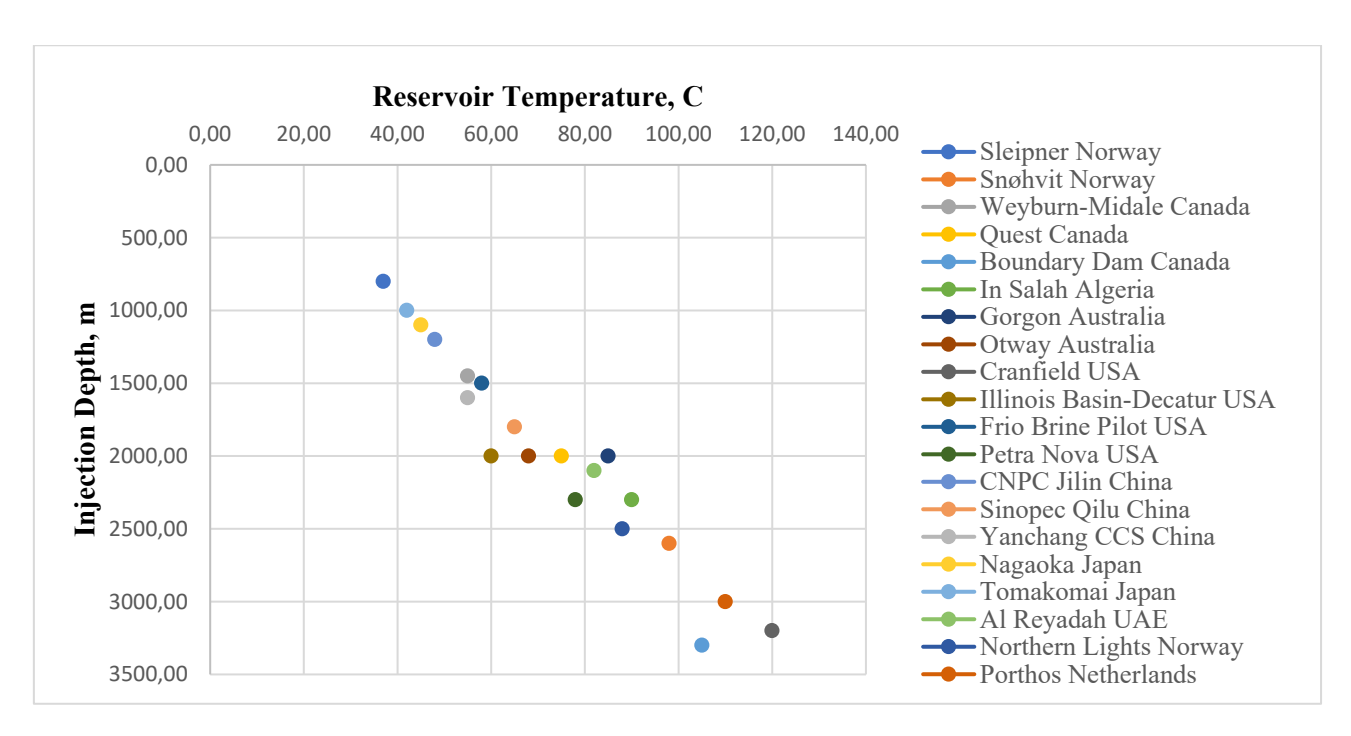
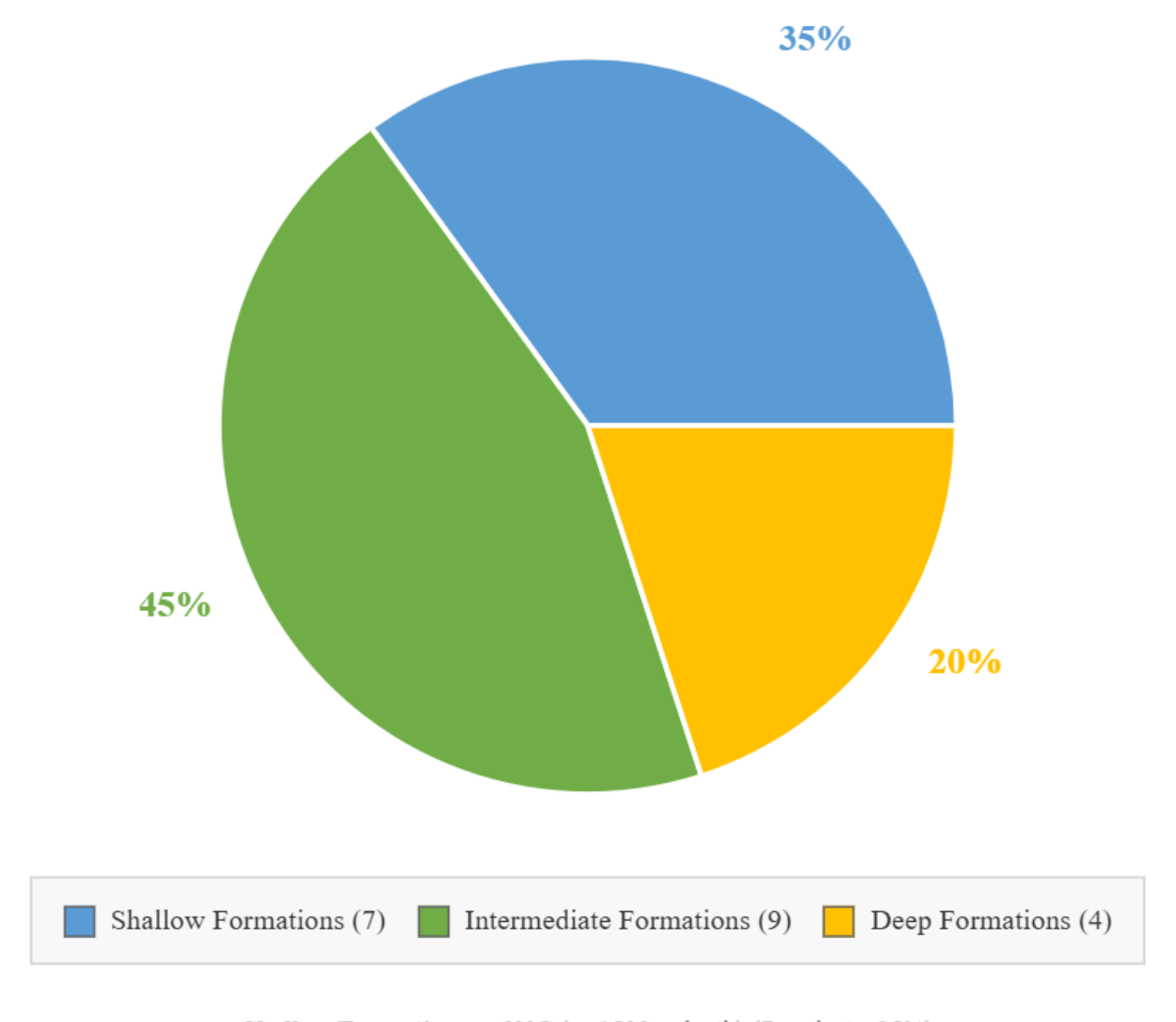


Figure 27. Reservoirs Temperature

Geothermal gradient variations ranging from 25°C/km in stable cratonic regions to 35°C/km in active sedimentary basins create significant temperature differences at similar depths across storage sites worldwide. The Gorgon project demonstrates moderate geothermal gradient of 32°C/km resulting in 85°C reservoir temperature at 2400 meters depth, providing favorable conditions for both storage density and geochemical stability. Ultra-high temperature storage environments above 100°C require enhanced materials selection and completion designs to ensure long-term wellbore integrity and operational safety.



Shallow Formations: <60°C (~<1500m depth) (7 projects, 35%)

Intermediate Formations: 60-90°C (~1500-2500m depth) (9 projects, 45%)

Deep Formations: >90°C (~>2500m depth) (4 projects, 20%)

Classification based on thermal gradient of 3°C/100m with surface temperature of 15°C

Figure 28. Reservoir Temperature Classification for Underground CO2 Storage Sites

Recent 2025 monitoring data indicates successful temperature management across all operational projects, with injection-induced cooling effects remaining within acceptable limits for formation integrity and completion performance. Advanced thermal modeling incorporating heat transfer, fluid flow, and geomechanical coupling enables optimization of injection strategies and prediction of long-term thermal behavior throughout storage lifecycles. Temperature-dependent geochemical reaction modeling becomes increasingly important for high-temperature storage environments where accelerated mineral reactions may affect both storage security and reservoir performance over extended timeframes.

3.4 Caprock Properties

The caprock formations in the twenty studied projects demonstrate exceptional diversity in lithology, thickness, and sealing mechanisms that provide primary containment security for stored CO₂ throughout operational and post-injection periods. Shale and mudstone caprocks represent

75% of storage systems, characterized by permeability values below 0.005 mD and capillary entry pressures ranging from 0.8 MPa at Nagaoka to 8.0 MPa at Quest. The Sleipner project's Nordland Shale caprock stands out with optimal sealing characteristics with an effective thickness of 100-150 meters, permeability below 0.001 mD, and capillary entry pressure higher than 2.5 MPa. This has successfully contained over 22 Mt of injected CO₂ for over 25 years of operation.

Evaporite caprocks, such as the Lotsberg Salt at Quest and anhydrite layers at Weyburn-Midale and Al Reyadah, provide exceptional sealing capacity with permeability values below 0.0001 mD and self-healing characteristics that accommodate stress changes without brittle failure. The Quest project's salt caprock system exceeds 150 meters thickness and demonstrates ultimate sealing integrity with capillary entry pressures of 8.0 MPa, representing the highest containment security among evaluated projects. Salt dissolution concerns in CO₂-saturated brine systems require careful evaluation through reactive transport modeling and long-term monitoring programs that assess dissolution rates and potential integrity impacts over storage timeframes.

The mechanical properties of caprock are important for ensuring operational safety and long-term containment security, with fracture pressure gradients ranging from 0.65 to 0.90 psi/ft, influenced by regional stress conditions and mechanical properties of the rock. Conservative operational practices maintain injection pressures below 80% of caprock fracture pressure to ensure adequate safety margins throughout project lifecycles. The In Salah project's experience where surface uplift surpassed 15 mm demonstrates the importance of integrated geomechanical monitoring that combines downhole pressure measurements, surface deformation tracking, and microseismic monitoring to ensure caprock integrity during injection operations.

Recent 2025 studies on caprock highlight the use of enhanced characterization techniques such as high-resolution seismic imaging, geomechanical testing, and long-term geochemical stability analysis that improve understanding of sealing mechanism efficiency and durability. Advanced monitoring technologies including distributed fiber-optic sensing and continuous electromagnetic monitoring enable real-time assessment of caprock integrity and early detection of potential sealing degradation that could compromise storage security over extended timeframes.

3.5 Brine Characteristics

Brine pH

The pH levels of formation water across various CO2 storage projects range from 6.8 at Cranfield to 8.2 at Nagaoka under ambient conditions, reflecting diverse geochemical environments and buffering capacity variations that significantly influence CO2-brine-rock interactions during storage operations. Reduction in initial pH due to CO2 dissolution creates acidic conditions that enhance mineral dissolution rates and affect geochemical equilibrium development within storage formations. The Sleipner project's comprehensive brine monitoring demonstrates typical pH evolution from initial values near 7.8 decreasing to approximately 6.2 within CO2 plume areas, followed by gradual recovery through carbonate and silicate mineral buffering reactions over decades to centuries.

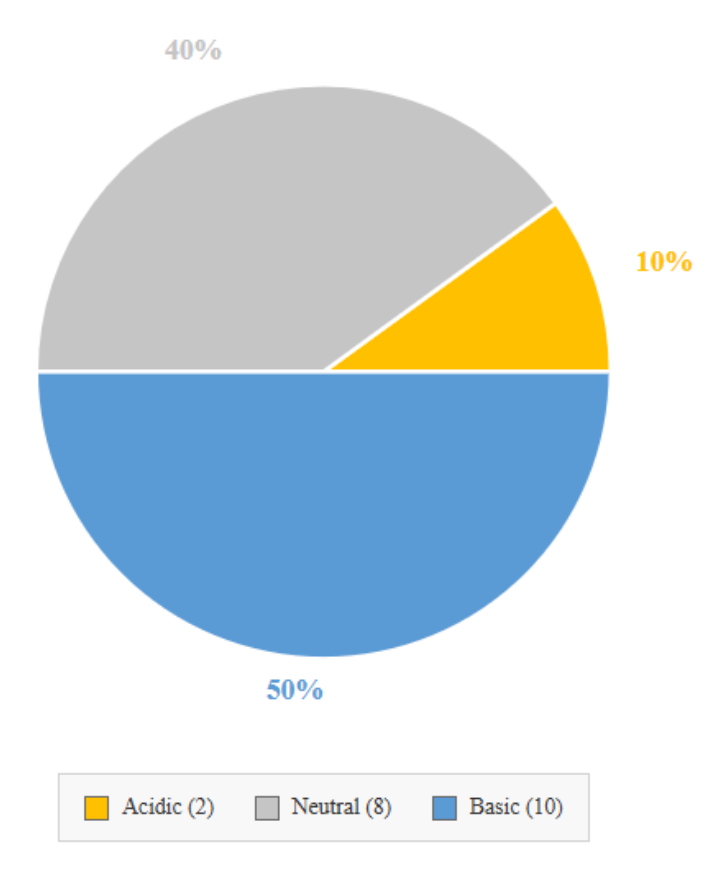


Figure 29. Formation Brine pH Distribution in Global CO2 Storage Projects

Buffering capacity variations among storage formations depend critically on reactive mineral content, particularly carbonate concentrations that neutralize CO₂-induced acidity through dissolution processes. High-carbonate formations including Weyburn-Midale (85% carbonate content) and Al Reyadah (90% carbonate content) provide substantial buffering capacity that limits pH depression and accelerates return to near-neutral conditions through calcite and dolomite dissolution mechanisms. In contrast, quartz-dominated sandstone formations with minimal carbonate content experience prolonged acidic conditions potentially persisting for decades, affecting mineral stability and requiring enhanced monitoring of trace metal mobilization and secondary mineral precipitation processes.

The kinetics of pH-dependent geochemical reactions control the long-term storage evolution of CO2 storage by influencing mineral dissolution, precipitation, and transformation processes that affect porosity, permeability, and trapping mechanism. Recent 2025 geochemical monitoring data indicates successful pH management across operational projects, with measured values remaining within predicted ranges and demonstrating expected temporal evolution patterns. Advanced pH monitoring technologies including downhole fiber-optic sensors and real-time electrochemical systems enable continuous assessment of geochemical conditions and validation of reactive transport models throughout storage lifecycles.

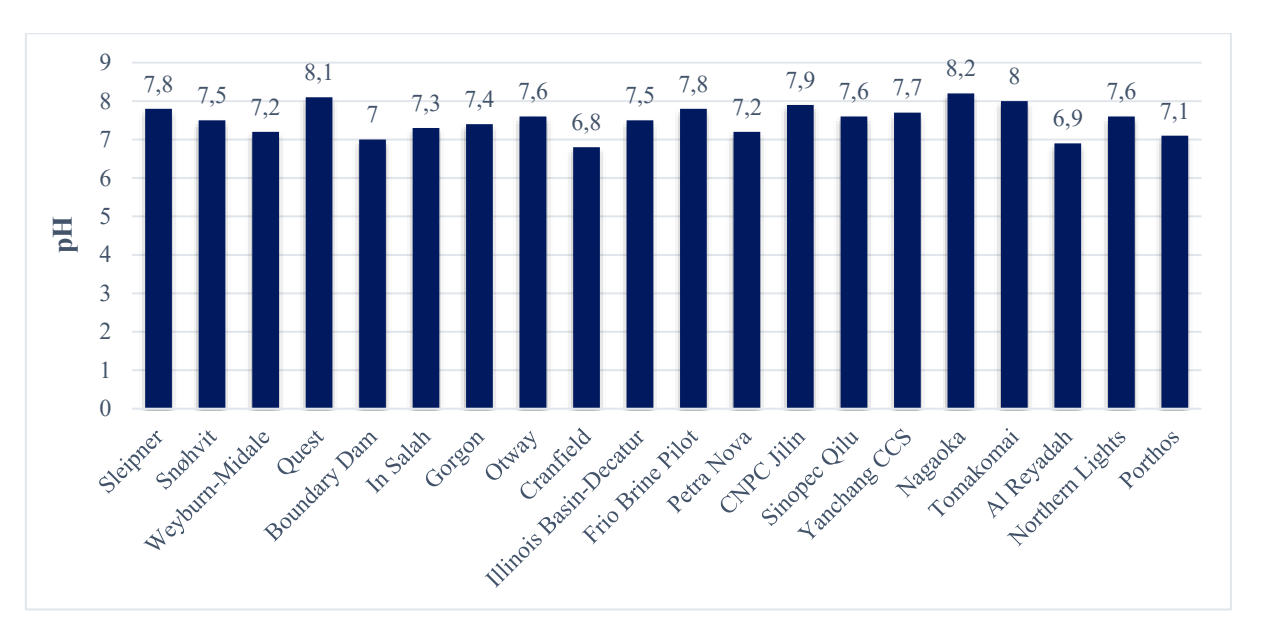
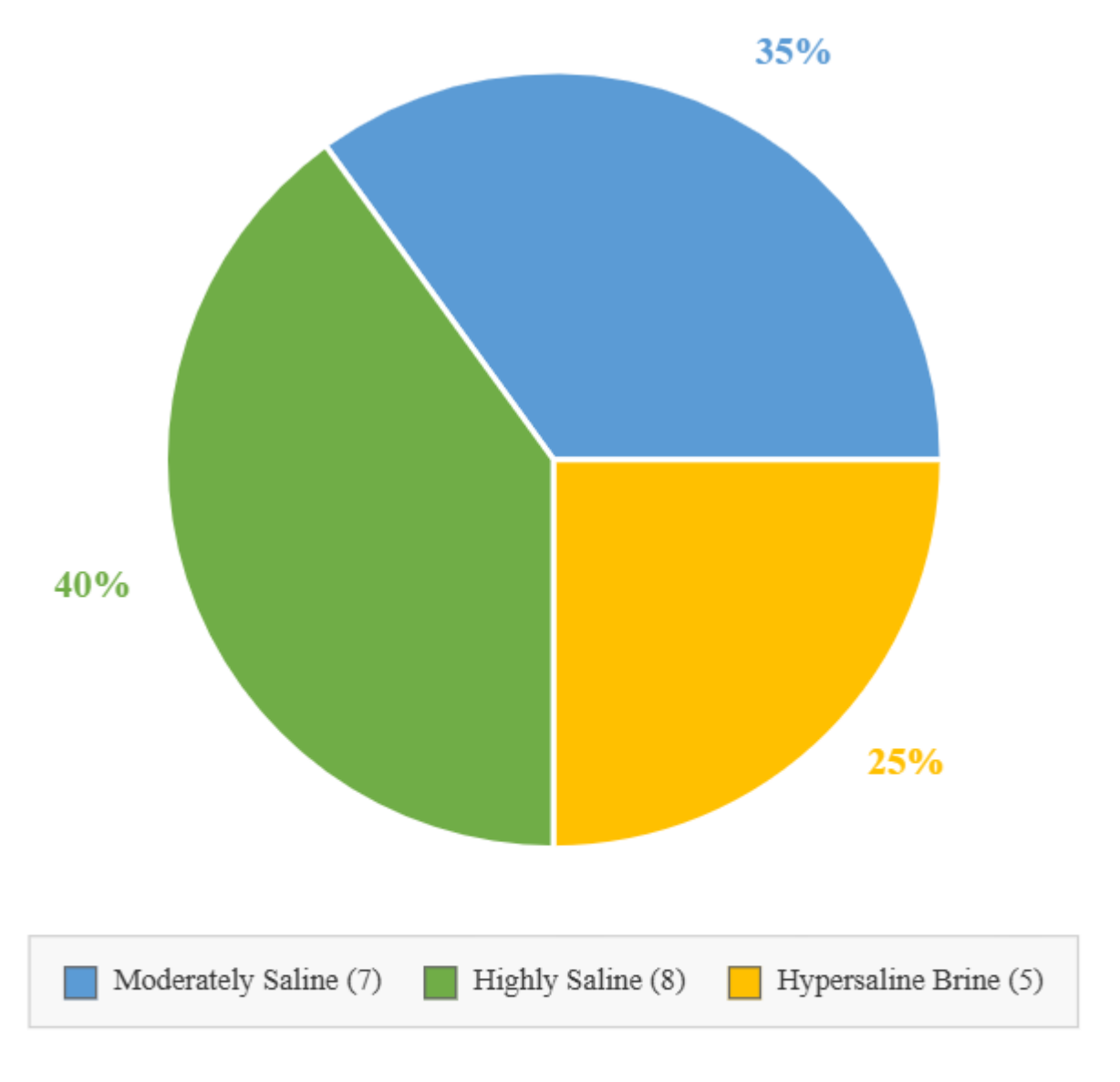


Figure 30. Brine pH

Brine Salinity

Formation water salinity demonstrates extraordinary variation from 15,000 mg/L TDS in fresh aquifer systems to 250,000 mg/L in deep hypersaline environments, fundamentally affecting CO₂ solubility, geochemical reactivity, and operational aspects across storage projects. Most operational storage systems exhibit moderate salinity levels between 35,000-85,000 mg/L TDS, providing favorable balance between CO₂ solubility and operational compatibility. The Quest project with a salinity of 15,000 mg/L represents optimal conditions for CO₂ dissolution trapping, while hypersaline systems like Boundary Dam (250,000 mg/L) require specialized corrosion management and adjustments for reduced solubility in storage mechanism assessments.



Moderately Saline: 10,000-50,000 mg/L TDS (7 projects, 35%) **Highly Saline:** 50,000-150,000 mg/L TDS (8 projects, 40%)

Hypersaline Brine: >150,000 mg/L TDS (5 projects, 25%)

Refined classification within saline ranges suitable for CO2 storage (all projects > 10,000 mg/L TDS)

Figure 31. Brine Salinity Classification for Underground CO₂ Storage Sites

Analysis of ionic composition shows that sodium and chloride are the dominant ions in most formation waters, with significant bicarbonate content providing natural buffering capacity against CO₂-induced acidification. Calcium and magnesium concentrations ranging from 1,000-15,000 mg/L influence carbonate mineral precipitation potential and scaling that may affect injection well productivity over extended operational periods. Variations in sulfate content between 100-5,000 mg/L require evaluation for potential bacterial sulfate reduction and hydrogen sulfide generation that could affect metallurgy selection and operational safety protocols throughout project lifecycles.

Salinity effects on multiphase flow properties become particularly important for storage efficiency assessments and reservoir simulation accuracy. High ionic strength conditions alter clay mineral behavior, wettability characteristics, and relative permeability relationships that control CO₂

displacement efficiency and residual trapping mechanisms. Recent 2025 laboratory research studies demonstrate salinity-dependent contact angle variations ranging from 20° to 55°, significantly affecting capillary pressure relationships and ultimate storage capacity predictions. Advanced brine characterization including isotopic analysis and trace element profiling enables enhanced understanding of formation water origin, flow patterns, and mixing processes that influence long-term storage behavior and monitoring interpretation.

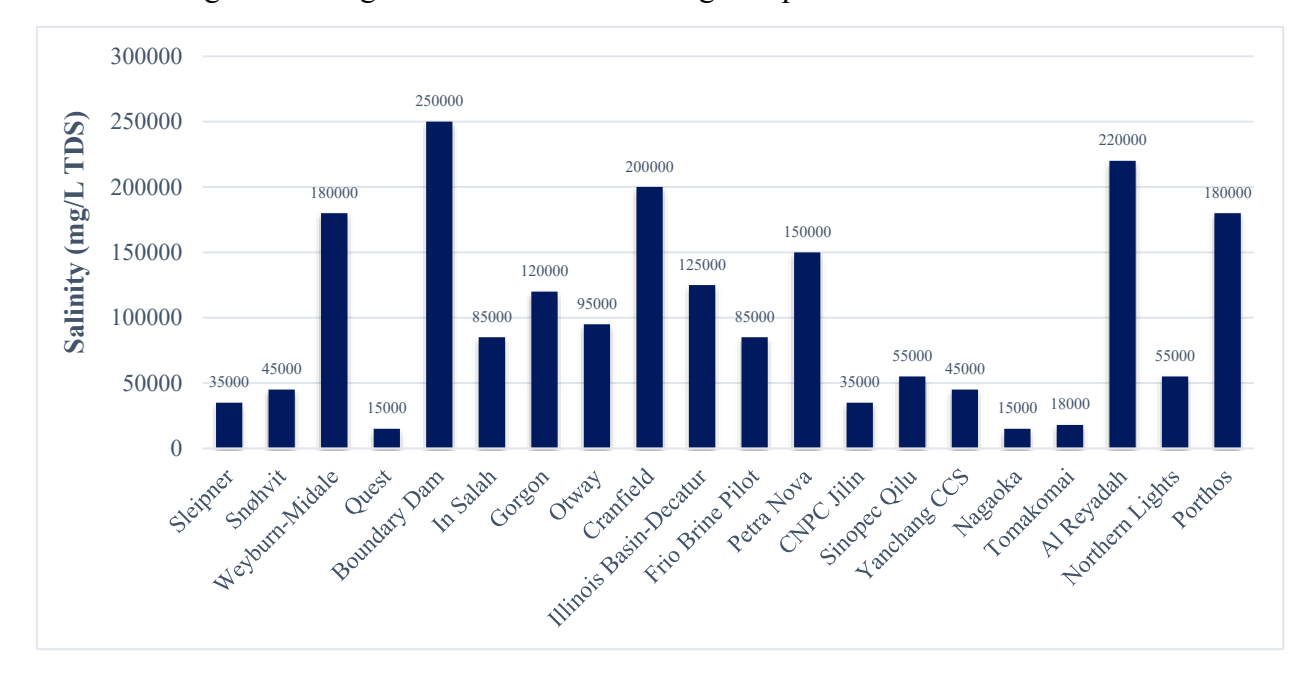
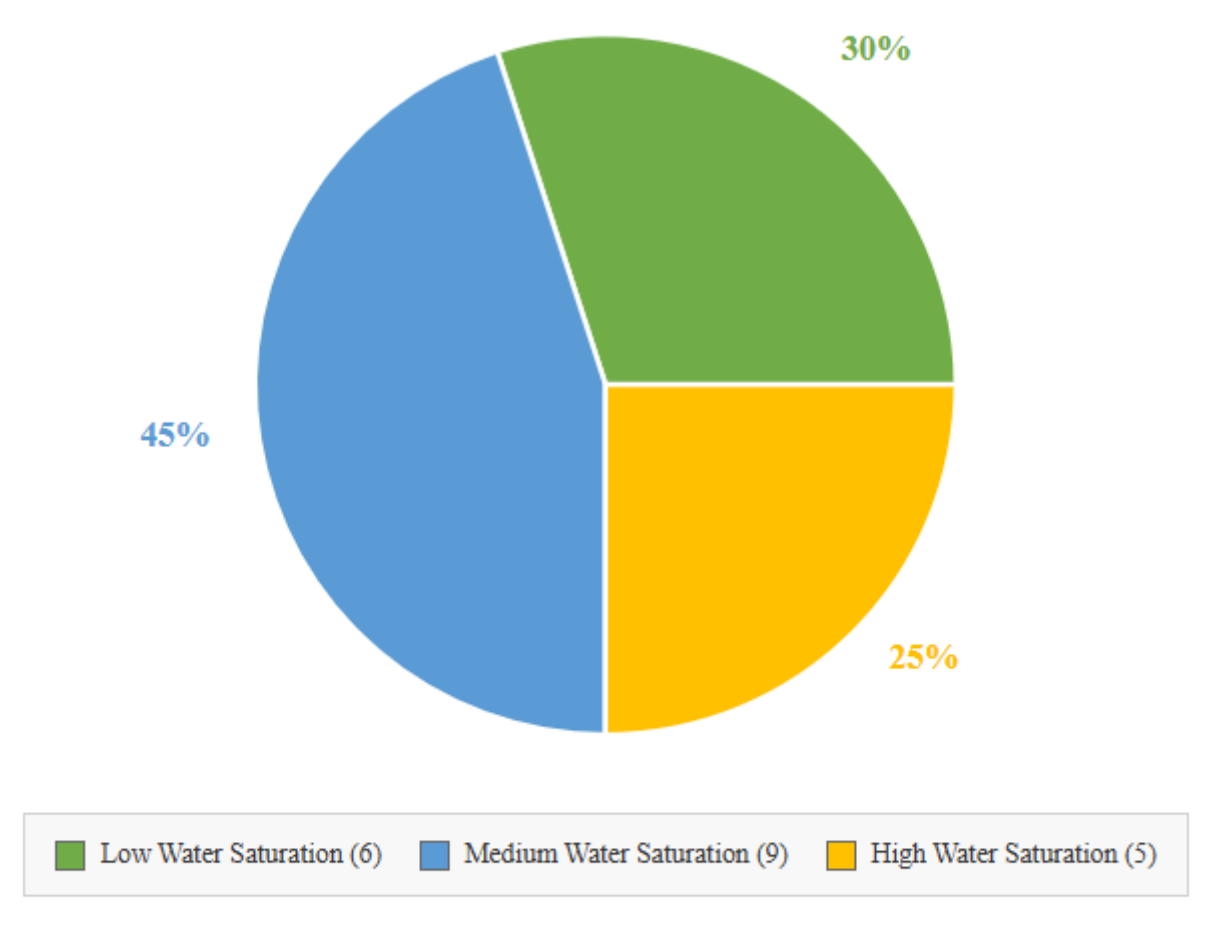


Figure 32. Brine Salinity

3.6 Fluid—Rock Interaction Properties

Initial and Residual Water Saturation

Enhanced oil recovery (EOR) projects including Weyburn-Midale, Cranfield, and Chinese EOR facilities demonstrate complex initial saturation distributions with remaining hydrocarbon saturations between 35-55%, providing additional storage capacity through three-phase displacement mechanisms during CO₂ injection. Saline aquifer systems typically exhibit water saturations exceeding 95%, with slight undersaturation potentially indicating natural gas presence or structural perching effects that require evaluation for storage capacity and injection strategy optimization.



Low Water Saturation: <60% Sw (6 projects, 30%)

Medium Water Saturation: 60-75% Sw (9 projects, 45%)

High Water Saturation: >75% Sw (5 projects, 25%)

Classification based on initial water saturation in CO2 storage reservoir formations

Figure 33. Initial Water Saturation Distribution in Global CO₂ Storage Projects

Residual water saturation after CO₂ displacement represents a critical parameter controlling ultimate storage efficiency and capillary trapping effectiveness, with measured values ranging from 40% at In Salah to 85% at Nagaoka depending on formation wettability, pore structure characteristics, and injection methodology. Formations with strong water-wet nature, typical of clean sandstone systems retain higher residual water saturations that reduce effective storage capacity but enhance security through increased CO₂-water interfacial area and improved capillary trapping mechanisms. Laboratory measurements indicate drainage residual water saturations typically 15-25% higher than imbibition values, creating significant hysteresis effects that influence post-injection CO₂ redistribution and trapping evolution.

The evolution of saturation during and after CO2 injection reflects complex interactions between viscous forces, capillary forces, and gravity (gravitational segregation) that control final CO₂ distribution patterns and storage security mechanisms. Advanced reservoir simulation incorporating hysteretic relative permeability effects enables prediction of saturation evolution and optimization of injection strategies to maximize residual trapping through controlled injection rate management and well placement strategies. Recent 2025 monitoring data from various projects align with these predictions showing measured residual CO₂ saturations ranging from 15-35% after

injection stops, demonstrating effective capillary trapping and enhanced storage security over operational time.

Wettability, Contact Angle, Capillary Pressure

Contact angle measurements conducted under reservoir conditions indicate predominantly waterwet behavior across various CO2 storage projects, with values ranging from 22° at Nagaoka to 55° at Weyburn-Midale depending on formation mineralogy, organic matter content, and brine chemistry. Temperature effects demonstrate general trends toward reduced water-wetness at higher temperatures, with contact angles increasing approximately 0.3-0.5° per °C temperature increase under typical storage pressure conditions. The Sleipner project's extensive contact angle characterization indicates stable water-wet conditions with values near 25° throughout the storage interval, contributing to favorable capillary trapping and enhanced storage security through strong CO₂ entrapment mechanisms.

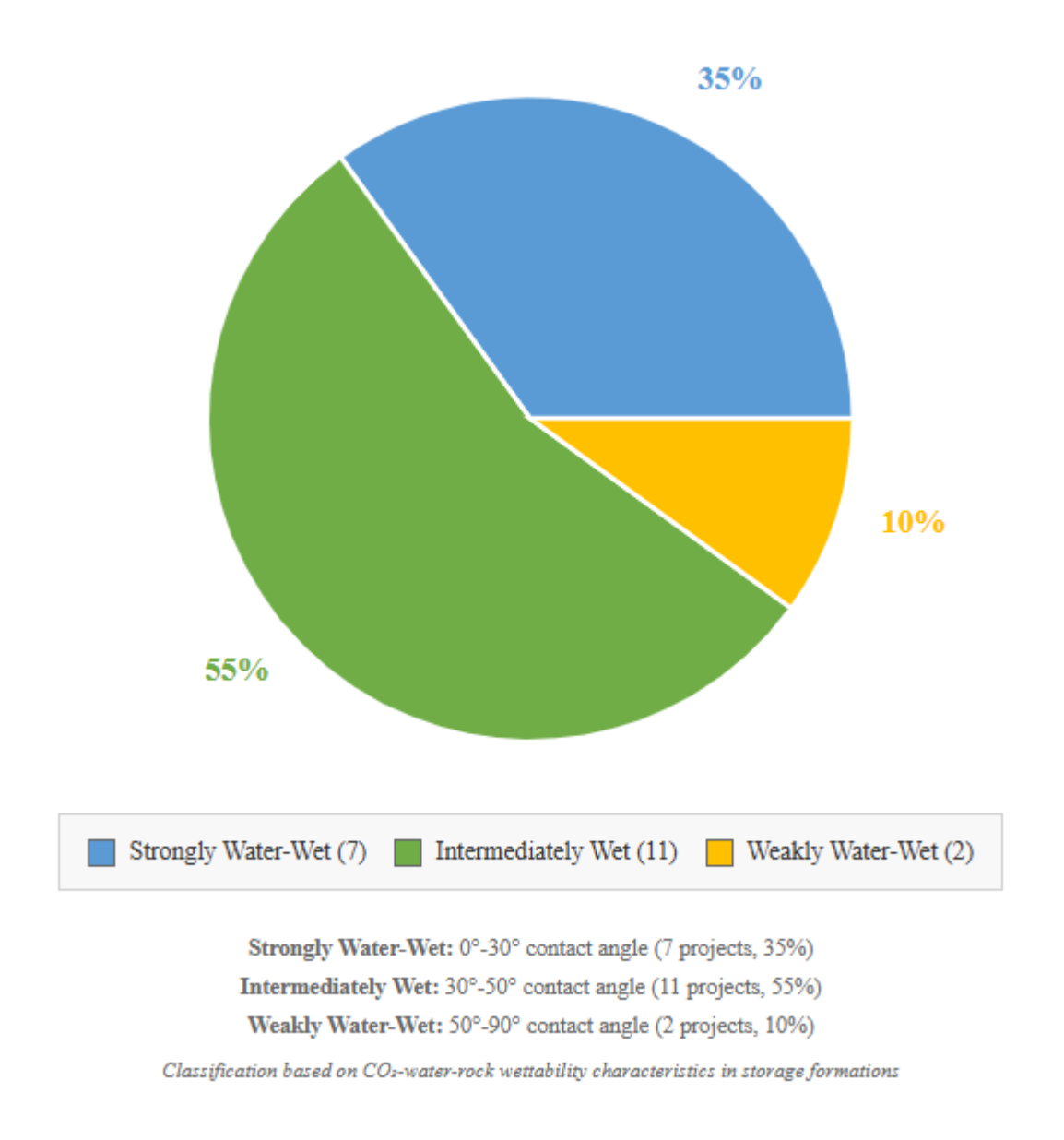


Figure 34. CO₂-Water-Rock Contact Angle Distribution in Global CO₂ Storage Projects

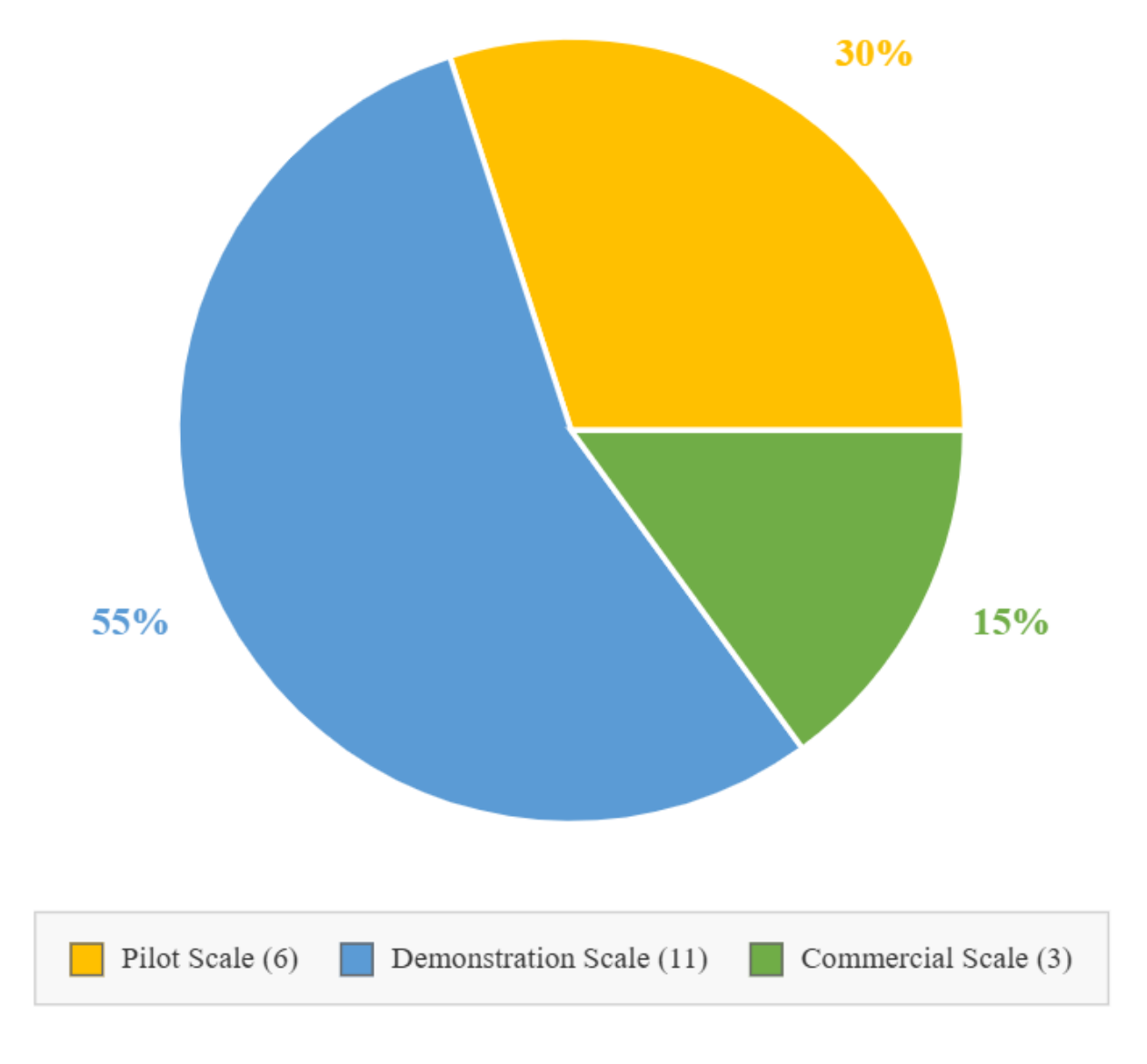
Wettability index calculations based on relative permeability measurements reveal strongly waterwet conditions (index > 0.7) in 60% of evaluated projects, moderately water-wet behavior (index

0.4-0.7) in 30% of systems, and mixed-wet characteristics (index < 0.4) in 10% of formations typically associated with carbonate reservoirs or hydrocarbon-bearing formations. Clay mineral content particularly influences wettability behavior, with high-clay formations exhibiting stronger water-wet characteristics compared to clean sandstone intervals. Advanced wettability characterization including contact angle hysteresis measurements and surface force analysis enables improved understanding of trapping mechanism effectiveness and storage security development over extended timeframes.

Capillary pressure relationships play important role in controlling CO₂ entry conditions, displacement efficiency, and residual trapping characteristics within storage formations, with capillary entry pressures ranging from 0.01 MPa in high-permeability systems to 2.5 MPa in tight formations depending on pore throat size distribution and interfacial tension conditions. Drainage and imbibition capillary pressure curves exhibit significant hysteresis effects with imbibition curves demonstrating 20-50% higher values and increased residual CO₂ saturation compared to drainage conditions. Recent 2025 laboratory studies highlight the importance of reservoir-condition measurements, as ambient condition testing potentially underestimates entry pressures by 30-60% due to interfacial tension and wettability variations under storage pressure and temperature conditions.

3.7 Injectivity and Storativity

Injectivity performance of existing CO₂ storage projects varies from 15 bbl/day/psi in tight formations to over 400 bbl/day/psi in high-quality aquifer systems, directly reflecting reservoir quality and the effectiveness of well completion optimization. The Sleipner project has maintained exceptional injectivity exceeding 300 bbl/day/psi throughout 25+ years of continuous operations, demonstrating sustainable performance in optimal reservoir conditions with minimal formation damage or operational complications. Chinese EOR projects including CNPC Jilin and Sinopec Qilu have demonstrated moderate injectivity values of 25-50 bbl/day/psi, requiring advanced well completion technologies and pressure management strategies to achieve injection targets while maintaining reservoir integrity.



Pilot Scale: <0.5 Mt CO₂/year (6 projects, 30%)

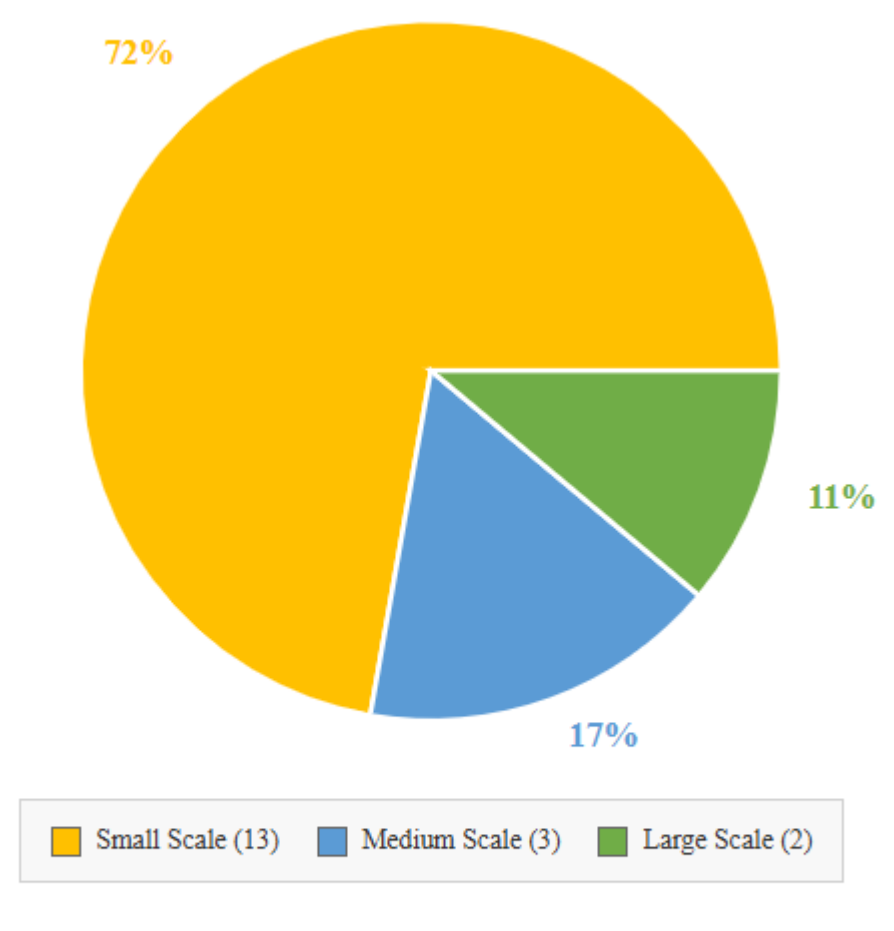
Demonstration Scale: 0.5-2.0 Mt CO₂/year (11 projects, 55%)

Commercial Scale: >2.0 Mt CO₂/year (3 projects, 15%)

Classification based on CO2 injection capacity and project development stage

Figure 35. CO₂ Injection Rate Distribution in Global CO₂ Storage Projects

Storage efficiency calculations show significant variations among project types and geological settings, with achieved values ranging from 2% in tight formations to 25% in optimal EOR applications where remaining hydrocarbon volumes provide additional storage capacity. Projects using saline aquifer typically demonstrate storage efficiency of 3-12%, limited by conservative pressure management and heterogeneity effects that limit effective reservoir utilization. The Weyburn-Midale EOR project achieves storage efficiencies of 15-25% through comprehensive reservoir characterization, optimized well placement, and integrated production and injection strategies that maximize both hydrocarbon recovery and CO₂ storage capacity.



Small Scale: <5 Mt CO₂ total (13 projects, 72%)

Medium Scale: 5-15 Mt CO₂ total (3 projects, 17%)

Large Scale: >15 Mt CO₂ total (2 projects, 11%)

Classification based on cumulative CO2 storage volume in operational projects (excludes projects at 0 Mt)

Figure 36. Cumulative CO₂ Storage Volume Distribution in Global CO₂ Storage Projects

Operational optimization requires continuous monitoring of injection performance parameters including wellhead pressure, flow rate, and reservoir formation response characteristics to maintain target storage rates while ensuring safety and environmental compliance. Advanced completion technologies including expandable screens, intelligent completion systems, and real-time downhole monitoring systems enable responsive performance management and early detection of potential issues including formation damage, scale precipitation, or mechanical integrity concerns. Recent 2025 technological developments emphasize automated injection control systems that optimize operating parameters based on real-time reservoir response data, improving both storage efficiency and operational safety throughout project lifecycle.

Well configuration strategies have a significant impact on both injectivity performance and storage capacity utilization, with horizontal completions becoming increasingly popular for thin formations and heterogeneous reservoirs. Multi-zone completion designs allow selective injection into optimal reservoir intervals, avoiding problematic zones with potential formation damage or inadequate sealing characteristics. The Northern Lights project utilizes advanced completion technologies including intelligent flow control devices and real-time monitoring systems to optimize injection distribution across multiple reservoir zones while maintaining individual zone pressure management.

3.8 Trapping Mechanisms

Structural trapping mechanisms provide primary containment security for 60-85% of stored CO₂ across evaluated projects, relying on buoyancy forces and geological architecture to maintain CO₂ accumulation beneath low-permeability caprock formations throughout storage lifecycles. The Sleipner project exemplifies successful structural trapping with CO₂ accumulating in small domal features within the Utsira Sand formation, where 4D seismic monitoring reveals plume development following subtle topographic variations on the caprock surface. Structural efficiency calculations indicate 60-85% of injected CO₂ remains within primary structural closures, with remaining volumes distributed through secondary trapping mechanisms including residual and solubility trapping that enhance overall storage security.

Residual trapping development provides increasingly important storage security over extended timeframes, with trapped CO₂ saturations ranging from 12% at Al Reyadah to 35% at Nagaoka depending on formation wettability, pore structure characteristics, and injection-production cycling history. Laboratory measurements indicate residual trapping efficiency increases significantly through imbibition processes following injection cessation, with typical saturation increases of 15-25% developing over post-injection periods of 5-20 years. The Otway project's detailed residual trapping studies demonstrate 25% residual CO₂ saturation development within two years following injection cessation, providing enhanced storage security through permanent immobilization of significant CO₂ volumes.

Solubility trapping occurs through CO₂ dissolution in formation brines, creating gravitationally stable CO₂-saturated water that eliminates free-phase CO₂ and provides ultimate storage security through molecular-scale immobilization. Dissolution rates vary significantly among storage formations depending on temperature, pressure, brine salinity, and convective mixing processes that control mass transfer between CO₂ and aqueous phases. The Frio pilot project demonstrated rapid CO₂ dissolution with over 60% of injected CO₂ dissolving within one year of injection, though higher-rate commercial projects typically experience slower dissolution due to reduced residence time and limited mixing enhancement.

Mineral trapping represents the most secure long-term storage mechanism by converting CO₂ into stable carbonate and other mineral phases, though reaction rates typically require decades to centuries for significant capacity development. Geochemical monitoring across multiple projects has documented early mineral trapping evidence through secondary carbonate precipitation, clay mineral alteration, and trace element mobilization that indicate active CO₂-mineral reactions. Recent geochemical studies indicate that mineral trapping rates range from 0.1% to 2% of injected CO₂ per decade in sandstone formations, with carbonate formations potentially achieving higher rates through enhanced reactivity and buffering capacity [8]. Advanced reactive transport modeling predicts potential mineral trapping capacities exceeding 50% of injected CO₂ over millennial timeframes, providing ultimate storage security through permanent chemical immobilization in stable mineral phases.

3.9 Monitoring Technologies and Results

Comprehensive monitoring programs are essential for verifying storage containment and detecting potential leakage pathways. Successful projects employ multiple monitoring technologies including seismic surveys, pressure monitoring, geochemical sampling, and surface flux

measurements. Table 4 compares the effectiveness and application of different monitoring technologies across major storage projects.

Table 7. Monitoring Technologies Used in Major CO2 Storage Projects

Technology	Detection Capability	Spatial Coverage	Temporal Resolution	Cost Level	Projects Applied
4D Seismic	CO ₂ plume migration	Regional (km²)	Years	High	Sleipner, Weyburn, In Salah
Pressure Monitoring	Reservoir response	Local (wells)	Real-time	Medium	All operational projects
Geophysical Sampling	Fluid coomposition	Point measurement	Monthly	Low	Quest, Gorgon, Boundary Dam
InSAR	Surface deformation	Regional (100s km²)	Daily- Monthly	Medium	In Salah, Gorgon
Soil Gas Monitoring	Near-surface leakage	Local (km²)	Weekly	Low	Weyburn, Cranfield
Microseismic	Induced seismicity	Local-Regional	Real-time	Medium	In Salah, Quest
Fiber Optic Sensors	Temperature/strain	Well-based	Real-time	Medium	Otway, Northern
Atospheric CO ₂	Surface emissions	Point/regional	Continuous	Low	Multiple projects

Time-lapse seismic monitoring has emerged as a highly effective method for tracking CO₂ plume migration and confirming containment integrity. The Sleipner project has demonstrated the effectiveness of 4D seismic imaging in mapping CO₂ distribution within the Utsira formation, showing stable plume behavior with no evidence of leakage over more than 25 years of operation.

Pressure monitoring provides real-time data on reservoir response to CO₂ injection and can detect anomalies that might indicate leakage or unexpected reservoir behavior. Successful projects maintain injection pressures well below fracture gradients while achieving target injection rates, demonstrating the importance of proper pressure management.

Geochemical monitoring of formation waters and soil gas provides additional verification of storage containment and can detect early indicators of possible leakage. The absence of CO₂ signatures in shallow groundwater and surface environments at successful projects confirms the effectiveness of geological containment mechanisms.

4. Risk Assessment and Management Strategies

4.1 Global and Local Risk Factors

Risk management represents a fundamental aspect of CO₂ storage implementation, requiring comprehensive assessment of potential hazards and development of appropriate mitigation strategies. The risk profile of storage projects encompasses both global risks related to climate change mitigation effectiveness and local risks associated with environmental and safety impacts.

Global risks primarily concern the potential release of stored CO₂ to the atmosphere, which could undermine the climate benefits of storage operations. However, geological evidence and operational experience from existing projects demonstrate that properly selected and managed storage sites can achieve retention rates exceeding 99% over century-long timescales. The natural

occurrence of CO₂ reservoirs and hydrocarbon fields provides analogues for long-term containment, with many formations having retained fluids for millions of years.

Local risks encompass potential impacts on groundwater quality, surface ecosystems, and human health from CO₂ leakage or associated contaminants. These risks require site-specific assessment considering local hydrogeology, ecological sensitivity, and population density. Risk mitigation strategies include comprehensive site characterization, robust monitoring systems, and emergency response protocols.

4.2 Monitoring and Verification Requirements

Effective monitoring and verification (M&V) systems are essential for demonstrating storage security and maintaining public confidence in CO₂ storage operations. Best practices developed from operational projects provide guidance for designing comprehensive M&V programs that address both technical and stakeholder requirements.

Monitoring strategies must be tailored to site-specific conditions and risk profiles, with greater intensity and duration required for higher-risk projects or locations. Baseline monitoring prior to injection is crucial for establishing reference conditions and detecting any changes attributable to CO₂ storage operations.

The integration of multiple monitoring technologies provides redundancy and enhances detection capabilities. Successful monitoring programs combine subsurface techniques (seismic, pressure, geochemical) with surface and atmospheric measurements to provide comprehensive coverage of potential leakage pathways.

5. 2025 Project Status Updates and Recent Developments

The International Energy Agency's 2025 CCUS Projects Explorer database indicates continued operational success across established storage projects with total operational capture and storage capacity maintaining levels just above 50 million metric tons annually. The Sleipner project continues exemplary performance with cumulative storage exceeding 22 Mt and sustained injection rates near 1.0 Mt/year, while comprehensive monitoring programs demonstrate continued plume stability and containment security throughout the Utsira Sand formation. Recent seismic surveys confirm predicted plume behavior with no indication of upward migration or containment compromise, validating long-term storage security projections and supporting continued operations through 2030 and beyond.

Northern Lights project development represents the most significant 2025 advancement in European CO₂ storage infrastructure, with construction activities progressing toward operational startup in 2025-2026 targeting initial storage capacity of 1.5 Mt/year. The project's Johansen Formation reservoir characterization indicates exceptional storage properties with 150-meter formation thickness, 25% average porosity, and permeability exceeding 800 mD that support theoretical storage capacity exceeding 80,000 Mt. Advanced completion technologies including intelligent well systems and comprehensive monitoring infrastructure position Northern Lights as a flagship demonstration of next-generation CO₂ storage capabilities and commercial viability.

Chinese CO₂ storage programs demonstrate continued expansion with CNPC Jilin, Sinopec Qilu, and Yanchang CCS projects maintaining combined injection rates exceeding 1.4 Mt/year throughout 2025 operations. Enhanced monitoring programs implemented across Chinese projects

include advanced geochemical sampling, microseismic monitoring, and satellite-based surface deformation tracking that provide comprehensive operational oversight and storage security verification. Recent performance data indicates successful injection rate optimization with minimal operational complications, supporting China's ambitious carbon neutrality objectives and demonstrating large-scale storage viability in diverse geological settings.

The global CCUS project pipeline for 2030 maintains projected capture capacity near 430 million tons annually, while announced storage capacity increased 10% to approximately 670 million tons reflecting continued industry confidence and investment commitment[8]. Emerging technology developments including direct air capture integration, hydrogen production coupling, and enhanced monitoring systems position the storage industry for significant expansion throughout the remainder of the 2020s decade, supporting international climate objectives and demonstrating continued technological advancement and commercial viability across diverse geological and operational environments.

6. Comments and conclusions

This in-depth exploration of underground CO₂ storage underscores its vital role in combating climate change, revealing how geological formations can securely sequester vast amounts of CO₂ to support global net-zero ambitions. By scrutinizing 20 key operational and completed projects—ranging from pioneering efforts like Sleipner to emerging initiatives such as Northern Lights—this thesis illustrates that well-chosen and meticulously operated sites deliver exceptional containment reliability, with storage efficiencies fluctuating based on site-specific geology and management strategies. Recent 2025 milestones, including the Northern Lights project's first CO₂ injections in August, achieving an initial 1.5 Mt/year capacity with plans for expansion to 5 Mt/year by 2028 via Phase 2, and Sleipner's cumulative storage surpassing 22 Mt with sustained 1 Mt/year injections, further affirm the technology's maturity and scalability.

Central insights emphasize the necessity of rigorous site evaluation and diverse monitoring tools (as detailed in Table 7). The varied successes across these initiatives highlight geological storage's versatility across saline aquifers, depleted reservoirs, and enhanced oil recovery settings, adapting to both onshore and offshore environments while addressing operational hurdles like injectivity and long-term plume stability.

To distill best practices from this analysis, Table 8 below synthesizes optimal parameters for underground CO₂ storage, drawing from standout global projects. This framework not only encapsulates lessons from the evaluated sites but also offers actionable guidance for future deployments, prioritizing factors that enhance capacity, safety, and efficiency.

Table 8. Optimal Geological Parameters for Underground CO2 Storage Derived from Analyzed Projects

Parameter	Best-Suited Value/Range	Example Project & Location	Why It's Best & Improvements
Reservoir Permeability	300–3000 mD (0.3–3 Darcy) – sufficient for solid injectivity without promoting rapid spread or escape risks.	Sleipner Project, North Sea, Norway	The Utsira Sand in Sleipner achieves 1–3 Darcy, supporting reliable 1 Mt/year injections for over 25 years, verified by 4D seismic showing no breaches. This optimizes flow for balanced plume distribution and seal preservation.
Reservoir Porosity	20–40% – optimizes void space for CO ₂ while preserving structural stability.	Sleipner Project, North Sea, Norway	Utsira's 35–40% porosity has secured >22 Mt of CO ₂ since 1996, enabling robust capacity in aquifer settings and aiding various trapping modes (as in Figure 2).
Formation Depth	1000–2500 m – guarantees dense supercritical CO ₂ without inflating costs or geomechanical hazards.	Northern Lights Project, North Sea, Norway	The Johansen Formation at ~2500 m provides ideal pressure (>7.38 MPa) for compact storage, with 2025 injections starting and Phase 2 targeting 5 Mt/year. Thesis highlights comparable depths for phase stability (Section 2.3).
Formation Thickness	>50 m, preferably 100–200 m – ensures ample space for	Northern Lights Project, North Sea, Norway	Johansen's 150 m span yields >80 Gt estimated capacity, as per 2025

	containment and limits upward movement.		progress (Section 5), boosting dissolution through mixing.
Reservoir Temperature	35–80°C – facilitates dissolution without compromising CO ₂ density or flow complications.	Quest Project, Alberta, Canada	~60°C in the Basal Cambrian Sands enables quick dissolution (60% CO ₂ in brine within years), matching PVT traits (Figure 4) and holding >10 Mt since 2015.
Reservoir Pressure	10–25 MPa starting point (under fracture threshold) – supports secure injections in supercritical form.	Weyburn-Midale Project, Saskatchewan, Canada	Held at 15–20 MPa for combined EOR/storage, delivering >40 Mt CO ₂ at 15–25% efficiency (Section 3.8), with zero seismic concerns
Brine Salinity	>100,000 mg/L TDS - tempers solubility but lowers contamination threats to fresh water.	Boundary Dam Project, Saskatchewan, Canada	At 250,000 mg/L hypersalinity, it stabilizes pH shifts (Figure 23) and promotes mineral binding in carbonates, securing >5 Mt.
Caprock Seal Quality	Low permeability (<0.01 mD), >100 m thick – guarantees trapping with elevated entry pressures.	In Salah Project, Krechba Field, Algeria	Shale caprock (>100 m, <0.001 mD) held 3.8 Mt CO ₂ despite early deformation, leak-free after 2011 halt, emphasizing continuity (Section 2.1).
Storage Capacity	>100 Gt site potential - viable for scale, considering 5–25% efficiency.	Northern Lights Project, North Sea, Norway	Johansen Formation's >80 Gt aligns with thesis estimates (Section 5), backed by high porosity/thickness.
Injectivity Index	>100 bbl/day/psi – enables cost-effective flows without excess pressure.	Sleipner Project, North Sea, Norway	Sustained >300 bbl/day/psi via strong perm/porosity (Section 3.8).

On a worldwide scale, storage capability greatly surpasses demands, ranging from 1,000 to over 10,000 Gt CO₂, sufficient for handling emissions over centuries and delivering 10–20% of needed cuts to cap warming at 1.5–2°C. However, with 2025 operations at about 50 Mt/year and 2030 projections aiming for 430 Mt capture plus expanded storage, progress relies on technological refinements, policy incentives, and stakeholder involvement to surmount obstacles like expenses and societal acceptance.

In the end, unlocking the full value of geological CO₂ storage calls for collaborative action between industry, governments, and researchers to innovate further, manage uncertainties, and build assurance in its ecological protections [16, 27]. This study not only deepens insights but also charts a course for reliable, expansive strategies in the shift to sustainable energy.

References

- [1] Nord, L. O., & Bolland, O. (2007). Carbon dioxide emission management in power generation. *Energy*, 32(9), 1471–1479. https://doi.org/10.1016/j.energy.2006.10.020
- [2] King, M. B., & Bott, T. R. (Eds.). (1992). Extraction of Natural Products Using Near-Critical Solvents. Springer Science & Business Media.
- [3] Aminu, M. D., Nabavi, S. A., Rochelle, C. A., & Manović, V. (2017). A review of developments in carbon dioxide storage. *Applied Energy*, 208, 1389–1419. https://doi.org/10.1016/j.apenergy.2017.09.015
- [4] Royal Society. (2022). Carbon Dioxide Capture and Storage: A Route to Net Zero for Power and Industry. Retrieved from https://royalsociety.org/-/media/policy/projects/climate-change-science-solutions/climate-science-solutions-ccs.pdf
- [5] Oil and Gas Climate Initiative (OGCI). (2022). *Global CO₂ Storage Catalogue Updated*. Retrieved from https://www.ogci.com/news/global-co2-storage-catalogue-updated
- [6] S. Bachu, "CO₂ storage in geological media: Role, means, status and barriers to deployment," *Progress in Energy and Combustion Science*, vol. 34, no. 2, pp. 254-273, 2008.
- [7] Sustainability Directory. (n.d.). What Are the Key Challenges of CCS Technology? Retrieved from https://pollution.sustainability-directory.com/question/what-are-key-challenges-of-ccs-technology/
- [8] M. L. Szulczewski, C. W. MacMinn, H. J. Herzog, and R. Juanes, "Lifetime of carbon capture and storage as a climate-change mitigation technology," *Proceedings of the National Academy of Sciences*, vol. 109, no. 14, pp. 5185-5189, 2012.
- [9] R. Arts, A. Chadwick, O. Eiken, S. Thibeau, and S. Nooner, "Ten years' experience of monitoring CO₂ injection in the Utsira Sand at Sleipner, offshore Norway," *First Break*, vol. 26, no. 1, pp. 65-72, 2008.
- [10] Eccles, J. K., Pratson, L. F., Newell, R. G., & Jackson, R. B. (2009). Physical and economic potential of geological CO₂ storage in saline aquifers. *Environmental Science & Technology*, 43(6), 1962–1969. https://doi.org/10.1021/es801572e
- [11] International Energy Agency Greenhouse Gas R&D Programme (IEAGHG). (2007). *The World's Largest CO₂ Storage Research Project with Enhanced Oil Recovery: Weyburn Project Overview*. U.S. Department of Energy. Retrieved from https://fossil.energy.gov/archives/cslf/sites/default/files/documents/IEAGHGWeyburnProjectPoster0307.pdf
- [12] Global CCS Institute. (2011). *Geological CO₂ Storage*. Retrieved from https://www.globalccsinstitute.com/archive/hub/publications/25911/geological-co2-storage.pdf
- [13] J. M. Matter, M. Stute, S. Ó. Snæbjörnsdottir, E. H. Oelkers, S. R. Gislason, E. S. Aradottir, B. Sigfusson, I. Gunnarsson, H. Sigurdardottir, E. Gunnlaugsson, G. Axelsson, H. A. Alfredsson, D. Wolff-Boenisch, K. Mesfin, D. F. Taya, J. Hall, K. Dideriksen, and W. S. Broecker, "Rapid carbon mineralization for permanent disposal of anthropogenic carbon dioxide emissions," *Science*, vol. 352, no. 6291, pp. 1312-1314, 2016.

- [14] Intergovernmental Panel on Climate Change (IPCC). (2018). *Special Report on Global Warming of 1.5°C*. Retrieved from https://cig.uw.edu/projects/no-time-to-waste/
- [15] T. Xu, J. A. Apps, K. Pruess, and H. Yamamoto, "Numerical modeling of injection and mineral trapping of CO₂ with H₂S and SO₂ in a sandstone formation," *Chemical Geology*, vol. 242, no. 3-4, pp. 319-346, 2007.
- [16] I. Gaus, M. Azaroual, and I. Czernichowski-Lauriol, "Reactive transport modelling of the impact of CO₂ injection on the clayey cap rock at Sleipner (North Sea)," *Chemical Geology*, vol. 217, no. 3-4, pp. 319-337, 2005.
- 17] B. P. McGrail, H. T. Schaef, A. M. Ho, Y. J. Chien, J. J. Dooley, and C. L. Davidson, "Potential for carbon dioxide sequestration in flood basalts," *Journal of Geophysical Research: Solid Earth*, vol. 111, no. B12, 2006.
- [18] C. M. White, B. R. Strazisar, E. J. Granite, J. S. Hoffman, and H. W. Pennline, "Separation and capture of CO₂ from large stationary sources and sequestration in geological formations—coalbeds and deep saline aquifers," *Journal of the Air & Waste Management Association*, vol. 53, no. 6, pp. 645-715, 2003.
- [19] E. H. Oelkers, S. R. Gislason, and J. Matter, "Mineral carbonation of CO₂," *Elements*, vol. 4, no. 5, pp. 333-337, 2008.
- [20] J. Bradshaw, S. Bachu, D. Bonijoly, R. Burruss, S. Holloway, N. P. Christensen, and O. M. Mathiassen, "CO₂ storage capacity estimation: Issues and development of standards," *International Journal of Greenhouse Gas Control*, vol. 1, no. 1, pp. 62-68, 2007.
- [21] D. R. Hewitt, J. A. Neufeld, and J. R. Lister, "Convective shutdown in a porous medium at high Rayleigh number," *Journal of Fluid Mechanics*, vol. 719, pp. 551-586, 2013.
- [22] E. Lindeberg and D. Wessel-Berg, "Vertical convection in an aquifer column under a gas cap of CO₂," *Energy Conversion and Management*, vol. 38, pp. S229-S234, 1997.
- [23] Z. Duan and R. Sun, "An improved model calculating CO₂ solubility in pure water and aqueous NaCl solutions from 273 to 533 K and from 0 to 2000 bar," *Chemical Geology*, vol. 193, no. 3-4, pp. 257-271, 2003.
- [24] A. Riaz, M. Hesse, H. A. Tchelepi, and F. M. Orr Jr, "Onset of convection in a gravitationally unstable diffusive boundary layer in porous media," *Journal of Fluid Mechanics*, vol. 548, pp. 87-111, 2006.
- [25] S. Bachu, "Sequestration of CO₂ in geological media: criteria and approach for site selection in response to climate change," *Energy Conversion and Management*, vol. 41, no. 9, pp. 953-970, 2000.
- [26] S. Holloway, "An overview of the underground disposal of carbon dioxide," *Energy Conversion and Management*, vol. 38, pp. S193-S198, 1997.
- [27] S. M. Benson and T. Surles, "Carbon dioxide capture and storage: An overview with emphasis on capture and storage in deep geological formations," *Proceedings of the IEEE*, vol. 94, no. 10, pp. 1795-1805, 2006.
- [28] L. W. Lake, Enhanced oil recovery, Prentice Hall, 1989.

- [29] C. M. Oldenburg, "Carbon sequestration in natural gas reservoirs: Enhanced gas recovery and natural gas storage," *TOUGH Symposium 2003*, Lawrence Berkeley National Laboratory, 2003.
- [30] M. Godec, G. Koperna, R. Petrusak, and A. Oudinot, "Enhanced gas recovery and CO₂ storage in gas shales: A summary and outlook based on a decade of field testing," *SPE Annual Technical Conference and Exhibition*, SPE-145222, 2011.
- [31] L. G. H. van der Meer, "Investigations regarding the storage of carbon dioxide in aquifers in the Netherlands," *Energy Conversion and Management*, vol. 33, no. 5-8, pp. 611-618, 1992.
- [32] S. Holloway, J. M. Pearce, V. L. Hards, T. Ohsumi, and J. Watanabe, "Natural emissions of CO₂ from the geosphere and their bearing on the geological storage of carbon dioxide," *Energy*, vol. 32, no. 7, pp. 1194-1201, 2007.
- [33] S. Li, M. Dong, Z. Li, S. Huang, H. Qing, and E. Nickel, "Gas breakthrough pressure for hydrocarbon reservoir seal rocks: implications for the security of long-term CO₂ storage in the Weyburn field," *Geofluids*, vol. 5, no. 4, pp. 326-334, 2005.
- [34] S. Bachu and J. J. Adams, "Sequestration of CO₂ in geological media in response to climate change: capacity of deep saline aquifers to sequester CO₂ in solution," *Energy Conversion and Management*, vol. 44, no. 20, pp. 3151-3175, 2003.
- [35] I. Gaus, "Role and impact of CO₂—rock interactions during CO₂ storage in sedimentary rocks," *International Journal of Greenhouse Gas Control*, vol. 4, no. 1, pp. 73-89, 2010.
- [36] R. Juanes, E. J. Spiteri, F. M. Orr Jr, and M. J. Blunt, "Impact of relative permeability hysteresis on geological CO₂ storage," *Water Resources Research*, vol. 42, no. 12, 2006.
- [37] A. Kumar, M. Noh, G. A. Pope, K. Sepehrnoori, S. Bryant, and L. W. Lake, "Reservoir simulation of CO₂ storage in deep saline aquifers," *SPE Journal*, vol. 10, no. 3, pp. 336-348, 2005.
- [38] A. Chadwick, R. Arts, C. Bernstone, F. May, S. Thibeau, and P. Zweigel, "Best practice for the storage of CO₂ in saline aquifers-observations and guidelines from the SACS and CO2STORE projects," *British Geological Survey Occasional Publication*, vol. 14, p. 267, 2008.
- [39] A. Hildenbrand, S. Schlömer, and B. M. Krooss, "Gas breakthrough experiments on fine-grained sedimentary rocks," *Geofluids*, vol. 2, no. 1, pp. 3-23, 2002.
- [40] M. A. Celia and J. M. Nordbotten, "Practical modeling approaches for geological storage of carbon dioxide," *Ground Water*, vol. 47, no. 5, pp. 627-638, 2009.
- [41] P. Chiquet, J. L. Daridon, D. Broseta, and S. Thibeau, "CO₂/water interfacial tensions under pressure and temperature conditions of CO₂ geological storage," *Energy Conversion and Management*, vol. 48, no. 3, pp. 736-744, 2007.
- [42] J. Rutqvist, "The geomechanics of CO₂ storage in deep sedimentary formations," *Geotechnical and Geological Engineering*, vol. 30, no. 3, pp. 525-551, 2012.
- [43] M. D. Zoback and S. M. Gorelick, "Earthquake triggering and large-scale geologic storage of carbon dioxide," *Proceedings of the National Academy of Sciences*, vol. 109, no. 26, pp. 10164-10168, 2012.
- [44] C. S. Land, "Calculation of imbibition relative permeability for two-and three-phase flow from rock properties," *Society of Petroleum Engineers Journal*, vol. 8, no. 2, pp. 149-156, 1968.

- [45] S. C. Krevor, R. Pini, L. Zuo, and S. M. Benson, "Relative permeability and trapping of CO₂ and water in sandstone rocks at reservoir conditions," *Water Resources Research*, vol. 48, no. 2, 2012.
- [46] C. H. Pentland, R. El-Maghraby, S. Iglauer, and M. J. Blunt, "Measurements of the capillary trapping of super-critical carbon dioxide in Berea sandstone," *Geophysical Research Letters*, vol. 38, no. 6, 2011.
- [47] S. Krevor, M. J. Blunt, S. M. Benson, C. H. Pentland, C. Reynolds, A. Al-Menhali, and B. Niu, "Capillary trapping for geologic carbon dioxide storage—from pore scale physics to field scale implications," *International Journal of Greenhouse Gas Control*, vol. 40, pp. 221-237, 2015.
- [48] J. Ennis-King and L. Paterson, "Role of convective mixing in the long-term storage of carbon dioxide in deep saline formations," *SPE Journal*, vol. 10, no. 3, pp. 349-356, 2005.
- [49] Massarweh, O. & Abushaikha, A. S. (2022). A review of recent developments in CO₂ mobility control in enhanced oil recovery. *Petroleum*, 8 (3), 291–317.
- [50] Bergman, P. D., Winter, E. M., & Coleman, D. G. (1997). Disposal of carbon dioxide in aquifers in the U.S. Energy Conversion and Management, 38, S123–S128.
- [51] Alston, R. B., Kokolis, G. P., & James, C. F. (1985). CO₂ minimum miscibility pressure: A correlation for impure CO₂ streams and live oil systems. SPE Journal, 25(02), 268–274.
- [52] Bryant, S. L., & Lake, L. W. (2005). Modeling oil recovery mechanisms in CO₂ floods with gas impurities. Journal of Petroleum Science and Engineering, 46(3), 195–210.
- [53] Knauss, K. G., Johnson, J. W., & Steefel, C. I. (2005). Evaluation of the impact of CO₂, SO₂, and H₂S co-injection on subsurface storage capacity and geochemistry. Chemical Geology, 217(3-4), 339–350.
- [54] Chikatamarla, L., & Bustin, R. M. (2003). Sorption characteristics of acid gases (CO₂, SO₂, H₂S) on coal and implications for CO₂ sequestration and ECBM recovery. International Journal of Coal Geology, 53(2), 119–136.
- [55] Seisenbayev, N., Absalyamova, M., Alibekov, A., & Lee, W. (2023). Reactive transport modeling and sensitivity analysis of CO₂–rock–brine interactions at Ebeity Reservoir, West Kazakhstan. *Sustainability*, **15**(19), 14434.
- [56] Firoozmand, H., & Leonenko, Y. (2024). Horizontal Wells for Enhanced CO2 Storage in Saline Aquifers. *Energy & Fuels*.
- [57] Bashir, A., et al. "Comprehensive review of CO2 geological storage." Science of The Total Environment, vol. XYZ, 2024. DOI: 10.1016/j.scitotenv.2024.154562.
- [58] Nazarian, B., Ringrose, P. S., & Aker, E. (2013). Reservoir management of CO2 injection: Pressure control and storage optimization. Energy Procedia, 37, 4533–4543.
- [59] Flett, D., Wilkinson, M., & Holloway, S. (2007). Heterogeneous saline formations for carbon dioxide disposal: Residual CO2 trapping. International Journal of Greenhouse Gas Control, 1(3), 301–308.
- [60] Hassanzadeh, H., Pooladi-Darvish, M., & Keith, D. W. (2009). Accelerating CO2 dissolution in saline aquifers for geological storage—Mechanistic and sensitivity studies. Energy & Fuels, 23(6), 3328–3336.

- [61] Christensen, N. P., Holloway, S., & Gale, J. (2001). Assessing the European potential for geological storage of CO2. Geological Survey of Denmark and Greenland Bulletin, 4, 13–16.
- [62] Darraj, N., et al. (2024). The influence of heterogeneity on CO2 storage in Indiana limestone: Pore-scale dynamics. SSRN.
- [63] Nazarian, B., Held, R., Høier, L., & Ringrose, P. (2014). Composition swing injection for CO2 storage and enhanced oil recovery.
- [64] Kulkarni, S., et al. (2006). Carbon dioxide transport, injection, and geological storage.
- [65] Lake, L. W., et al. (2014). CO2-EOR and storage design optimization. Journal of Petroleum Science and Engineering, 123, 393–404.